DEVELOPMENT OF A ROBOTIC ORTHO-PROSTHESIS FOR TRANS-HUMERAL AMPUTEES

Rammuni Achintha Mihiran Abayasiri

(168041U)

Degree of Master of Science

Department of Mechanical Engineering

University of Moratuwa

Sri Lanka

January 2019

Development of A Robotic Ortho-prosthesis for Trans-humeral Amputees

Rammuni Achintha Mihiran Abayasiri

(168041U)

Thesis submitted in partial fulfillment of the requirements for the degree Master of Science by research in Biomedical Engineering

Department of Mechanical Engineering

University of Moratuwa

Sri Lanka

January 2019

DECLARATION

I declare that this is my own work and this dissertation does not incorporate without acknowledgement any material previously submitted for a Degree or Diploma in any other University or institute of higher learning and to the best of my knowledge and belief it does not contain any material previously published or written by another person except where the acknowledgement is made in the text.

Also, I hereby grant to University of Moratuwa the non-exclusive right to reproduce and distribute my dissertation, in whole or in part in print, electronic or other medium. I retain the right to use this content in whole or part in future works (such as articles or books).

Signature: Date:

The above candidate has carried out research for the MSc thesis under my supervision.

Signature of the Supervisor(s): Date:

Prof. R. A. R. C. Gopura
Head/Professor,
Department of Mechanical Engineering,
University of Moratuwa, Sri Lanka.

Abstract

Over the years trans-humeral prostheses have been developed as a remedy for trans-humeral amputation: the amputation occurs between shoulder and elbow. For the best usage of the trans-humeral prostheses, amputee should have a strong residual arm (stump arm) after the amputation. Furthermore, the ranges of motions and also the full functionality of the prosthesis will be limited if the amputee has a weak stump arm. Moreover, prolonged applying of the loads on the stump arm can cause musculo-skeletal disorders.

In order to improve the dexterity of the prosthesis, they are developed with more joints and actuators. Hence, the weight of the prosthesis increases. There is a need for power assisting the weak stump arm while the prosthesis is at work. Trans-humeral ortho-prosthesis is a device which assists the power of stump arm from an orthosis while replacing the missing upper limb with trans-humeral prosthesis. This research is carried to develop a 9 Degrees of Freedom trans-humeral ortho-prosthesis. It consists of 4 DoF motions: shoulder horizontal flexion/extension, shoulder vertical flexion/extension, shoulder abduction/adduction and shoulder internal/external rotation, at the orthosis and 5 DoF motions: elbow flexion/extension, forearm supination/pronation, wrist ulnar/radial deviation, wrist flexion/extension and compound motion of thumb and index finger, at the prosthesis. Moreover, shoulder abduction/adduction is supported as a passive DoF in order to compensate the misalignments of the joints caused by the motions of clavicle and the scapula in the sagittal plane while enabling shoulder abduction/adduction . Even though the orthosis is designed to achieve 4 DoF motions, it contains 6 DoF motions. Therefore, the whole ortho-prosthesis becomes a redundant manipulator.

Simulation experiments have been carried out to determine the workspace of the hand of the ortho-prosthesis and to determine the manipulability of the ortho-prosthesis. Workspace plots show that it can reach the workspace of a human hand. Manipulability measures: manipulability index, minimum singular values, condition number and manipulability ellipsoids verify that the trans-humeral ortho-prosthesis would not reach singular configurations. Furthermore, it is confirmed that the ortho-prosthesis is capable of performing dexterous motions due to its high manipulability after carrying out experiments with the fabricated prototype of the trans-humeral ortho-prosthesis.

***Keywords*-Trans-humeral, ortho-prosthesis, manipulability measures, singular configurations, musculo-skeletal disorders, linear velocity jacobian**

DEDICATION

To my loving family

who keeps lifting me up with unconditional love,

every time I fall down ...

ACKNOWLEDGMENTS

After immense ups and downs, I am writing this thanking note in remembrance of the great assistance provided by everyone who were there with myself for the successful completion of this research work. It has been a great run for me and it is time for myself to pay my sincere gratitude towards all these great people.

The long list of the people who have my unending homage, should be started with my thesis supervisor Prof. R. A. R. C. Gopura. For me choosing the path of higher studies was challenging and life changing. I am eternally grateful to him for accepting myself as his research student and for the continuous support given to reach great milestones which I would not have even imagined. Over the entire period of my research, his humane qualities left an example for me to look up to and I am honoured to be a student of him.

I wish to extend my gratitude to Dr.Thilina Lalitharatne and Dr.Buddhika Jayasekara for providing their valuable insights for the successful completion of this research work. Moreover, special thanks should go to Eng.Pubudu Ranaweera for the assistance given during the Computer Aided Design phase.

Doing a research alone can be tiresome and restless at most of the time. However, it is the people around you who make that feeling disappear. I am very grateful to all the members of Bionics Laboratory, Department of Mechanical Engineering, University of Moratuwa, who had my back in each step of the way. Among them I would like to appreciate the support Dr. Kanishka Madusanka in shaping my Master's Degree work. Moreover, I would like to recall the motivational advices of Mr. Tharindu Prabatha and Dr. Viraj Muthugala. My homage

paid to the support of Bionics Laboratory will not be complete if I do not mention the fraternity displayed by Mr. Sanka Chandrasiri, Mr. Isuru Ruhunage, Mr. Chamika Perera, Mr. Thilina Weerakkody, Mr. Chathura Semasinghe, Mr. Chamara Herath, Mr. Chanaka Premarathna and Mr. Rancimal Arumathanthri, apart from the support as the Bionics Laboratory members.

I wish to express my sincere thanks to Mr. Dashanka De Silva, Mr. Ravindu Thalagala and all my fellow batch mates from 11^{th} batch who are currently pursuing academic career in University of Moratuwa for their friendly and insightful feedbacks during my research work.

I wish to dearly mention the unwavering support and the trust I had from Ms. Gayeshi Jayakody throughout the times where the hope was bleak for myself.

Finally, this thanking note will be incomplete if I do not mention the unconditional support, love and motivation provided by my loving family. I would pay my sincere homage to them, with heavy heart for being the reason to keep moving forward when the things get hard.

Achintha Abayasiri
achintha.mihiran@ieee.org

TABLE OF CONTENTS

LIST OF FIGURES

LIST OF TABLES

LIST OF ABBREVIATIONS

ADL	Activities of Daily Living
DoF	Degrees of Freedom
U/R	Ulnar/ Radial
F/E	Flexion/ Extension
ROM	Range of Motions
Abd/Add	Abduction/Adduction
S/P	Supination/ Pronation
I/E	Internal/ External
DH	Denevit-Hartenberg
HRI	Human Robot Interaction
N/A	Not Applicable

Chapter 1

INTRODUCTION

Using robots for Activities of Daily Living (ADL) has been a popular research area for decades. According to Merriam-Webster dictionary, a robot is referred to as a machine that resembles a living creature in being capable of moving independently and performing complex actions [1]. However the word "robot" originated from the Czech word "robota" which has the meaning of "labor" [2]. Getting the assistance of robots for ADL can be a challenging task [3]. As the definition states, resembling living creatures should be brought into the robot design. Identifying the user intention [4], [5] and acting according to that, are two distinctively different and challenging tasks while designing of robots.

The history of robots runs back till 400 BC when Archytas of Arentum developed a steam-driven, self-propelling wooden bird capable of flying 200m [2]. Since then robots have been evolved in leaps and bounds in the fields of robot design and control architecture. The evolution of the robotics have been outreached the conventional use of robots in ADL to fileds like aerospace industry, medicine, military purposes etc.

In the field of medicine, robots play a vital role in making complexed prostheses to imitate the missing body part after the replacement. However, the first prosthesis which by definition replaces the missing body part, is dated back to 300 B.C. It was a bronze lower limb which was unearthed in Capua, Italy in 1858 [6]. In the early days, the prostheses were worn for cosmetic purposes. Even though American Orthotic and Prosthetic Association (AOPA) was formed after world

war I, the transformation of the prostheses from cosmetic purposes to working prostheses was occurred after the world war II.

With the development of science and technology dexterous prostheses came in to the globe. However, addressing the remedies for upper limb amputation has become a challenging task due to various reasons [7]. Trans-humeral amputation occurs between elbow and shoulder [8]. Trans-humeral prostheses are developed as a remedy for trans-humeral amputation. When developing the dexterous trans-humeral prostheses the weight of the prosthesis becomes a huge challenge. Researches are being carried out to reduce the weights of the trans-humeral prostheses by introducing sophisticated actuators to the design [9]. However, these actuators would increase the cost of the prostheses. Furthermore, trans-humeral prostheses should maintain the co-existence of both dexterity and the weight of the prosthesis. Therefore, it is difficult to limit the weights of the trans-humeral prostheses since the dexterous prostheses need many degrees of freedoms (DoF).

1.1 Motivation

Addressing the mental and physical health issues of post-amputation has become a challenging task for the scientists over the years [10]. These challenges raised with the type of amputation and level of amputation are different from each other and each of them may need different solutions. A weak residual arm (stump arm) has been a great obstacle for finding remedies of the trans-humeral amputation. Trans-humeral amputation occurs between elbow and shoulder due to congenital disorders, accidents, neuroma, injuries etc. The amputation and the way which it has occured make the stump arm weak.

In general, trans-humeral prostheses are worn on stump arm. Therefore, stump arm motions has a direct impact towards the end effector pose of the prosthesis. In some cases trans-humeral prostheses do not contain two wrist motions:

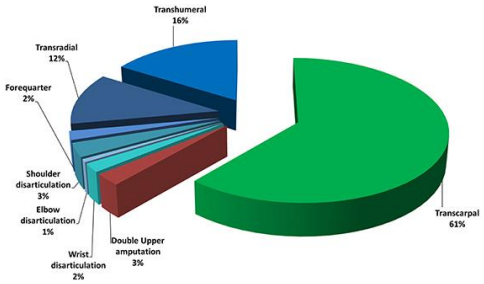

Figure 1.1: Statistics on level of upper limb amputation in Italy and United Kingdom [14]

ulnar/radial (U/R) deviation and wrist flexion/extension (F/E). Then the shoulder motions should take over the wrist motions to carryout daily activities. If there is a weak stump arm, the shoulder is unable to take over the wrist motions. Even in the cases where the both wrist motions are present [11], weak stump arm would limit the ranges of motions of the prosthesis.

Moreover, the amputees with healthy stump arms often get diagnosed with musculo-skeletal disorders due to prolonged load application on the stump arm [12, 13]. As mentioned in the previous section, it has been a difficult task to maintain the co-existence between the dexterity and the weight of the prosthesis.

1.1.1 Trans-humeral ortho-prosthesis

As mentioned in section 1.1 trans-humeral amputation occurs due to several reasons. Approximately 3500 and 5200 upper limb amputations are reported each year in Italy and in UK, respectively. 16% of them are recorded as trans-humeral amputations [14] (see Figure 1.1). Sri lanka has also faced an internal conflict for nearly three decades leaving thousands of upper limb amputees.

It is an apparent fact that the shoulder orthosis should be developed with a mechanism to bear the loads applied by the prosthesis on the stump arm while being able to provide the required assistance to the stump arm. **A trans-humeral ortho-prosthesis** can be considered as a solution to these problems. Trans-humeral ortho-prosthesis is a combination of an orthosis (to assist stump arm

and bear the loads of the prosthesis) and prosthesis (to replace the missing upper limb). Combination of orthosis and prosthesis to make an ortho-prosthesis is being used for lower limb prostheses [15]. However, the application of this concept for upper limb prostheses is rarely found in the literature.

This thesis proposes a trans-humeral ortho-prosthesis with novel redundant orthosis mechanism. With the introduced redundancy in shoulder orthosis, the proposed trans-humeral ortho-prosthesis has been able to perform dexterous motions. Initial experiments have been carried out to validate the effectiveness of the prosthesis and orthosis. Then experiments were carried with prototype of the proposed trans-humeral ortho-prosthesis to evaluate its ability to perform dexterous motions and to monitor its ability to perform human like motions.

1.2 Contributions of the Thesis

The research work described in this thesis is carried out for the development of trans-humeral robotic ortho-prosthesis. The major contributions of this thesis is listed down below.

- Validating trans-humeral prosthesis "MoBio"
- Proposing the concept of Trans-Humeral Ortho-Prosthesis
- Proposing a design of trans-humeral ortho-prosthesis for human like motion generation
- Validation of the proposed trans-humeral ortho-prosthesis with a fabricated prototype

1.3 Thesis Overview

The thesis consists of 5 chapters. Chapter 2 includes the literature review. Chapter 3 explains the mechanical design of the trans-humeral ortho-prosthesis. Chapter 4 illustrates the experimental results. Chapter 5 concludes the thesis. Figure 1.2 shows the summary of the overview of the thesis.

Chapter 2:- Literature Review

This chapter covers the biomechanics of the human upper limb and other areas relevant for designing trans-humeral ortho-prosthesis. These areas include kinematics of the human upper limb, kinematic redundancy of the robot manipulators, shoulder orthoses/exoskeletons, kinematic performance analyzing of the robot manipulators and finally the issues regarding the trans-humeral prostheses. Further description towards the thesis motivation is presented in later part of the chapter.

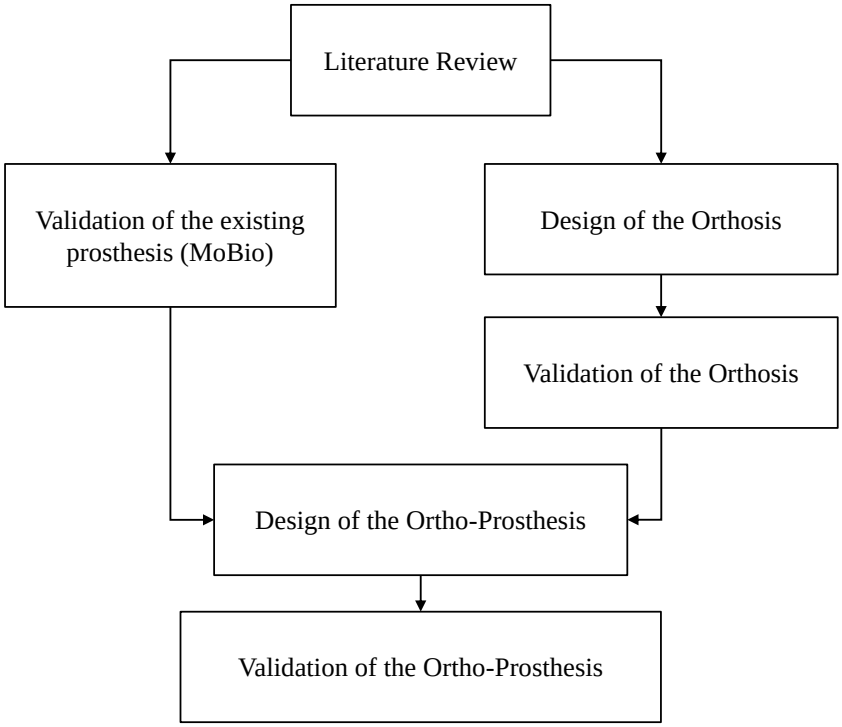

Figure 1.2: Summary of the research work

Chapter 3:- Mechanical Design of the trans-humeral ortho-prosthesis

A detailed description of the mechanical design of the trans-humeral ortho-prosthesis is included in this chapter. The chapter is devided into three sections which describe the design of shoulder orthosis, design of the trans-humeral prosthesis and the prototype of the trans-humeral ortho-prosthesis respectively.

Chapter 4:- Results

This chapter discusses the experimental results obtained for the trans-humeral ortho-prosthesis. Results are discussed under three sections namely validation of the existing trans-humeral prosthesis, validation of the shoulder orthosis and validation of proposed trans-humeral ortho-prosthesis.

Chapter 5:- Conclusion

This chapter concludes the thesis with future directions.

Chapter 2

LITERATURE REVIEW

From the motivation of this thesis [see section 1.1] it is apparent that a device is required to assist the stump arm of trans-humeral amputee while the prosthesis is at work. A literature review was carried out to find out the relevant factors for designing a robotic trans-humeral ortho-prosthesis. Furthermore, this chapter presents comprehensive information on the background of the trans-humeral ortho-prostheses. Moreover, performance evaluatiion methods of the robots and the anatomical details regrading the trans-humeral ortho-prostheses are discussed under this chapter.

2.1 Biomechanics of the human upper limb

Human upper limb can be divided into four major components: shoulder complex, elbow complex, wrist and hand [see Figure 2.1 (a)]. The shoulder complex is built by clavicle, scapula and humerus [see Figure 2.1 (b)]. The other end of the humerus is joined with radius and ulnar which then build the elbow complex. These bones are placed on the arm and forearm respectively. Shoulder complex and elbow complex have 4 DoF and 2 DoF respectively. Wrist has DoF motions namely U/R deviation and wrist F/E. Hand provides the platform for 21 DoF motions with its individual motions of the five fingers [16].

Table 2.1 and Table 2.2 show the ranges of motions (ROM) of the human upper limb [18]. Even though the motions are depicted as separate entities [see

Figure 2.2 and Figure 2.3] each motion effects the other motion in performing the hand motions. Further details about the upper limb motion generation will be discussed in section 2.2 and sub section 3.2.1.

Figure 2.4 shows the classification of the finger grasping patterns. Hand can be considered as the section with the most sophisticated structure which consists of carpal, metacarpal and phalangeal bones. Five metacarpal and 14 phalangeal

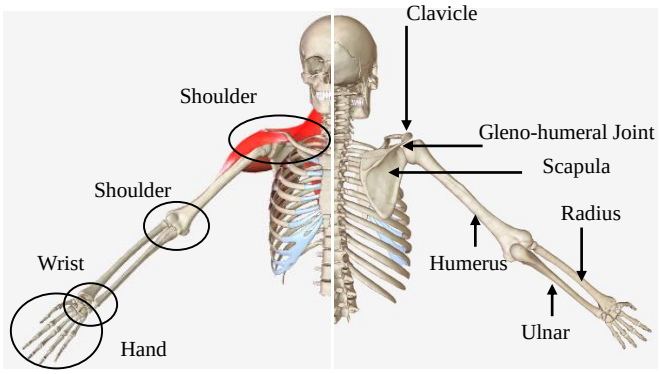

Figure 2.1: Human upper limb: (a) Anterior view of the upper limb (b) Posterior view of the upper limb

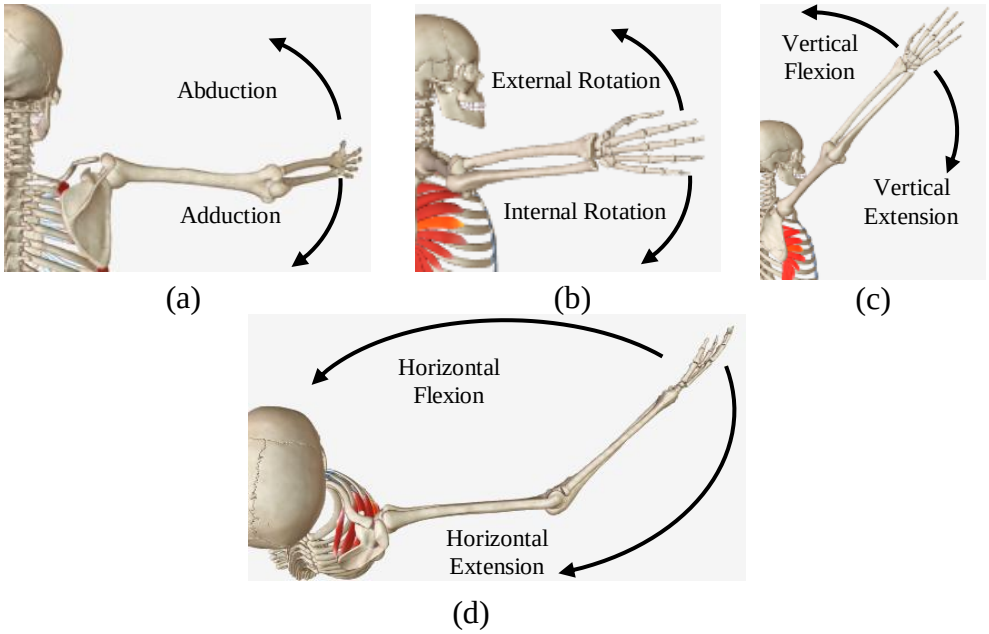

Figure 2.2: Motions of the shoulder: (a) Shoulder Abduction/Adduction (Abd/Add) (b) Shoulder Internal/External (I/E) rotation (c) Shoulder vertical F/E (d) Shoulder horizontal F/E

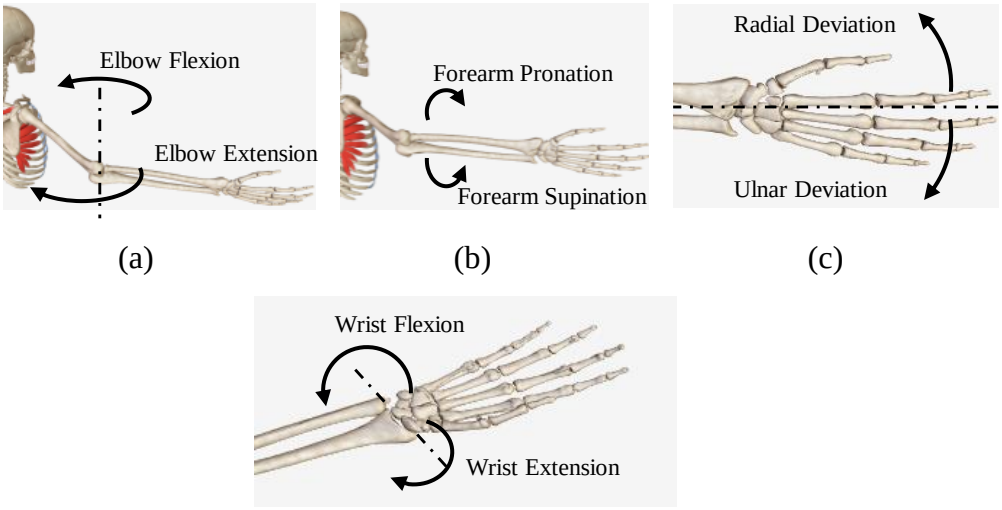

Figure 2.3: Motions of elbow and wrist complexes: (a) Elbow F/E (b) Forearm Supination/Pronation (S/P) (c) U/R deviation (d) Wrist F/E

Table 2.1: ROM of human upper limb and the trans-humeral ortho-prosthesis (Shoulder motions)

Motion	**Human Upper Limb (Deg)**	**Trans-humeral Ortho-prosthesis (Deg)**
Shoulder vertical F/E	-60 - 180	-50 - 180
Shoulder Horizontal F/E	-30 - 135	-30 - 120
Shoulder Abd/Add	0 - 180	0 - 180
Shoulder I/E rotation	-50 - 100	-40 - 90

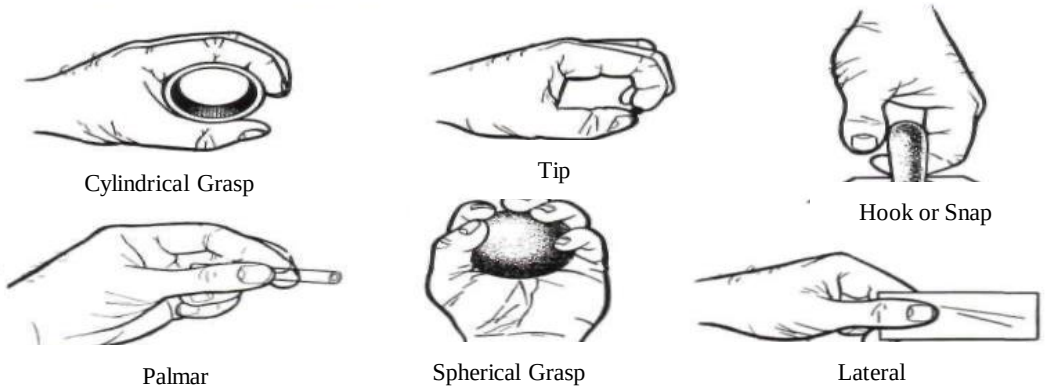

Figure 2.4: Taxonomy of grasps [17]

Table 2.2: ROM of human upper limb and the trans-humeral ortho-prosthesis (Forearm motions)

Motion	**Range (deg) Human Limb**	**Range (deg) MoBio arm**
Elbow Flexion/Extension	0 - 145	0 - 150
Supination/Pronation	-85 - 70	-85 - 70
Wrist Flexion/Extension	-70 - 70	-70 - 70
Wrist Ulnar/Radial deviation	-35 - 20	-27 - 25

bones form the palm and fingers of the hand and eight carpal bones form the wrist [16, 19–21].

Human hand acts as the end effector if the upper limb is considered as a manipulator. However, its pose (position + orientation) is decided with the of shoulder, elbow and the wrist motions. The Kinematic structure of the upper limb will be discussed in the next section.

2.2 Kinematics of the human upper limb

As mentioned in the previous section there are 4 DoF motions in shoulder complex, 2 DoF motions in elbow complex and 2 DoF motions wrist. Figure 2.5 shows the simplified kinematic model of the upper limb. In order to perform shoulder motions, scapula, clavicle and gleno-humeral joint work as a compound unit. Considering the 4 principle motions of the shoulder: shoulder Abd/Add, shoulder horizontal F/E, shoulder vertical F/E and shoulder I/E rotation, kinematic model is derived for these compound motions but not for the individual motions of the bones. Hence the kinematic model is considered as a simplified

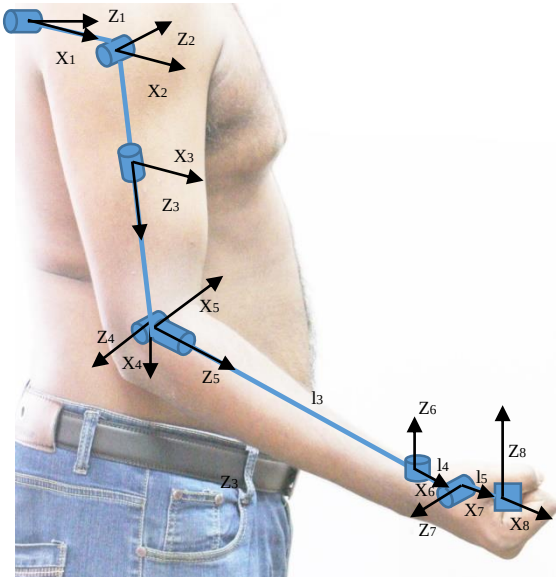

Figure 2.5: Simplified kinematic model of the human upper limb

Table 2.3: D-H parameters of human upper limb [11]

Link	α_i	$\mathbf{a}_i$	$\mathbf{d}_i$	θ_i
1	$\pi/2$	0	0	θ_1
2	$\pi/2$	0	0	θ_2
3	$\pi/2$	0	304	θ_3
4	$-\pi/2$	0	0	θ_4
5	$-\pi/2$	0	271	θ_5
6	$-\pi/2$	5	0	θ_6
7	0	0	0	θ_7

model. Furthermore, hand is considered as the end effector of the manipulator assuming upper limb as a robot manipulator as mentioned above. Here the "Z" axes denotes the joint axes. Denavit-Hartenberg (DH) parameters [22, 23] of the upper limb kinematic model is depicted in Table 2.3.

2.3 Kinematic redundancy of robot manipulators

Robots are designed to mimic living beings [see Chapter 1]. In order to perform tasks, living beings posses several DoF motions. Sometimes the number of DoF that are required for the motion, is less the DoF motions of the living being. However, putting this phenomena to the robot is a challenging task. The major deviations of the motions of the robots from the living beings, occur due to the lack of the redundancy of the robot. This section briefly discusses the aspects regarding the robot manipulability.

2.3.1 Class of tasks

Class of task can be defined as the number of DoF required to achieve a task through a robot [24, 25]. For example shoulder is built to perform shoulder horizontal F/E, shoulder vertical F/E, shoulder Abd/Add and I/E rotation of the shoulder. Therefore, the class of task of the human shoulder is four. In general, class of task is the crucial parameter to be looked at when designing a robot.

2.3.2 Kinematic redundancy

As mentioned at the beginning of section 2.3 and sub section 2.3.1 living beings posses DoF more than the class of task to achieve a given task. If the number of DoF of robot (manipulator) available for a given task is higher than the class of task of the particular task, manipulator is said to be redundant. Human upper limb itself is a redundant manipulator. The redundancy of the shoulder is further described in sub section 2.5.2.

2.4 Kinematic Performance analyzing of robot manipulators

As mentioned in Chapter 1 robots resemble the living creatures. In order to keep up the resemblance studies on kinematic structure is paramount. In order to evaluate the kinematic performances of a robot, Tsune Yoshikawa introduced "manipulability measures" in 1984 [24, 25]. Further details on manipulability measures are discussed under this section.

2.4.1 Manipulability Measures

Manipulability measure is a mathematical representation of the joint configurations of a particular manipulator. Manipulability measures directly associate with the velocity Jacobian of the manipulator [26] [see equation 2.1].

$$V = \begin{bmatrix} J_v \\ J_\omega \end{bmatrix} \dot{\theta} \tag{2.1}$$

Where V, J_v, J_ω and $\dot{\theta}$ are the velocity of the manipulator, translational velocity Jacobian of the manipulator, rotational velocity Jacobian and joint angle velocity respectively. However, manipulability measures take only the translational velocity Jacobian (J_v) for the calculations. Furthermore, manipulability measures depicts whether the manipulator is close to singularity or is in a singular configuration.

Manipulability Index

Manipulability index [27], [25] is a scalar defined with the translational velocity Jacobian [see equation 2.2].

$$w = \sqrt{det(J.J^T)} \tag{2.2}$$

Where w, J and J^T are manipulability index, translational velocity Jacobian of the given configuration and transpose of the translational velocity Jacobian of the given configuration respectively. Since translational velocity Jacobian is a configuration dependent term manipulability index also becomes configuration dependant. Therefore, manipulability index varies over a given trajectory. If the manipulability index value is zero manipulator is in a singular configuration or its manipulability is completely lost. If the manipulability index value is very high the manipulator can reach the same point with many different configurations.

Minimum Singular Value

Minimum singular value is another scalar value which depicts the manipulability of a manipulator. For any matrix $J \epsilon R^{m \times n}$ there exists orthogonal matrices $U \epsilon R^{m \times m}$ and $V \epsilon R^{n \times n}$ such that

$$J = U \Sigma V^T \tag{2.3}$$

where,

$$\Sigma = \begin{bmatrix} \sigma_1 & \dots & 0 \\ \vdots & \ddots & \vdots \\ 0 & \dots & \sigma_m \end{bmatrix} \epsilon R^{m \times n} \tag{2.4}$$

with,

$$\sigma_1 \geq \sigma_2 \geq \sigma_3 \geq \cdots \geq \sigma_m \geq 0 \tag{2.5}$$

"σ_m" is called the minimum singular value and "J" is the translational velocity Jacobian of the manipulability measure. The method used to obtain the minimum singular value is called Singular Value Decomposition (SVD). Low σ_m values indicate the closeness to the singular state where as the high σ_m values depict the improved manipulability. Furthermore, this measure is also configuration dependent.

Condition Number

Condition number is the ratio between maximum singular value (σ_{max}) and minimum singular value (σ_{min}) [see equation 2.6].

$$ConditionNumber = \frac{\sigma_{max}}{\sigma_{min}} \tag{2.6}$$

If the condition number is equal to one or close to one, the system is said to be well conditioned and its manipulability is very high. If the condition number is very high (close infinity) manipulability of the manipulator is lost and it is in singular state. Since singular values are calculated using translational velocity Jacobian, condition number too depends on the joint configuration of manipulator.

Manipulability Ellipsoids

Manipulability ellipsoid for a given joint configuration is the graphical representation of the manipulation of the manipulator. The volume of the ellipsoid is equal to the manipulability index value of the given configuration. Furthermore, manipulability ellipsoid depicts the directions of the velocities which the manipulator can achieve. If the manipulability ellipsoid becomes an ellipse for a given joint configuration manipulator said to be in a singular state and the directional velocity profile is limited to 2D planar velocity.

2.5 Shoulder orthoses/exoskeletons

Orthosis is an orthopedic appliance or apparatus used to support, align, prevent, or correct deformities or to improve function of movable parts of the body [28]. Depending on their tasks orthoses can be categorized into two categories: devices that are made to align the end effector with the user (category 1) and devices that have been made to mechanically align its joints with the joints of the user [5] (exoskeletons). However, developing an orthosis with the capability to cope up with the complicated structure of the human upper limb is still a widely researched area to the present [29–31].

2.5.1 Recent shoulder orthoses/exoskeleton designs

Assistive robots can be categorized in to several categories [5]. Classification of upper limb orthosis is shown in Figure 2.6. However, the upper limb orthoses can be classified further by considering their area of application. In this research a shoulder orthosis is going to be incorporated with the trans-humeral prosthesis. Therefore, exoskeletons which have the assistive design structures are discussed

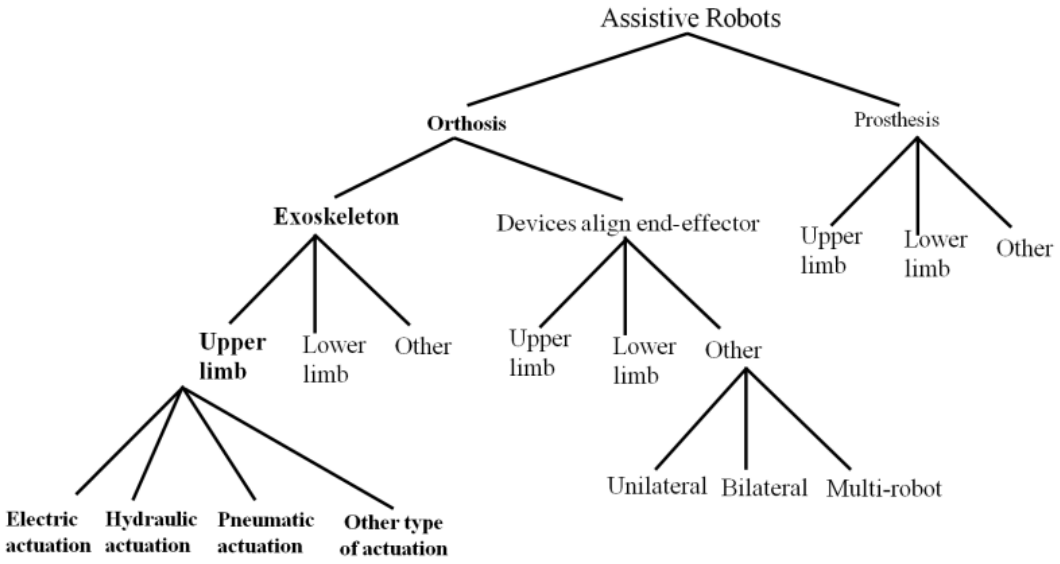

Figure 2.6: Classification of upper limb orthoses [5]

under this section. Furthermore, the focus of this section is directed only to electrically powered shoulder orthoses/exoskeletons. Since the ortho-prosthesis should be a portable and a design with desirable weight to the user, pneumatically and hydraulically powered designs are omitted from this section. Since, adding such configuration can result in a heavy design, only the electrically powered designs are discussed here. In order to prove that fact and considering the uniqueness of the design of the shoulder orthosis, [32] is discussed under this section. Even though though few shoulder orthosis designs can be found in literature [33, 34] most of the designs are dated bect to past ten years. However, those designs are still being used as a base for developing sophisticated controlling algorithms in order to improve the HRI (eg. [35, 36]).

Cable Driven ARm EXoskeleton (CAREX) [37, 38]

This device contains cuffs around the joints of human upper limb which are driven by the power transmitted from the motors. Instead of having a exoskeleton with serial link mechanism, this device focuses on each joint motion. It is designed for robot-aided rehabilitation. With three cable driven cuffs, CAREX has the ability assist the human motions from shoulder to to forearm in all directions. [see Figure 2.7 (a)]

SUEFUL-7 [39]

SUEFUL-7 was developed by Saga University, Japan. With 7DoF powered motions it can assist 7DoF human upper limb motions. The 7DoF consists shoulder vertical and horizontal F/E, shoulder I/E rotation, elbow F/E, forearm S/P, wrist U/R deviation and wrist F/E. In order to give the portability to the exoskeleton it is mounted to a wheel chair. Furthermore, SUEFUL-7 has the ability to train motions for 7DoF separately or simultaneously. [see Figure 2.7 (b)]

Cable-Actuated Dexterous Exoskeleton for Neurorehabilitation (CADEN)-7 [30]

CADEN-7 is an exoskeleton developed for neurorehabilitation purposes. It has the capability to enable full glenohumeral, elbow, and wrist joint functionality. Motors of the exoskeleton are located in a separate place. Cables and pulleys are used to transmit the power generated from the motors to exoskeleton motions. CADEN - 7 can be used as a haptic device with in a virtual reality simulation and a master device for tele-operation. [see Figure 2.7 (c)]

ARMin III [40]

This device has an exoskeleton structure that enables the training of ADL. ARmin III is capable of providing 3DoF motions assist to shoulder. 3 DoF motions are shoulder F/E, shoulder Abd/Add and shoulder I/E rotation. Apart from that it contains 1 DoF at forearm and wrist enabling forearm S/P and wrist F/E. ARmin III has the adaptability according to different human anthropometries. Vertical translation capability of the robot gives the platform for exoskeleton to perform dexterous motions. [see Figure 2.7 (d)]

L-EXOS [41, 45]

L-EXOS (Light Exoskeleton) [12] is an exoskeleton based haptic interface for the human arm. This exoskeleton introduced user a mechanism to insert and remove the arm easily excluding the conventional closed ring structure. It is capable of assisting 3DoF shoulder motions: shoulder horizontal and vertical F/E and shoulder I/E rotation, and elbow F/E. In order to transmit the power from the motors L-EXOS has used a tendon driven mechanism. [see Figure 2.7 (e)]

Portable haptic arm exoskeleton [42]

The exoskeleton provides shoulder F/E, shoulder Abd/Add, shoulder I/E rotation, elbow F/E, forearm S/P, wrist F/E and wrist U/R deviation. However, this exoskeleton is designed for the tele-operation purposes. It is a prototype of a master device used for tele-operation of future International Space Station (ISS). [see Figure 2.7 (f)]

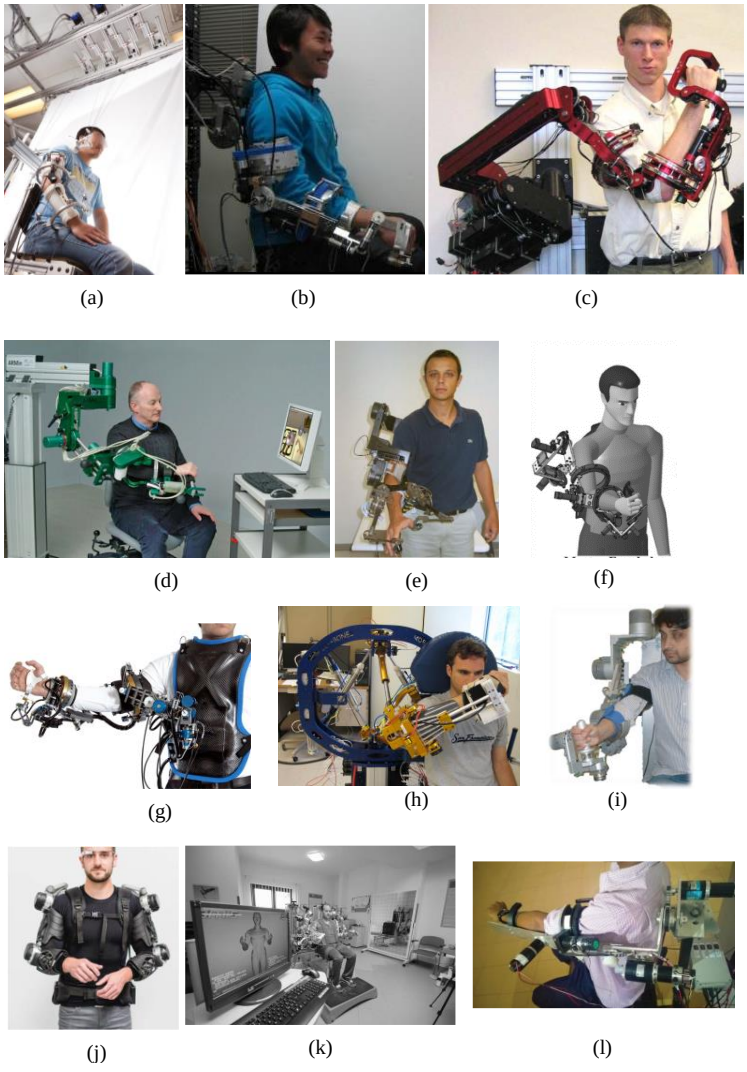

Figure 2.7: Recently Developed shoulder orthoses/exoskeletons: (a) CAREX [37] (b) SUEFUL-7 (c) CADEN-7 [30] (d) ARMin III [40] (e) L-EXOS [41] (f) Portable haptic arm exoskeleton [42] (g) X-Arm-2 [43] (h) BONES [32] (i) ETS-MARSE [44] (j) Stuttgart Exo-Jacket [33] (k) Automatic Recovery Arm Motility Integrated System (ARAMIS) [36] (l) 4DoF Exo-skeleton Robot [34]

X-Arm-2 [43]

This exoskeleton robot has been built to allow bilateral control of anthropomorphic space robots with force-feedback. It has 14DoF motions containing 6DoF passive DoF and 8DoF active DoF. Passive DoF are introduced in the design to reduce the misalignments occurred between joints of the exoskeleton and the human upper limb joints. In this exoskeleton, Bowden cables are used to transmit the power from the motors to the joints. [see Figure 2.7 (g)]

Biomimetic orthosis for the neurorehabilitation of the elbow and shoulder (BONES) [32]

The BONES is a pneumatically actuated shoulder orthosis. It has replaced the conventional circular bearing mechanism of the shoulder orthoses for shoulder I/E rotation with rotating a mechanism enabled by a pneumatic actuator arrangement. Four, mechanically grounded pneumatic actuators are placed behind the main structural frame to control shoulder motion via the sliding rods, and a fifth cylinder is located on the structure to control elbow F/E. [see Figure 2.7 (h)]

ETS-MARSE [44]

ETS-MARSE is a electrically powered 7DoF upper limb exoskeleton. It is capable of assisting 3DoF motions at the shoulder (shoulder vertical and horizontal F/E and I/E rotation), 1DoF at elbow (Elbow F/E), 1DoF at forearm (forearm S/P) and 2DoF at the wrist (wrist F/E and U/R deviation). This exoskeleton has used Harmonic Drive gear boxes forthe power transmission from motors to the exoskeleton. [see Figure 2.7 (i)]

Stuttgart Exo-Jacket [33]

The Stuttgart Exo-Jacket is an upper body exoskeleton designed at Fraunhofer IPA. It is designed to achieve 3DoF motions namely shoulder Abd/Add, shoulder vertical F/E and elbow F/E. The drives are constructed modularly and can be enhanced and replaced according to the requirements of a particular task. With a compact arrangement of the exoskeleton, the joints are supported with flat high power density EC-motors combined with flat Harmonic Drive gearing. [see Figure 2.7 (j)]

Automatic Recovery Arm Motility Integrated System (ARAMIS) [35, 36]

ARAMIS system is a robotic platform featuring a couple of fully-motorized 6 DOF symmetric exoskeletons. It can support all 4DoF of the shoulder while supporting 1DoF motion each at elbow and forearm. In the exoskeleton EC motors, have used to power up the joint motions and gear drives have used to transmit the power from motors to the joints.[see Figure 2.7 (k)]

4DoF Exo-skeleton Robot [34]

This exoskeleton is developed by the bionics laboratory of University of Moratuwa. It consists of 4DoF motions namely shoulder vertical and horizontal F/E, shoulder Abd/Add and shoulder I/E rotation. With a combination of belt drive and gear drives mechanism power is transmitted to three powered joint motions. Horizontal F/E of the exoskeleton is kept as a passive DoF. [see Figure 2.7 (l)]

2.5.2 Degrees of Freedom of shoulder orthoses/ exoskeletons

Shoulder orthoses interacts with the human as a external device. Since the upper limb has a complicated kinematic structure, the number of DoF of the device is crucial in the context of Human Robot Interaction (HRI). As mentioned in the subsection 2.3.1, human shoulder is built to perform class of task of four. However, shoulder motions involve more than four DoF motions to achieve the mentioned class of task.

In literature, upper limb exoskeletons can be found where the motions of upper limb is considered as a whole but not as motions of individual sections (i.e. shoulder complex). For these exoskeletons, the class of task of the shoulder is not important but the class of task of the whole upper limb. Therefore, it can be seen that the exoskeletons available in the literature possess less than or equal to 4 DoF motions for the shoulder [32–34, 36, 41, 42, 44, 46] in most instances [see Table 2.4]. Thus, they lack the redundancy (refer section 2.3) required for the human like motion generation. Furthermore, exoskeletons which enable all 4 motions of the shoulder are rarely found in the literature [30, 35, 40, 43]. Moreover, they do not include compound motion of several joints for the shoulder motions. Hence, they stay far back from generating human like motions.

Table 2.4: Comparison of existing shoulder orthoses

Reference	Location of Application	DoF	Actuator	Power Transmission	Presence of redundancy
CAREX [30]	Shoulder & Elbow	5	DC Motors	Cable Drives	N/A
SUEFUL-7 [39]	Shoulder,Elbow, Forearm & Wrist	7	DC Servo Motors	Cable & Gear Drives	No
L-EXOS [41, 45]	Shoulder & Elbow	5	Frameless DC permanent magnet torque motors	Tendon drive	No
ARmin III [40]	Shoulder & Elbow	6	DC Motors	Cable & gear drives & linkage	Yes
CADEN-7 [37, 38]	Shoulder,Elbow, Forearm & Wrist	7	Brushed Motors	Cable drives	Yes
Portable haptic arm exoskeleton [42]	Shoulder,Forearm, Elbow & Wrist	7	DC Motors	Gear drives	No
X-Arm-2 [43]	Shoulder, Elbow, Forearm & Wrist	7	Motors	Tendons	Yes
BONES [32]	Shoulder Elbow & Wrist	6	Pneumatic Actuators	Pneumatic Lines	No
ETS-MASRE [44]	Shoulder Elbow & Wrist	7	DC Motors	Gear Drives	No
Stuttgart Exo-Jacket [33]	Shoulder & Elbow	3	EC Motors	Gear Drives	No
ARAMIS [35, 36]	Shoulder, Elbow & forearm	6	EC Motors	Gear Drives	No
4 DOF Exoskeleton [34] Robot	Shoulder, Elbow & Forearm	4	DC Motors	Gear Drives & Belt Drives	No

2.6 Trans-humeral prostheses

Trans-humeral prostheses are developed to replace the missing limb due to trans-humeral amputation. Since, this research work uses an existing active trans-humeral prosthesis this section is focused on the facts which shaped this research work towards the motivation. Furthermore, the details of the trans-humeral prosthesis used for the final design is discussed extensively in section 3.5 and it is omitted from this section. Even though there are recent developments for trans-humeral prostheses [11], very few trans-humeral prostheses can be found in the literature. Hence, the upper limb designs which are designed to replace the whole upper limb with the prosthesis, are also included into this section [47].

2.6.1 Recent trans-humeral prosthesis designs

Trans-humeral prostheses can be devided in to three categories namely cosmeses, body powered prostheses and externally powered prostheses. Cosmeses are worn to replace the missing limb and are worn only for cosmetic purposes. Externally powered prostheses use an external power source to power up the prosthesis to move its components so that the prosthesis can perform missing motions. Body powered or passive prostheses can also perform motions but they acquire the required power form the wearer's body motions. These type of prostheses do not poses motors because there are no powered DoF (active DoF) in the prosthesis. This section discusses the details of the design aspects of the recently developed trans-humeral prostheses.

Dean Kamens Luke Arm (DEKA Arm) [47, 48, 51]

This is a modular type prosthesis which can replace the lost arm from shoulder to hand. It has 10 powered DoF at its full configuration with powered shoulder, humeral rotator, and wrist flexor with ulnar/radial deviation. It has the ability

to move multiple powered DoF at the same time and has the pre-programmed grips using four individually controlled DoF. At its trans-humeral configuration, straps around shoulder, chest and stomach have used to fix the prosthesis to the stump arm. [see Figure 2.8 (a)]

(a)

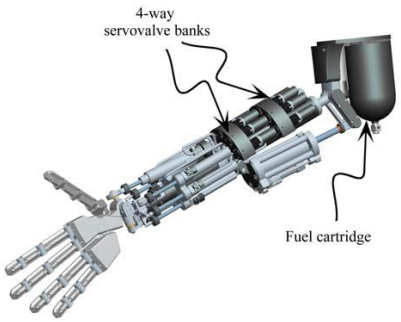

(b)

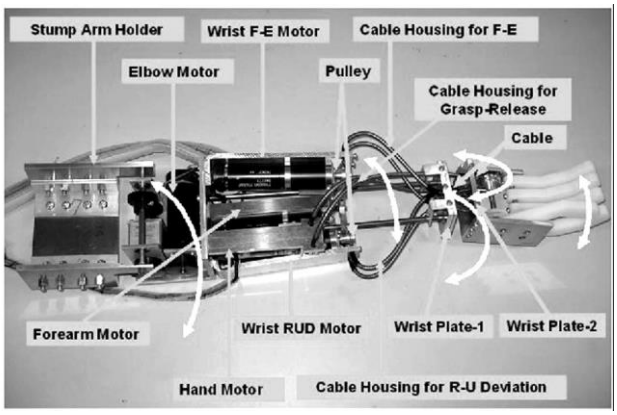

(c)

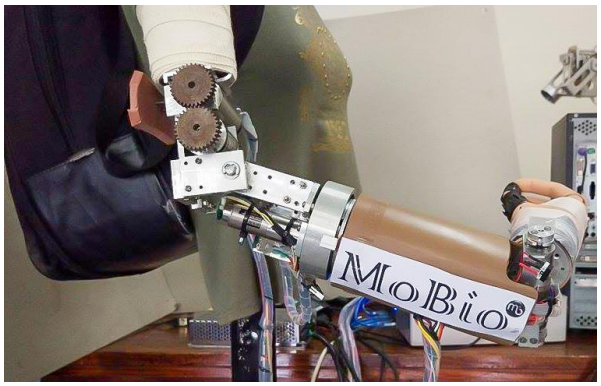

(e)

Figure 2.8: Existing trans-humeral prostheses: (a) DEKA Arm [48] (b) Gas-Actuated Anthropometric Trans-humeral prosthesis [49] (c) Saga University prosthetic Arm [50] (d) MoBio

Gas-Actuated Anthropomorphic Trans-humeral Prosthesis [49, 52]

This trans-humeral prosthesis possesses 21DoF motions. In order to achieve that it has used 9 degrees of actuation of pneumatic actuators. Out of 21 DoF 17 DoF are located in hand of the prosthesis. Power transmission to the hand is done through the cables. 5 degrees of actuation is allocated for the actuation of the hand. The fuel cartridge of the trans-humeral prosthesis, carries 200 mL of hydrogen peroxide, which provides 55 kJ based on 70% concentration. With anthropometric prosthesis design, projected weight of the prosthesis is 17.9N. It is expected to have 50% of force, power and energy of an anatomical human arm [see Figure 2.8 (b)].

Saga University Prosthetic Arm [50]

Saga University Prosthesis is a trans-humeral prosthesis which is capable of performing 5DoF motions, namely elbow F/E, forearm S/P, U/R deviation, wrist F/E and cylindrical grasp. Hand of the prosthesis is connected to the wrist via a ball joint. Two wrist motions are generated around the ball joint and cables are used to transmit the power from the motor to the joint [see Figure 2.8 (c)].

Proto-2 [53]

Proto-2 is a Defense Advanced Research Projects Agency (DARPA) funded project carried out by Applied Physics Laboratory of Johns Hopkins University. From elbow to the fingers, this prosthesis contains 25 DoF motions. However, the objectives of this projects are more directed towards making the amputee feel the sensations acquired from the prosthesis than designing a dexterous prosthesis.

2.6.2 Fixing trans-humeral prostheses to human body

Trans-humeral prosthesis is an external device which should be connected to the human body with carefully selected method. In order to perform compound motions generated from the stump motions and trans-humeral prostheses, they are fit to the stump arm directly. Further details about motion generation will be discussed under the sub section 2.6.5. The most popular method of fitting trans-humeral prostheses to the body is by means of sockets and straps. In this method a socket is made according to the dimensions of the stump arm of the amputee and it is fitted to the trans-humeral prosthesis. This socket will fit to the stump arm rigidly and would not come out easily [54–59]. However, it can be seen that these sockets come with straps to wind up around stump arm to ensure the firm fit between the stump arm and the prosthesis.

Another method to connect trans-humeral prostheses to body is connecting them through an osseo-integrated implant [60–67]. In this method, a metal implant is surgically connected to the humerus. This implant comes out from the stump arm providing a platform to connect the trans-humeral prosthesis through nuts [11] or other fastening method.

2.6.3 Load application by the prosthesis

In all the methods mentioned in subsection 2.6.2 trans-humeral prostheses are directly connected to the stump arm. Hence, the loads applied by the prosthesis directly go to the humerus [49, 52, 68–70]. Furthermore, these load application would extend towards the gleno-humeral joint through the humerus. Thus, the load of the prosthesis is applied on the shoulder joint.

2.6.4 Musculo-skeletal disorders vs trans-humeral prostheses

As deduced in subsection 2.6.3, loads of the trans-humeral prostheses are directly applied on the shoulder joint. However, the prolonged application of the loads by the trans-humeral prostheses on the stump arm, is proven unhealthy to human body [71]. It is common to have musculo-skeletal disorders among trans-humeral amputees due to the amputation [72, 73]. Due to the constraints provided by the prosthesis to the natural limb motion due to the load application of the trans-humeral prosthesis, musculo-skeletal disorders occurred. Therefore amputees find it is difficult to use the prosthesis anymore and often give up on using the prosthesis.

2.6.5 Effect of the stump arm motions toward the motion generation of trans-humeral prostheses

As mentioned in sections 2.1 and 2.2 human upper limb is complicated in its built and the kinematic structure. From a trans-humeral prosthesis it is expected to achieve the ADL with dexterously and effectively. In order to do that, the kinematic structure of the stump arm + trans-humeral prosthesis should match with the upper limb of the human. Since there is a combination of two kinematic structures: kinematic structure of the stump arm and the kinematic structure of the trans-humeral prosthesis, both sections should have the prefect kinematic capabilities in order to match with the human upper limb. As mentioned in previous subsection, the stump arm often meets with musculo-skeletal disorders after and due to the amputation. Due to that, stump arm motions are limited for small range of motions and in some case it is impossible to move. The kinematic chain of the trans-humeral prosthesis should begin from the shoulder join just like the human upper limb [see Figure 2.5]. When the stump arm motions are absent or they are limited to small range due to weak stump arm, the achievable ROM and orientations of the hand of the prosthesis will also be limited to some

ranges and sometimes it may cause the loss of whole DoF [74–77]. Therefore, it is important to have the full range of motions of the stump arm for the human like motion generation from the trans-humeral prosthesis.

Table 2.5 shows a comparison of the existing trans-humeral prostheses. It can be seen that the load application by the prosthesis is always on to the stump arm. If there is a musculo-skeletal disorder is with the stump arm or such thing has occurred due to prolonged use of the prosthesis, amputees should give up the prosthesis use. It is obvious that there must be a way to bear the loads of the prosthesis and to supply assistance to the stump arm while using the trans-humeral prosthesis. Without having that feature, prosthesis would not be able to generate human like motions and dexterous motions in the long run.

Table 2.5: Comparison of existing trans-humeral prostheses

Reference	**Fixing Area**	**DoF**	**Actuator**	**Power Transmission**	**Prosthesis load applied area**
DEKA Arm [47, 48, 51]	Between Shoulder & Elbow	18	DC Motors	Gear Drives	Stump arm
Gas-Actuated Trans-humeral Prosthesis [49, 52]	Elbow	21	Pneumatic Actuators	Pressurized Fluid	Stump Arm
Saga University Prosthesis [50]	Between Shoulder & Elbow	5	DC Motors	Gears & Cables	Stump Arm
MoBio [11]	Between Shoulder & Elbow	5	DC/EC Motors	Gears	Stump Arm
Proto-2 [53]	Between Shoulder & Elbow	25	DC Motors	Tendons	Stump Arm

2.7 Trans-humeral ortho-prostheses

there is **no** evidence in the literature for active upper limb ortho-prostheses. Even though the fact remains as such lower limb ortho-prostheses can be found in the literature.

2.7.1 Lower limb ortho-prostheses

Most of the lower limb ortho-prostheses are made for lengthening the lower limbs of the patients with disproportionate short stature due to achondroplasia [80][see Figure 2.9 (b)]. Moreover, the concept of lower limb ortho-prosthesis is used as a remedy for patients who are suffering from rotationplasty after a lower limb amputation or congenital disorder [81][see Figure 2.9 (a)]. All of the previously mentioned instances are for the cosmetic purposes.

(a) (b)

Figure 2.9: Lower limb ortho-prostheses for cosmetic purposes: (a) Lower limb ortho-prosthesis for patient with rotationplasty [78] (b) Lower limb ortho-prosthesis for patient with achondroplasia [79]

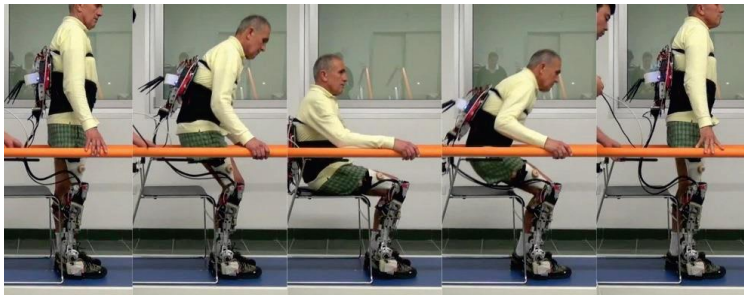

Figure 2.10: CYBERLEGs Beta-Prosthesis: An active lower limb ortho-prosthesis at work [15]

CYBERLEGs is a project launched to develop lower limb prostheses to replace missing lower limb while assisting the residual limb segment [15]. This project successfully developed ortho-prostheses and clinical trials are being carried out to date [see Figure 2.10]. It is the only available literature for an active lower limb orth-prosthesis.

As deduced in previous sections, stump arm of the trans-humeral amputees often meets with musculo-skeletal disorders. Even the healthy stump arms get diagnosed with musculo-skeletal disorders due to prolonged application of the loads by the prosthesis. It is evidently proved that a shoulder orthosis should be incorporated with the trans-humeral prostheses for the long term use of the prosthesis and for the human like motion generation. Since the concept of trans-humeral ortho-prosthesis has not been introduced, the need of a trans-humeral ortho-prosthesis is raised.

Chapter 3

MECHANICAL DESIGN OF THE TRANS-HUMERAL ORTHO-PROSTHESIS

This chapter describes the steps involved towards the end of the design of the trans-humeral ortho-prosthesis. Since ortho-prosthesis is a combination of orthosis and prosthesis, orthosis and prosthesis designs (for prosthesis its the existing trans-humeral prosthesis) were developed separately before developing the design of the proposed trans-humeral ortho-prosthesis [see section 3.2 and section 3.5]. When combining both proposed 6DoF orthosis and MoBio, some minor modifications had to be carried in to the design of MoBio.

The proposed trans-humeral ortho-prosthesis is designed for a right arm trans-humeral amputee [see Figure 3.1(a) and Figure 3.1(b)]. Since it is designed to replace the missing limb while assisting the stump arm, it can be divided into two main sections; orthosis and prosthesis [see Figure 3.1(c)]. Design of MoBio [11]is used as the prosthesis. In order to generate human like motions, ortho-prosthesis is designed with 9 DOF motions including 4 DOF in the orthosis section and 5 DOF in the prosthesis section.

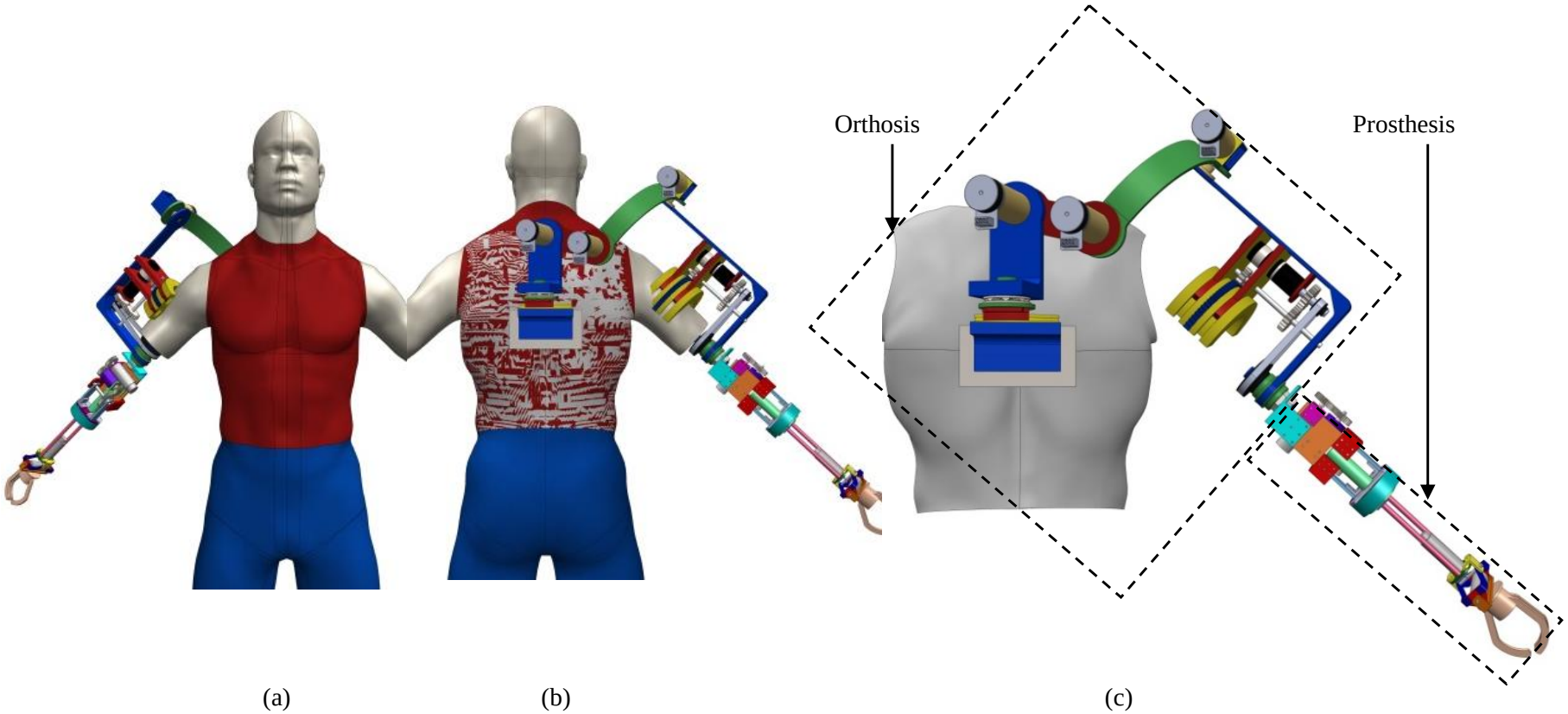

Figure 3.1: Proposed trans-humeral ortho-prosthesis (a) Front view of the amputee wearing the ortho-prosthesis (b) Rear view of the amputee wearing the ortho-prosthesis (c) Rear view of the proposed ortho-prosthesis

3.1 Design specifications

The proposed trans-humeral ortho-prosthesis is designed to enable the lost functions of the upper limb due to the amputation. The main design consideration for MoBio is that it should be able to perform ADL. For this purpose few activities were selected as the benchmarks. One of the most common ADL is the pick and place task. Here the object that is going to pick and place from MoBio should have a maximum weight of 300g. Furthermore, force applied by the hand of the prosthesis on the object is limited to 1Nm in order to avoid crushing object. Furthermore, the whole prosthesis is designed to have weight of 3.2kg which is similar to the weight of the same section of a grown human.

The orthosis of the proposed trans-humeral ortho-prosthesis is designed on the basis of that there is a prosthesis of weight of 3.2kg+300g (weight of the object) is attached to it. Furthermore, the orthosis section should not limit the motions of the prosthesis with its design constraints. Hence, the proposed ortho-prosthesis has the ability to achieve the same ROMs as the human upper limb [see Table 2.1and Table 2.2]. Moreover, the designed orthosis has the capability to assist a healthy stump arm for 5% in its general torque requirements.

3.2 Design of the shoulder orthosis

Shoulder orthoses are often made to power assist the given tasks: shoulder vertical F/E, shoulder horizontal F/E, shoulder Abd/Add and I/E rotation of the humerus section. Therefore, the existing shoulder orthoses are designed as 4DoF manipulators. However, the design concept often meets singular configurations constraining the natural upper limb motions [82]. Redundant manipulators can be used to eliminate the singular configurations of the robots. Since the redundant manipulators are capable of achieving the same point with different configurations, this concept can be brought into shoulder orthoses. Constraints to the natural motions of the shoulder by the shoulder orthosis mainly occurs because they are focused on the class of tasks [24] of the orthosis and are not designed to mimic the natural motions. A redundant shoulder othosis reduces the constraints to the natural limb motions while enabling dexterous motions [83]. Moreover, it can facilitate the ability to adapt according to the different shoulder anthropometry.

Orthosis is designed to perform shoulder vertical F/E, shoulder horizontal F/E, shoulder Abd/Add and I/E rotation. Excluding shoulder horizontal F/E all other orthosis motions are designed to power assist the amputee. Considering the rare usage of the shoulder horizontal F/E during ADL compared to other three shoulder motions [84], the motion is kept as a passive DOF motion. This design aspect provides the opportunity to compensate the misalignments of the joints between the ortho-prosthesis and the amputee due to the scapula motions.

In order to mount the ortho-prosthesis and to keep its portability, a back brace [see Figure 3.2] is added to the design. Back brace is attached to the back of the amputee. In order to make sure the successful attachment of the back brace, straps are introduced to it. Furthermore, it consists of back stage [see Figure 3.2] which provides the platform to mount the parts of the ortho-prosthesis.

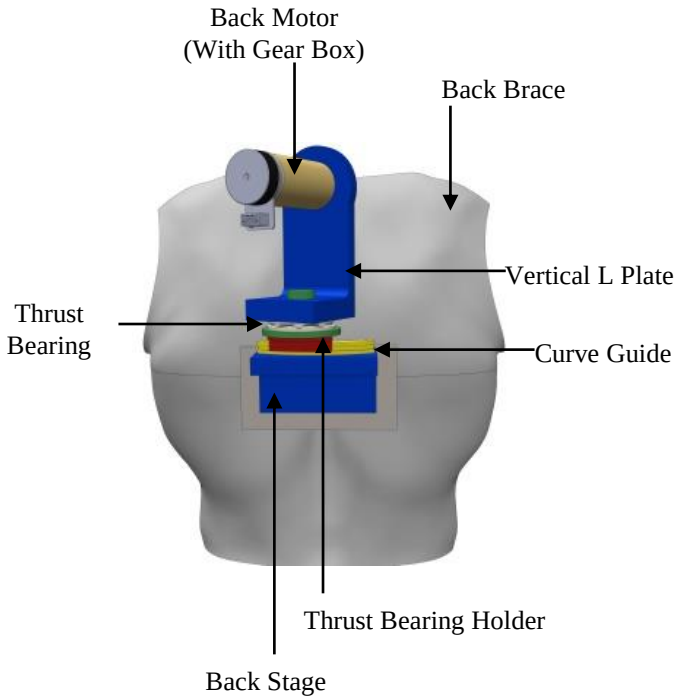

Figure 3.2: Components required for horizontal F/E

On top of the back stage, a curve guide (HCR12A+60/100R, THK) is mounted [see Figure 3.2]. The curve guide has been introduced to the design to facilitate the passive DOF. Thrust Bearing Holder [see Figure 3.2] is rigidly fit on top of the slider of the curve guide. To minimize the radial movements of the Thrust Bearing (Roller thrust bearing, NSK) and the Vertical L Plate [see Figure 3.2], Thrust Bearing Holder is designed with a shaft. Vertical L Plate is tight fit on top thrust bearing so that the L plate can rotate around the thrust bearing axis while moving along with the curve guide slider as a whole unit.

To generate the motions of the orthosis section (except I/E rotation) 4 links (including vertical L plate) are connected serially through motor shafts, ball bearings, gears and flanges. Back motor (with gear box) (EC 45 flat, Maxon Motors) is fixed to the vertical L plate so that the motor shaft would go through a ball bearing [see Figure 3.2 and Figure 3.3]. Through this design aspect, it is expected to minimize the load applied on the motor shaft. A flange is rigidly attached to the Abd/Add flat plate [see Figure 3.3]. Back Motor gear box shaft goes through

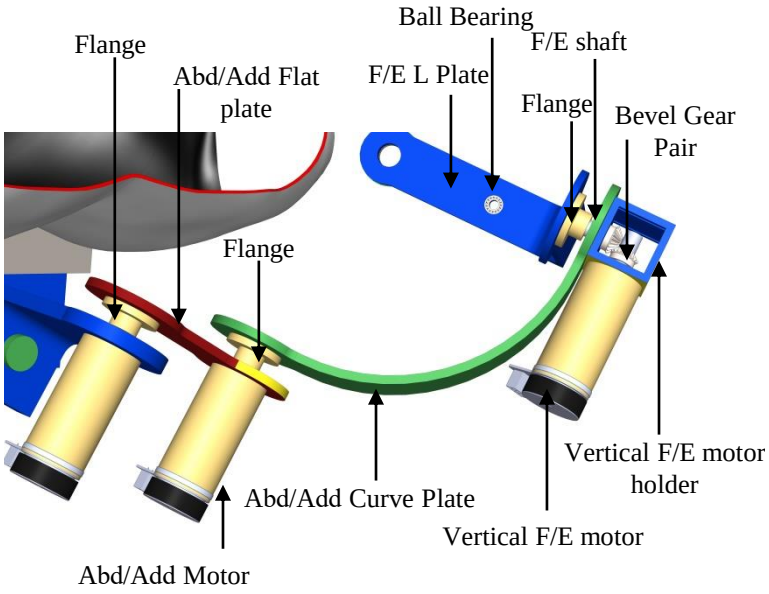

Figure 3.3: Components required for vertical F/E and Abd/Add

the other end of the flange so that the rotary motion generated by the Back Motor will be transmitted to the Abd/Add flat plate. Same mechanism is used to transmit the Abd/Add motor power to Abd/Add curve plate [see Figure 3.3]. Furthermore, motions of the vertical L plate, Abd/Add Flat plate and Abd/Add curve plate generate the shoulder Horizontal F/E and Abd/Add. Vertical F/E motor holder is rigidly attached to the other end of the Abd/Add curve Plate. Since the Vertical F/E Motor is fixed to the Vertical F/E Motor Holder, this design aspect enables compound motion of the Abd/Add curve plate, Vertical F/E Motor Holder and Vertical F/E Motor as one unit [see Figure 3.3].

A bevel gear is connected to the Vertical F/E motor gear box shaft inside the Vertical F/E motor holder. In order to transmit the Vertical F/E motor power to F/E L plate through a flange and F/E shaft, another bevel gear is paired with this bevel gear [see Figure 3.3]. Moreover, the F/E shaft is mounted through a ball bearing. The motion of the F/E L plate generates the Vertical F/E of the shoulder [see Figure 3.3]. Two I/E Rotator Holders and the I/E Rotation Motor Holder are connected to the F/E L plate by means of screws. I/E rotation motor is mounted to the I/E Rotation Motor Holder so that the back end of it would

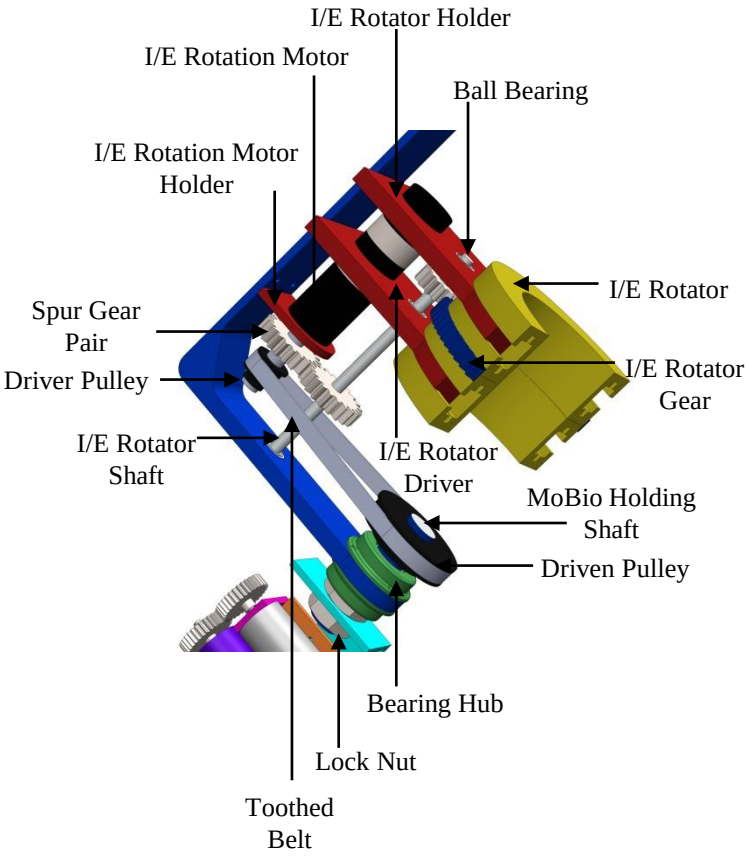

Figure 3.4: Components required for I/E rotation

go through the I/E rotator holders [see Figure 3.4]. I/E Rotator is mounted on the I/E rotator holders. It is designed to make though 3D printing method [9]. Furthermore, it can travel around the rails of the I/E the amputees stump arm by means of the straps. The I/E Rotator gear which is rigidly fixed on to the I/E rotator, is driven by the I/E Rotator Driver [see Figure 3.4].

In order to transmit the I/E Rotation Motor power to the I/E rotator, a gear mechanism is used. When the I/E rotation Motor shaft starts to rotate, spur gear pair transmits motor power to the I/E rotator shaft [see Figure 3.4]. Moreover, I/E rotator shaft goes through three ball bearings located at F/E L plate and I/E Rotator holder [see Figure 3.3 and Figure 3.4] to ensure its smooth rotation. Since I/E Rotator driver is mounted on the I/E Rotator shaft, the motor power is transmitted from the spur gear pair to I/E rotator driver to drive the I/E rotator gear; thus I/E rotation of the stump arm is achieved.

Table 3.1: Specifications of Motors

Actuator name	**Max: Continuous Torque Output (Nm)**	**Associated Motion**
EC45 Flat, Maxon motors (with gear box (91:1))	15	Shoulder vertical F/E Shoulder Abd/Add Shoulder Abd/Add
RH-8-6006-E50DO, Harmonic drive systems	2.7	Shoulder I/E rotation

Considering the facts that there is a prosthesis with 3.2kg attached to the orthosis and serial link chain would cause different torque requirements on the joints, motors and gear boxes were selected [see Table 3.1]. Since shoulder vertical F/E and shoulder Abd/Add requires high joint torques than the torque required for the shoulder I/E rotation, brush less motors with high torque outputs have selected for these motions.

3.2.1 Motion generation of the proposed redundant orthosis

Kinematic structure of the orthosis is very important in the context of facilitating the natural limb motions of the stump arm of the amputee. Human shoulder motions are generated as combined motions of clavicle, scapula and

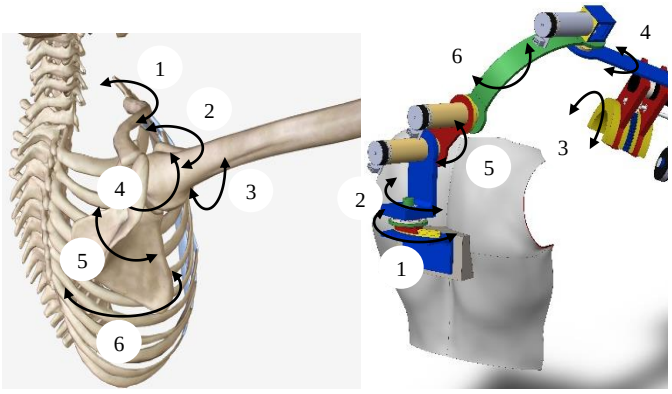

Figure 3.5: Redundant 6DoF shoudler orthosis: (a) Motions of the bones of the human shoulder during the shoulder motions (b) Motions of the links of the novel 6DoF shoulder orthosis of the trans-humeral ortho-prosthesis

gleno-humeral [85]. Since gleno-humeral joint is a spherical joint it can generate motions in infinite directions. Considering the usage in activities of daily living, the motions of the shoulder in the principle planes of the body: sagittal, transverse and coronal, along with the I/E rotation of the shoulder, shoulder orthoses are considered as manipulators for class of task of 4 [24]. Even though the fact remains as such, more than 4DoF motions are involved in the human body to achieve this task. If class of task is less than the DoF available for the task, then it is said to be a redundant manipulator. Therefore, human shoulder complex itself is a redundant manipulator.

Currently available shoulder orthoses have failed to match this redundancy of the shoulder [34, 86, 87]. It has lead to the constraints of the shoulder orthosis in natural limb motions. The proposed shoulder orthosis has 6 DoF to achieve the shoulder vertical F/E, shoulder horizontal F/E, shoulder Abd/Add and I/E rotation of the stump arm. Figure 3.5(a) dispalys the bone motions involvement in the shoulder motions discussed above. Here, **1** shows the clavicle motion during the shoulder motions. **5,6** and **2-4** depict the scapula motions and gleno-humeral joint motions respectively. Figure 3.5(b) depicts the link motions of proposed shoulder orthosis mechanism of the trans-humeral ortho-prosthesis. **1** and **2** motions are kept as passive motions. This mechanism can compensate the misalignments cause by the scapula and clavicle motions of the human shoulder motions [see Figure 3.5(a) **1** and **6**]. Serial link mechanism [see Figure 3.5(b) **5, 6** and **4**] has introduced to the orthosis to match the scapulohumeral rhythm [88] of the human shoulder motion [see Figure 3.5(a) **5** and **4**]. **3** of both Figure 3.5(a) and (b) depicts the shoulder I/E rotation and it is kinematically pretty much the same for both human shoulder and the novel shoulder mechanism. It is evident that none of the shoulder motions are done with one link motion involvement. For each and every task at least two bone motions are involved. Thus, addition of passive DoF [see Figure 3.5(b) **1** and **2**] gives the flexibility of the orthosis required to match the scapula and clavicle motions while providing a platform to orthosis to keep up with inherent redundancy of the human shoulder.

3.3 Major changes added to shoulder orthosis from initial design

Figure 3.6 shows the key areas where the major changes were added to the shoulder orthosis to build the final shoulder orthosis design. In Figure 3.6 (b), the major change 1 depicts the modification added to the I/E rotator. In the final design of shoulder orthosis, I/E rotator consists of two sliders where as the initial design has only one slider. This design feature was added to improve the stability of the I/E rotator during the motion generation and to improve the effectiveness of the power transmission of the motor to the I/E rotator.

It can be seen that the F/E L plate of the final design extends up to the point where both orthosis and prosthesis connects with each other, replacing the mechanism of fixing the prosthesis directly to the I/E rotator in the initial design

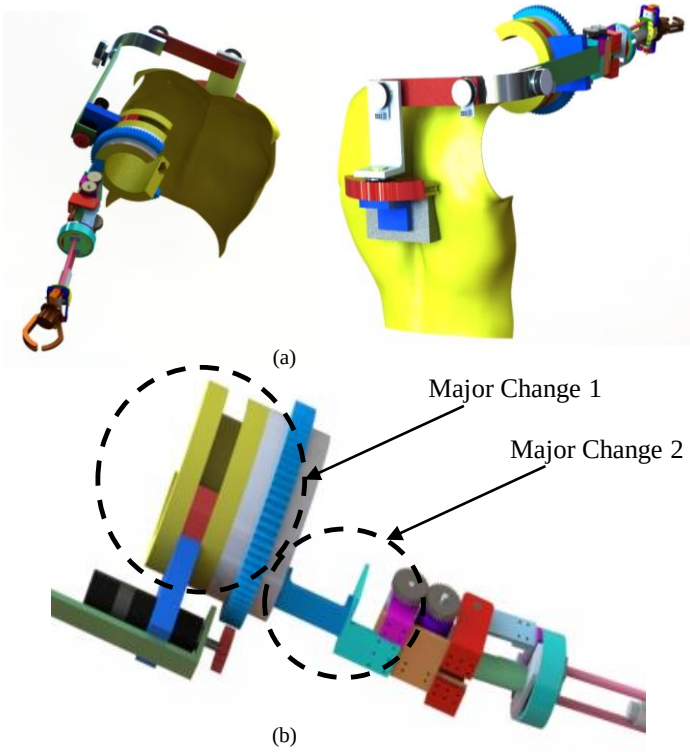

Figure 3.6: Major changes added to the shoulder orthosis: (a) Initial design of the trans-humeral ortho-prosthesis (b) Modified areas of the shoulder orthosis in the final design

[see Figure 3.6 (b)- Major Change 2]. This design modification has been added to eliminate the buckling of the I/E rotator due to the direct application of the loads on the I/E rotator by the prosthesis.

Due to these two modifications, power transmission mechanism of the final design of shoulder orthosis is completely different from the initial design. In order to transmit the power of I/E rotation Motor to the I/E rotator, two gear couples mounted at different levels are used. Furthermore, I/E rotation shaft is used to mount the gears and to act as the common gear shaft for the gear mechanism. Moreover, a belt drive mechanism has been used to transmit the power from the I/E rotation motor to the prosthesis, in the final design.

3.4 Rationale behind Passive DoF in the shoulder orthosis

In the proposed shoulder orthosis, shoulder horizontal F/E is generated as a passive DoF motion. The proposed ortho-prosthesis is designed for an amputee with a weak stump arm which has the motor functions for some extent. Hence, the stump arm has the ability to move the shoulder orthosis in the passive DoF direction.

As discussed in the previous sections [refer section 2.1] human upper limb has a complex kinematic structure with inherent redundancy. Due to its complexed kinematic structure it is important to have a close kinematic structure in shoulder orthosis to co-aligned with it. The main offsets of joints of the shoulder orthoses and the joints of the shoulder complex occur due to the motions of the clavicle and scapula. In the proposed shoulder orthosis [see Figure 3.5 (b)] **1,2** motions are kept as passive DoF motions to enable the shoulder horizontal F/E and to enable a platform to compensate the misalignments of the joints of the shoulder orthosis with the shoulder due to clavicle motion and motions of scapula motion in the transverse plane.

Furthermore, these two passive DoF motions can absorb the sudden accident motions and involuntary motions of the shoulder and provide the smooth flow of the motions of the shoulder orthosis.

3.5 Design of the trans-humeral prosthesis

The prosthesis [11] section includes 5DOF motions; Elbow F/E, Forearm supination/pronation, ulnar/radial deviation, wrist F/E and compound motion of thumb and first fingers. Attachment of the prosthesis to the orthosis in order to make the ortho-prosthesis should be carefully designed. MoBio [see Figure 3.7] is designed to attach to the stump by means of osseointegrated implant. This configuration tend to apply axial loads on the stump arm. Therefore, prosthesis rotation and I/E rotator rotation should be synchronized while distributing the vertical forces applied on the MoBio holding shaft among the ortho- prosthesis. In order to synchronize two rotation the motor power is transmitted to MoBio Holding Shaft by means of a Driven pulley, Driver Pulley and a toothed belt. Furthermore, the two pulleys have the same radius ratio same as the I/E rotator driver and I/E Rotator (1:6) [see Figure 3.4].

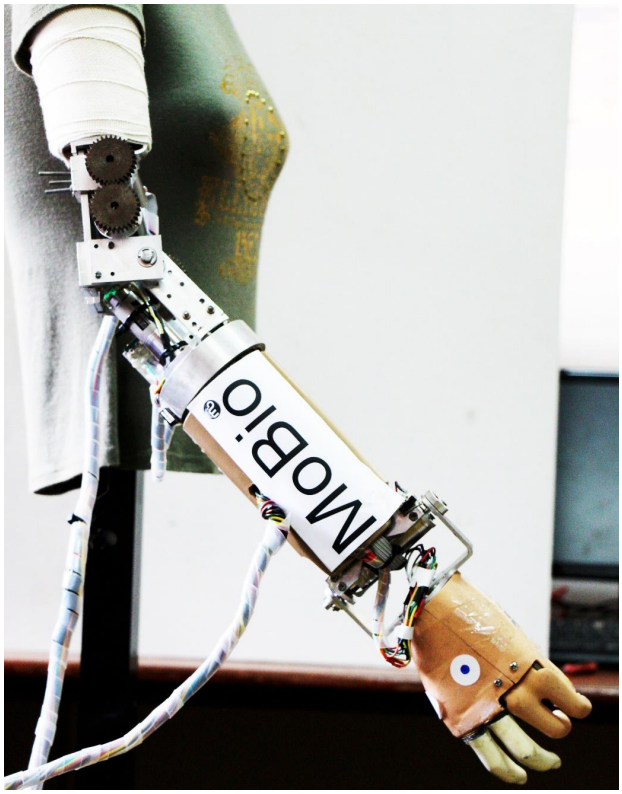

Figure 3.7: MoBio: The existing trans-humeral prosthesis

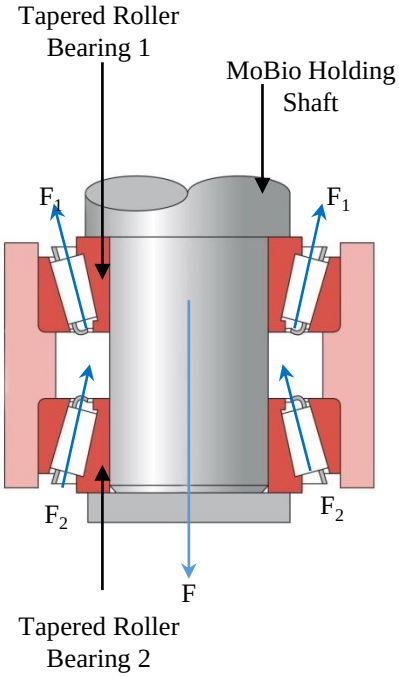

Figure 3.8: Simplified view of tapered roller bearings arrangement

To prevent MoBio Holding shaft from going downwards, the shaft section above the Driver Pulley which is mounted co-axially on the MoBio Holding Shaft, has a higher radius than the other section. The end section of the shaft is threaded so that MoBio can be mounted on the shaft by means of Lock Nuts. Furthermore, two tapered roller bearings are mounted in opposite directions to withstand the axial loads applied on the MoBio Holding shaft [see Figure 3.4 and Figure 3.8]. Two bearing hubs are introduced to ensure correct fixing of two bearings. In order to withstand the axial loads as well as the radial loads applied on the MoBio Holding Shaft while enabling the axial rotation, two tapered roller bearings have included into the design. Figure 3.8 shows how the vertically applied force (F) is compensated by two roller bearings. (With forces F_1 and F_2)

3.6 The prototype of the proposed trans-humeral ortho-prosthesis

Figure 3.9 shows the overview of the build of the proposed trans-humeral ortho-prosthesis. The prototype of the trans-humeral ortho-prosthesis [see Figure 3.10 and Figure 3.12] is developed for right arm trans-humeral amputees. It is fixed to the body of the amputee with a back brace attached to his/her body by means of straps around torso and collar bones (clavicle).

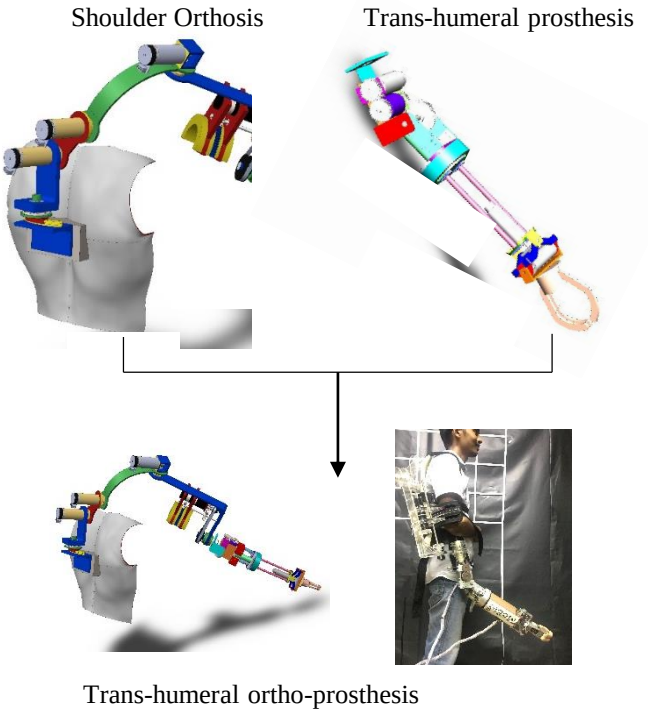

Figure 3.9: Overview of the trans-humeral ortho-prosthesis: Combination of 6DoF redundant orthosis and 5DoF trans-humeral prosthesis build the proposed trans-humeral ortho-prosthesis.

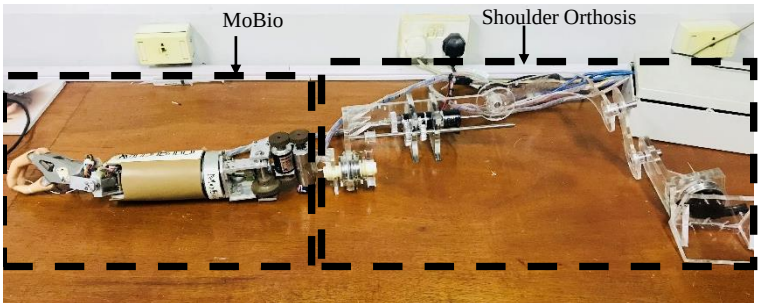

Figure 3.10: Fabricated prototype of the trans-humeral ortho-prosthesis

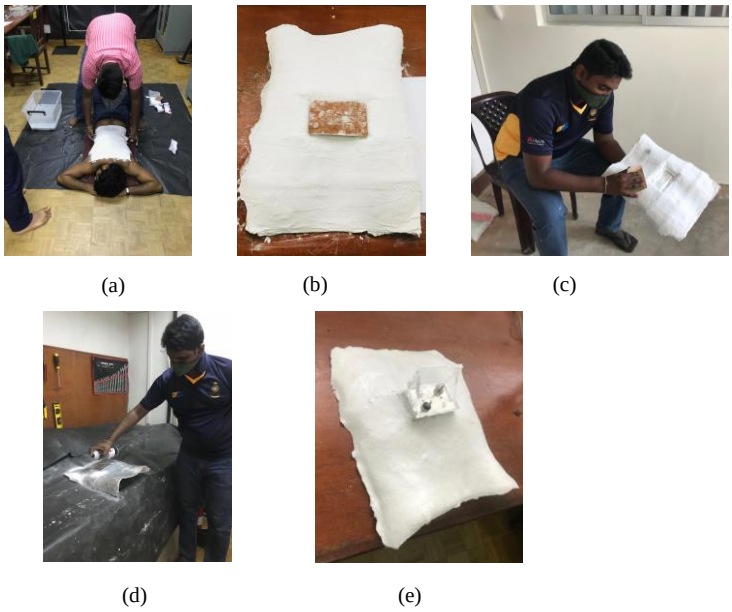

Figure 3.11: Steps of the fabrication of the back brace: (a) Mould (b) Fabricated plast-of-paris mould (c) Smoothening the mould surface (d) Painting the mould surface (d) Fabricated back brace

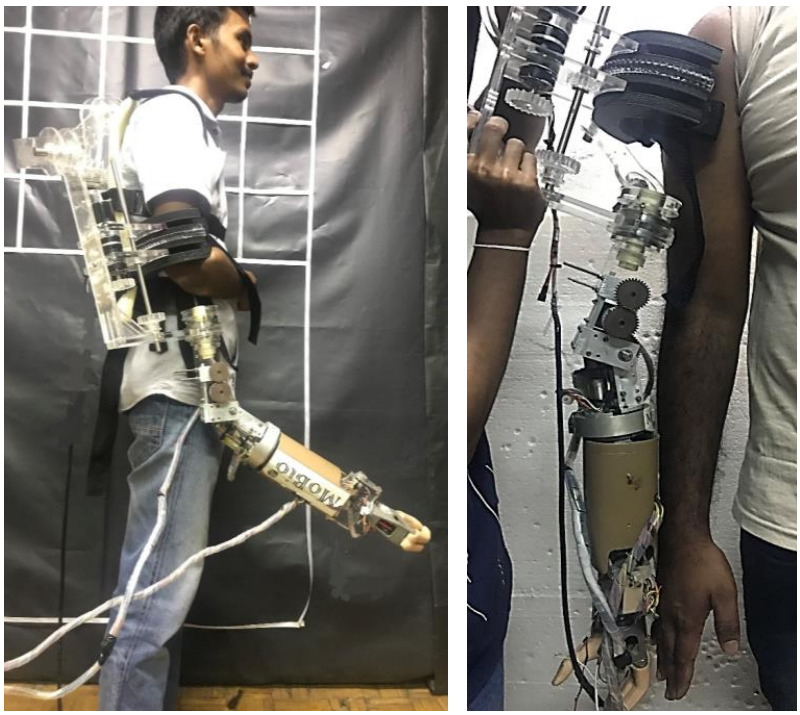

Figure 3.12: The test subject wearing the proposed trans-humeral ortho-prosthesis

In order to fabricate the links of the prototype of the trans-humeral ortho-prosthesis Acrylic was used. Furthermore, fiberglass was used to fabricate the back brace of the prototype. Figure 3.11 shows some steps involved in the making of back brace. Due to the toxicity of the glass fibre laying up process, laying up was done in a secluded environment and the photographs of that process could not be taken.

For the purpose of monitoring the ability to adapt according different human anthropometries and the ability to support human like motion, all the joints of the orthosis of the prototype was kept to enable passive DoF motions. Further details will be discussed in sub section 4.3.2.

Chapter 4

RESULTS

The proposed trans-humeral prosthesis is a combination of a 6DoF shoulder orthosis and a 5DoF trans-humeral prosthesis. Therefore, validation results were

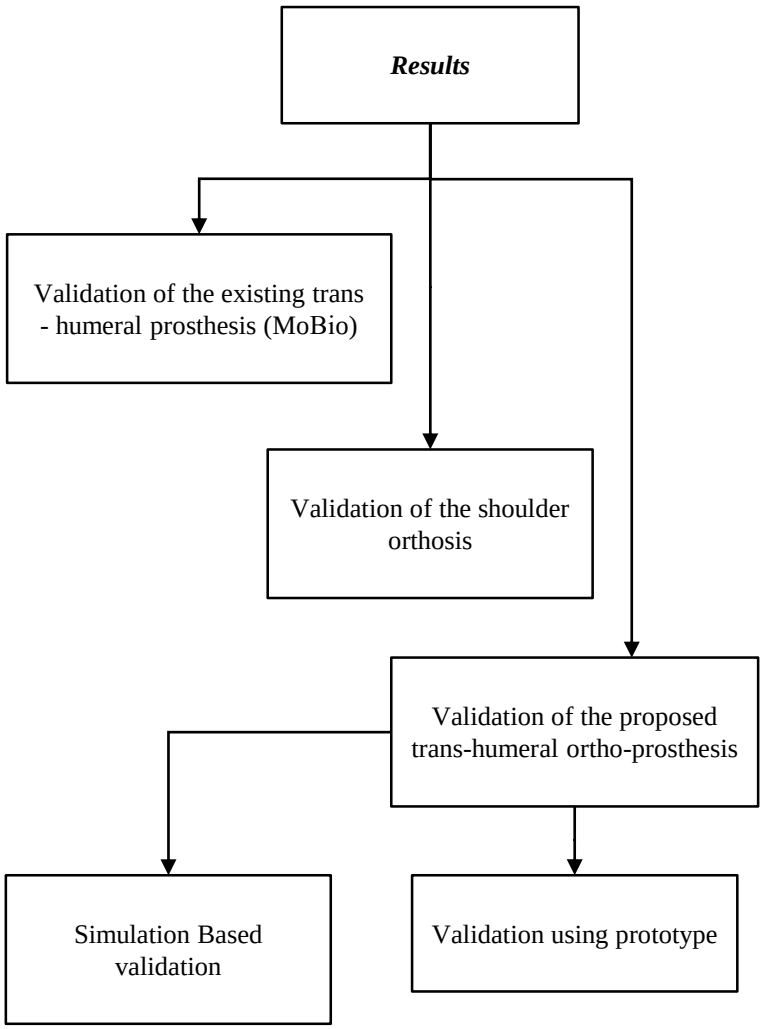

Figure 4.1: Categorization of results

carried out as 3 sections [see Figure 4.1]. First, the validation of the existing trans-humeral prosthesis was carried out for the fine tuning of the prosthesis. Then, the validation of the shoulder orthosis was carried out to evaluate its kinematic performance and durability of its critical parts. Finally validation of the whole trans-humeral ortho-prosthesis was carried out to evaluate its kinematic performances. Furthermore, a prototype of the proposed trans-humeral ortho-prosthesis was fabricated for the further evaluation of the design.

4.1 Validation of the existing trans-humeral prosthesis

Design of "MoBio" [11] was used as the design of the trans-humeral posthesis. MoBio was developed as a requirement for under graduate project of the Department of Mechanical Engineering, University of Moratuwa [see Figure 3.7].This trans-humeral prosthesis is designed to achieve 5DoF motions. They are elbow F/E, forearm S/P, U/R deviation, wrist F/E and compound motion of thumb finger and index finger. Controlling of the prosthesis is done using the EMG signals of the biceps and triceps of the stump arm. Controlling algorithm consists of a motion sequence [see Figure 4.2] where each of the five motions are shifted sequentially via a motion switcher. This controlling algorithm has the ability to skip the motions in the sequence if needed. Figure 4.2 shows how to skip two consecutive motions (U/R deviation and wrist F/E) in the motion sequence.

Even though the designing and manufacturing of MoBio was done already, the validation of the prosthesis had not been carried out. As a contribution from this research work, the validation of MoBio was carried out. Further details of the validation are discussed in the next section (4.1). Moreover, the design of the trans-humeral ortho-prosthesis was developed on the basis that MoBio is designed to attach the stump arm through osseointegrated implant [89] and has a weight of 3.2kg.

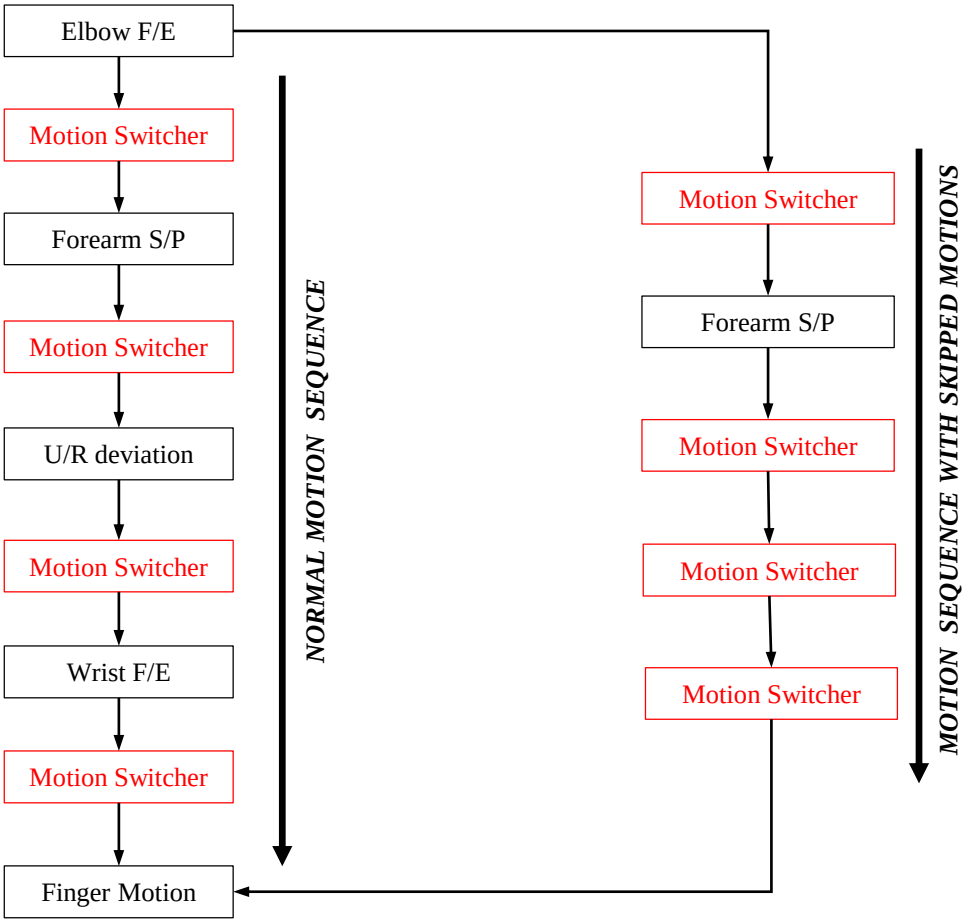

Figure 4.2: Summary of the motion sequence

4.1.1 Experimental setup

Experimental setup was consisted of MoBio, angle measuring device [see Figure 4.4], 3 microcontrollers (ATmega 2560, Atmel), BLDC motor controller (EPOS2, Maxon Motors), 3 H-bridges (L298), data acquisition (DAQ) card (6220, National Instruments), EMG extraction system (16 channel Bagnoli^{TM} desktop EMG system, DELSYS) [see Figure 4.5] and a personnel computer with MATLAB software. For the purpose of controlling the brushed DC motors of the prosthetic device H-bridges were used and EPOS2 motor controller was used for the controlling of the brush less DC motor. Summary of the experimental setup is shown in Figure 4.3

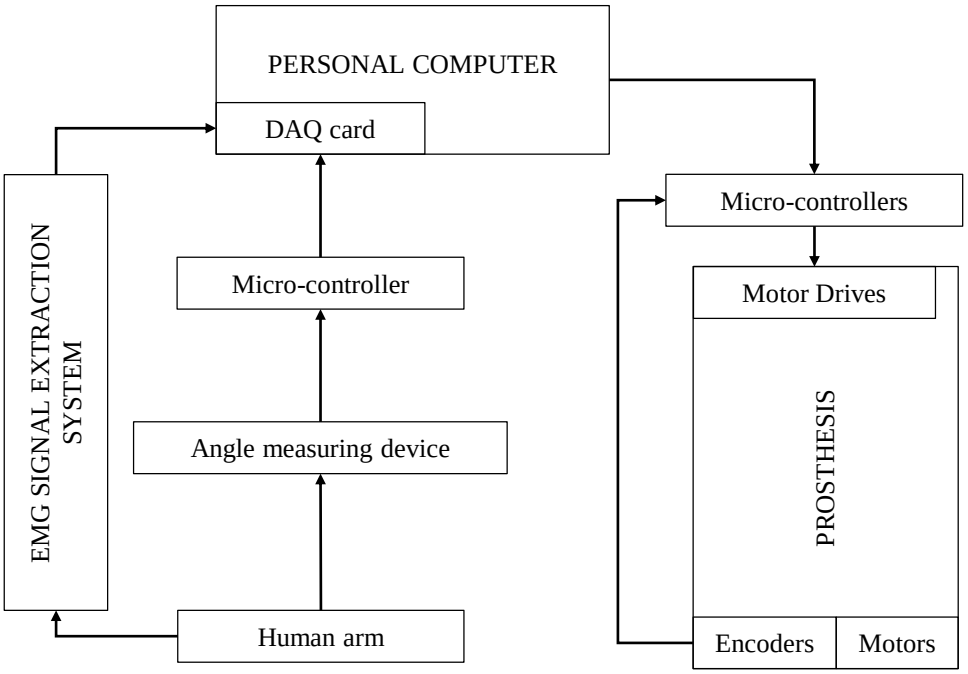

Figure 4.3: Summary of the experimental setup

Figure 4.4: Angle Measurement Device

The extracted EMG signals were sampled at frequency of 2000Hz and band pass filtered to 50Hz to 450Hz. The extracted signals were displayed in the PC monitor while the experiments were carried out.

4.1.2 Joint angle responses according to the PID controller

In order to evaluate the response of the joint motors of the trans-humeral prosthesis according to its Propotional-Integral-Derivative (PID) controllers, this experiment was carried out. This experiment was done for the three PID con-

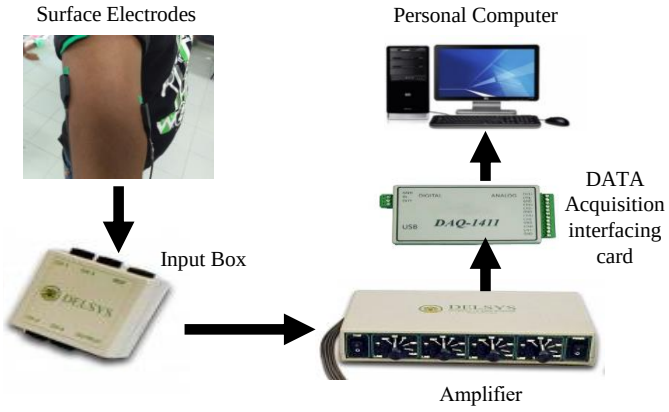

Figure 4.5: EMG signal acquisition system

trollers of its three brushed DC motors located at its forearm and wrist. A sinusoidal wave was given to the PID controller as an input. This input was considered as the desired motion and the encoder feedback according to the input was considered as the output motion. For each of the three PID controllers input (desired motion) and the encoder feedback(output motion) was plotted in the same graph. Motor commands (input signal) are sent through PWM outputs of the micro-controllers(ATmega 2560,Atmel) to the motor controller(L298,H-bridge). Implemented Proportional-Integral-Derivative controller (PID) is shown in Equation 4.1.

$$M_s = K_p \times E_p + K_i \times E_i + K_d \times E_d \tag{4.1}$$

where M_s,K_s, K_i,K_d, E_p, E_i and E_d are motor control, proportional gain, integral gain, derivative gain, proportional error integral error and derivative error respectively.

$$E_p = P_d - P_a \tag{4.2}$$

where, P_a and P_d are actual angular position and desired angular position of a prosthetic joint respectively.

$$E_d = \frac{(E_p(t) - E_p(t-1))}{t} \tag{4.3}$$

where, $E_p(t)$, $E_p(t-1)$ and t are current angular position error, previous angular position error and sample time respectively.

$$E_i = E_p(t-1) + E_p(t) \tag{4.4}$$

where, $E_p(t-1)$, $E_p(t)$, and t are, previous angular position error, current angular position error and sample time respectively.

Figure 4.6 and Figure 4.7 depict the motion output of the S/P motor, wrist F/E motor and wrist U/R motor according to the desired motion input respectively. In each graph it can be seen that output motions are not reached to the same peaks as the desired motion. Since the ranges of motions prosthesis are limited to the values as shown in Table, prosthesis cannot achieve desired peak to peak ranges of motions. The values for the human were taken from [90].

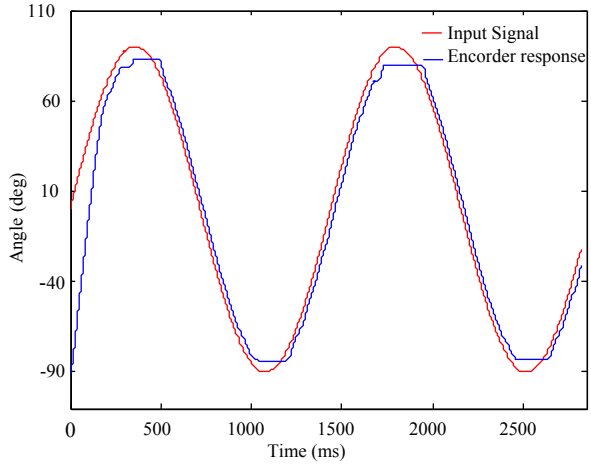

Figure 4.6: Motion output of the S/P motor to a desired motion input

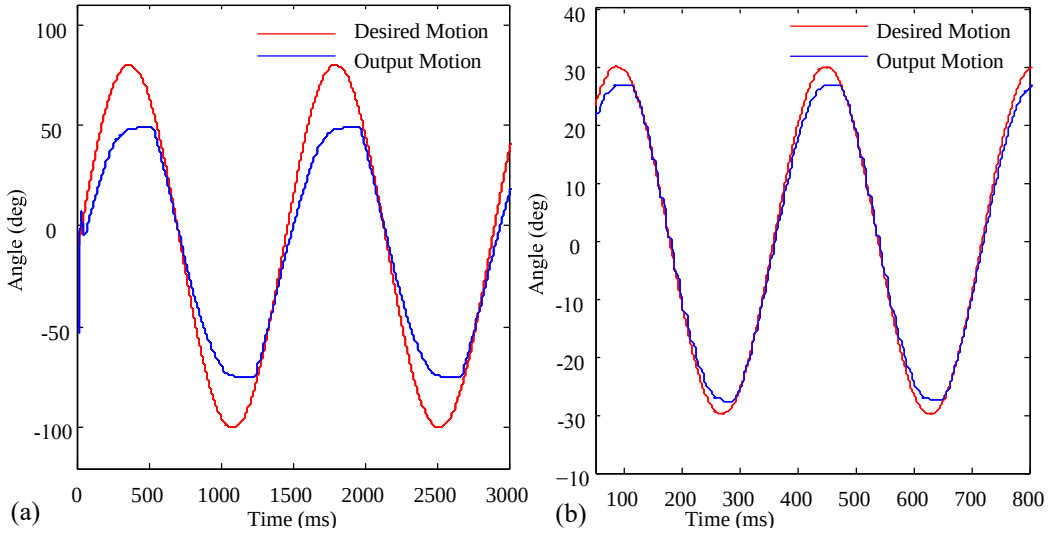

Figure 4.7: Motion outputs of motors: (a) Motion output of the wrist F/E motor to a desired motion input (b) Motion output of the wrist U/R motor to a desired motion input

4.1.3 Effectiveness of the EMG based proportional controller

In order to measure the effectiveness of the EMG based proportional controller of MoBio, joint angles of the actual arm and MoBio are plotted after taking the joint angle readings at the same time using an attachment. In order to measure

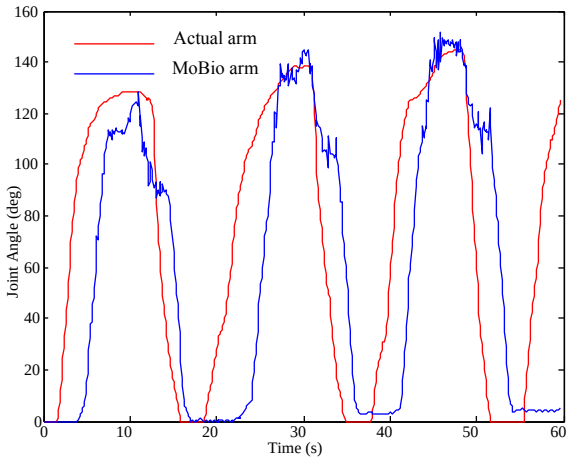

Figure 4.8: Elbow motion comparison between actual human arm and prosthetic arm

the angle of both human arm and prosthesis, an angle measuring device was used.

Figure 4.8 shows the motion comparison between elbows of both MoBio and the human arm. It can be seen that there is a lag in the robotic arm motion compared to the actual arm motion. This situation mainly occurs due to the delay generated by the signal processing and communication in the micro-controllers and softwares. The distortion which has occurred at the peak of the robotic arm motion curve, has generated due to the noise interferences.

4.1.4 Spatial motion comparison between actual arm and MoBio

In order to monitor the effectiveness of MoBio when reaching towards object this experiment was conducted. Healthy human subject controlled the prosthesis and its path when reaching towards an object was recorded using a camera. Markers were pasted on the trans-humeral prosthesis in order to track the path. Kinovea software was used to determine the path followed by the prosthesis [91]. Finally the spatial motion of MoBio along X and Y axes against the time was plotted and the deviation of the EMG signal pattern of the healthy human subject with respect to the same time interval was also plotted. Path followed by the prosthesis is shown in Figure 4.10. Throughout this path, the user controls MoBio through his motion intentions while taking the vision feed back from the eyes, to reach the hand towards a specific object. The motion is performed in a plane parallel to sagittal plane.

Figure 4.9 depicts the vertical movement (along Y-axis) and horizontal movement (along X-axis) of the prosthesis during this task. Furthermore, EMG pattern recorded at the same time is also included in the graph so that the shifting regions can be identified. Here the hand motion is not available in the graph because it only reveal MoBio's ability to reach an object.Two consecutive isometric contractions are performed during the reaching process without any visible time gap to skip the wrist U/R deviation and hand motion at respective intervals.

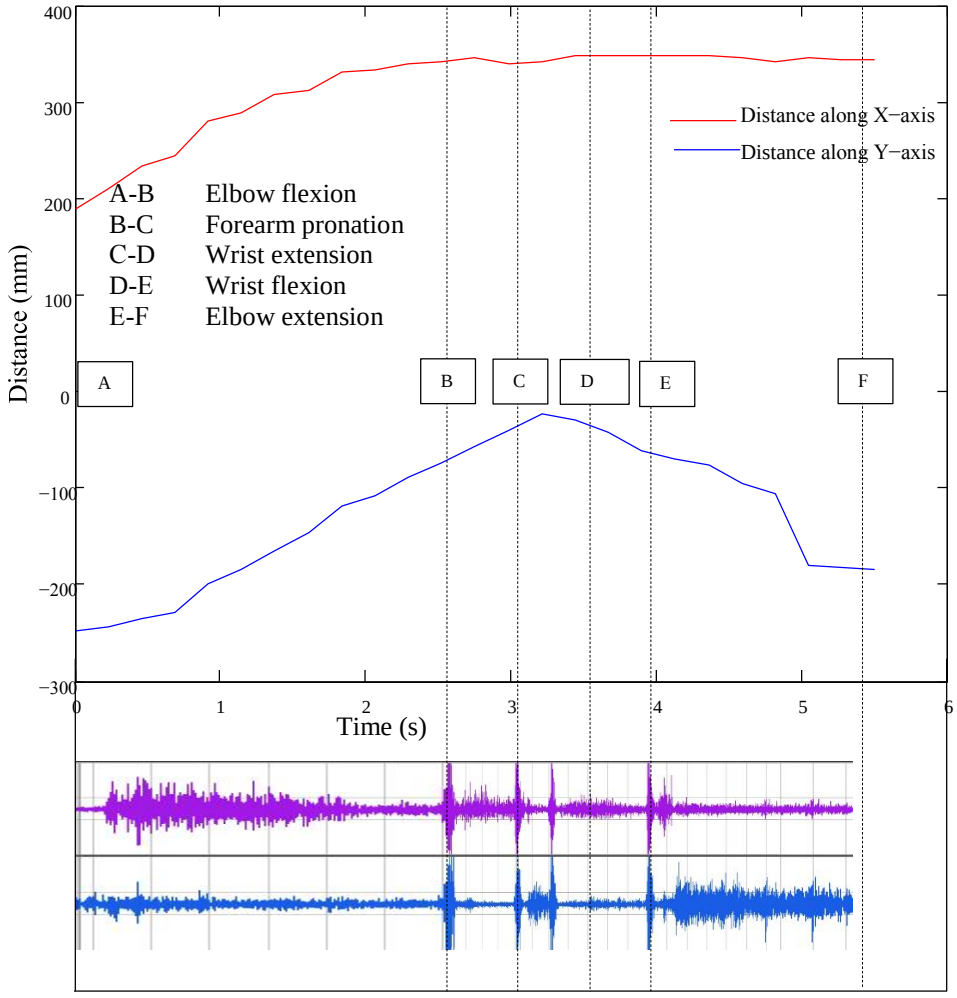

Figure 4.9: Spacial motion of MoBio along X and Y directions in reaching a object and EMG signal pattern change with time

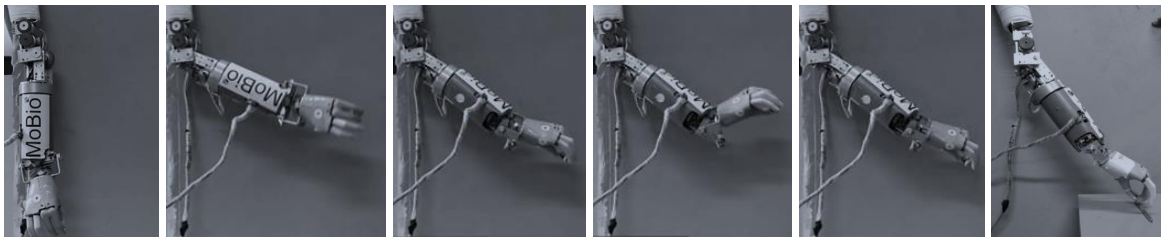

Figure 4.10: MoBio's reach towards an object

4.2 Validation of the shoulder orthosis

Shoulder orthosis is designed to assist 3DoF shoulder motions: shoulder vertical F/E, shoulder Abd/Add and I/E rotation of the stump arm. Furthermore it enables horizontal F/E as a passive DoF. Simulation experiments have carried out to evaluate its kinematic performances since the stump arm motions directly affects the hand motions of the ortho-prosthesis.

4.2.1 Redundancy of the shoulder orthosis

Human upper limb has a very complicated structure which makes it very hard to replicate or impossible at all. Since gleno-humeral joint of the shoulder is a spherical joint, human upper limb has infinite number of DoF around that joint. However, any shoulder orthosis or prosthesis should be able to perform the 4 DoF motions which lie parallel to the main three planes: sagittal, coronal and transverse plane. Those motions are shoulder vertical F/E, shoulder horizontal F/E, shoulder Abd/Add and I/E rotation of the shoulder. The dexterity of these motions depends on the redundancy of the shoulder orthosis or prosthesis.

Shoulder orthosis of the proposed trans-humeral ortho-prosthesis plays a vital role when it comes to the final design. Since the ortho-prosthesis is designed to withstand the loads applied by the prosthesis and to assist the stump arm to perform the motion while replacing the missing limb, the shoulder orthosis should be able to achieve both power assisting and load bearing. In doing so, it should not lose its dexterity too.

The shoulder orthosis of the trans-humeral ortho-prosthesis,extends up to the end of the stump arm and connects with the prosthesis. In order to discuss the kinematic properties of the shoulder orthosis it is considered as a robot manipulator which has its end effector at the point where the prosthesis is connected.

Since the shoudler orthosis should be able to perform main 4 DoF motions, the class of task which should be carried out by it equals to four. Therefore, the manipulator should contain minimum of four joint to achieve the task. Shoulder orthoses and prostheses are often made as 4DoF manipulators (up to elbow) [34]. In the proposed trans-humeral ortho-prosthesis, shoulder orthosis is designed as 6DoF manipulator. This aspect makes it a redundant manipulator. Due to its redundancy the manipulability of the shoulder orthosis has improved compared to the conventional 4DoF orthosis. This fact is proven in the next sub section 4.2.2.

4.2.2 Manipulability comparison between conventional 4 DoF shoulder orthosis and the proposed 6 DoF shoulder orthosis

Series of simulation experiments were carried on the kinematic models of both 4 DoF shoulder orthosis and 6 DoF shoulder orthosis. In order to perform the simulation kinematic models of both orthoses were modeled inside the MATLAB Robotics Toolbox environment using DH parameters.

Protocol of simulations

Inside the MATLAB Robotics Toolbox environment link models of both 4 DoF and 6 DoF orthoses [see Figure 4.13] were generated using the DH parameters [see Table 4.1 and Table 4.2]of two both kinematic models[see Figure 4.11 and Figure 4.12]. When choosing the trajectory the usage of the shoulder motions were considered. Since shoulder Abd/Add, shoulder horizontal and vertical F/E

Table 4.1: DH parameters of 4DoF orthosis

Link	α_i	a_i	d_i	θ_i
1	0	r	0	θ_1
2	$-\pi/2$	0	L_1	θ_2
3	$\pi/2$	0	0	θ_3
4	0	0	L_2	θ_4

Table 4.2: DH parameters of proposed 6DoF orthosis

Link	α_i	a_i	d_i	θ_i
1	0	r_2	0	θ_1
2	$-\pi/2$	0	l_3	θ_2
3	0	l_4	0	θ_3
4	$\pi/2$	0	r_{5b}	θ_4
5	$\pi/2$	0	0	θ_5
6	0	0	l_{6a}	θ_6

are the most critical motions in ADL [92], a trajectory which is a combination of these motions was chosen. The trajectory is more like the trajecory which the human upper arm (up to elbow) follow, when drinking from a cup, combing heir and etc. .

$$ {}^{0}_{n}T = {}^{0}_{1}T \times {}^{1}_{2}T \times {}^{2}_{3}T \times \ldots \times {}^{n-1}_{n}T \tag{4.5} $$

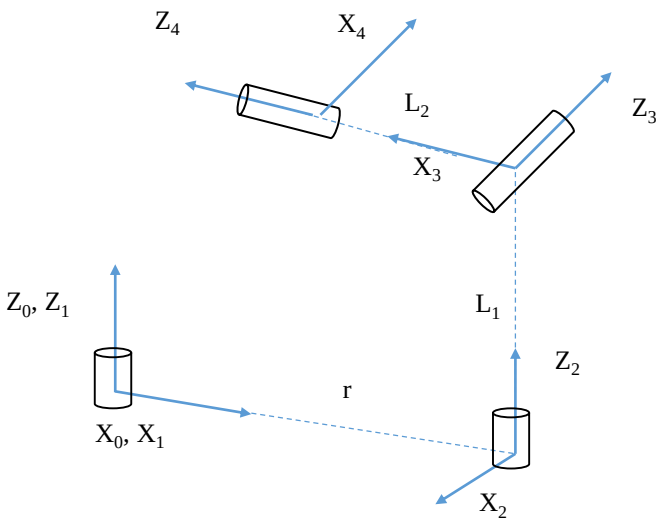

Figure 4.11: Kinematic Model of 4DOF orthosis

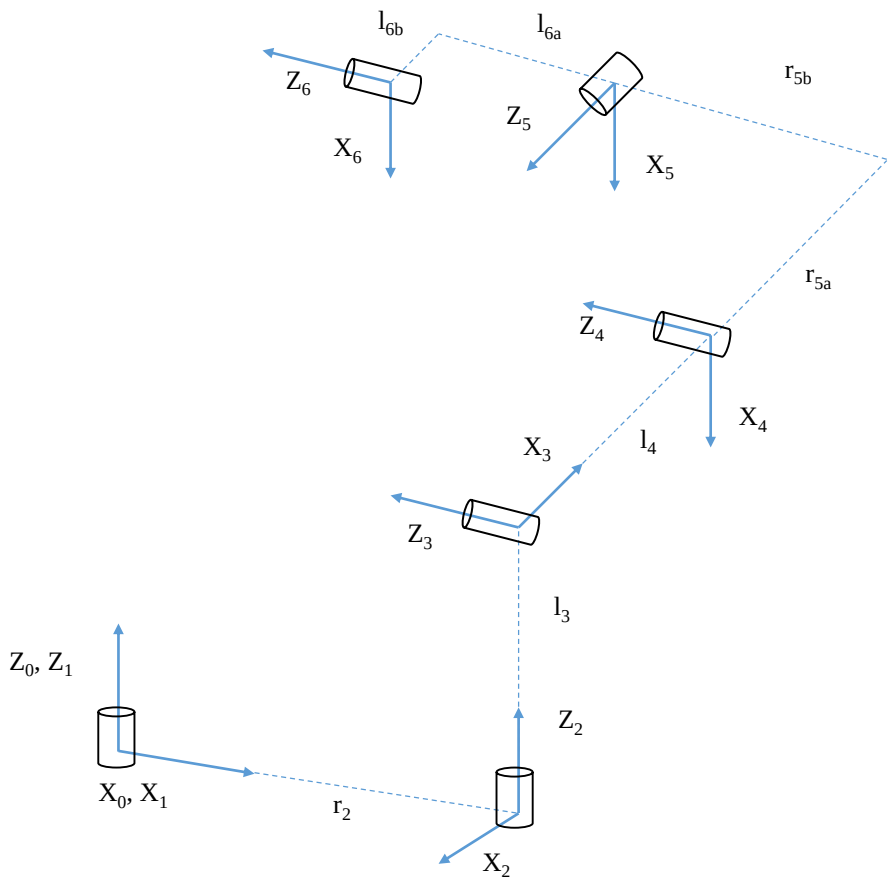

Figure 4.12: Kinematic Model of the proposed 6DOF orthosis

$$
{}^{i-1}_{i}T = \begin{bmatrix} cos\theta_i & -sin\theta_i cos\alpha_i & sin\theta_i sin\alpha_i & a_i cos\theta_i \\ sin\theta_i & cos\theta_i cos\alpha_i & -cos\theta_i sin\alpha_i & a_i sin\theta_i \\ 0 & sin\alpha_i & cos\alpha_i & d_i \\ 0 & 0 & 0 & 1 \end{bmatrix} \tag{4.6}
$$

Two link models were subjected to follow trajectories in the simulation environment. In order to calculate position and orientation of the end effector of the orthoses at each point, transformation matrices were used[see equation 4.5 and equation 4.6). Equation 4.6 is used to calculate the transformation matrix of the i^{th} frame relative to $(i-1)^{th}$ frame. Equation 4.5 determines the final position and orientation of the proposed ortho-prosthesis's end effector (hand) relative to the base frame. Initial point and end point of the trajectory was decided con-

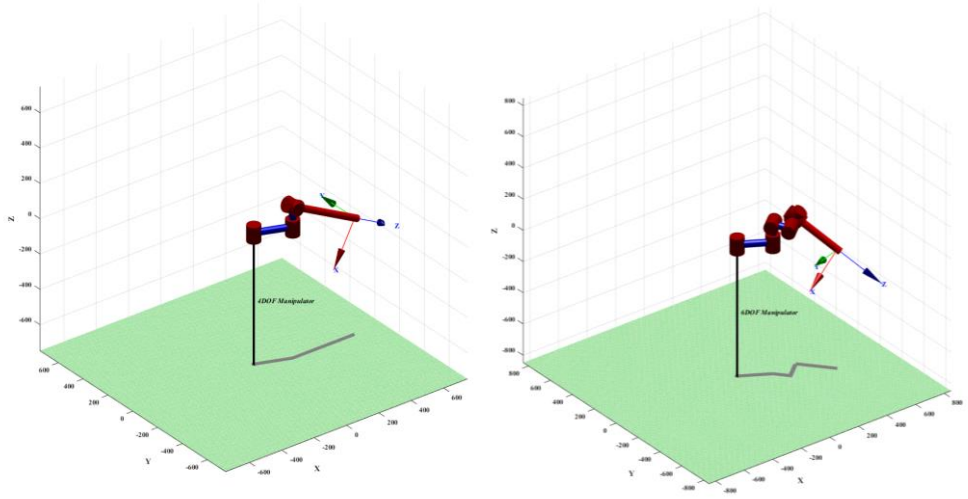

(a) (b)

Figure 4.13: Generated Link Models inside the MATLAB Robotics Toolbox Environment: (a) Link Model of 4DoF orthosis (b) Link Model of proposed orthosis (6DoF manipulator)

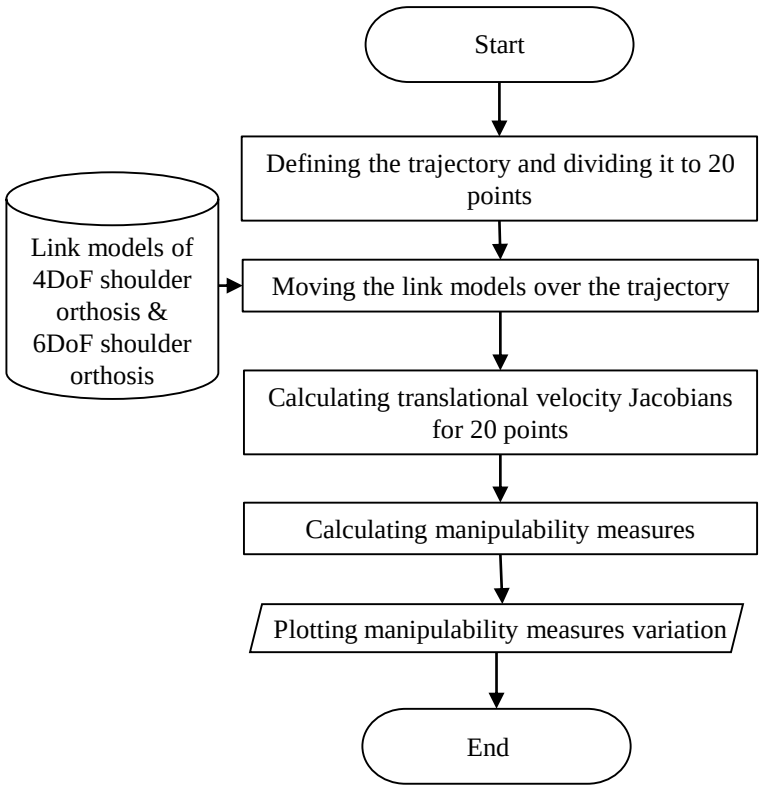

Figure 4.14: Summary of the experimental protocol

sidering the position and orientation of the actual human arm when doing these activities. "R.teach(Q)" command is used to find the initial and final pose of the orthoses. Here, "R" represent the"SerialLink"(link model) inside the MATLAB robotics toolbox environment where as "Q" denotes the joint angle vector of the manipulator. Then the link models were allowed to follow the trajectory which connects the initial and initial and final poses of the orthoses using "jtraj" command of MATLAB software. This trajectory consists of 20 linearly spaced vectors including initial and final poses. For each point, manipulability measures were calculated. Finally, the obtained results for both models were compared, in order to determine which has the better manipulability than the other. Figure 4.15 and Figure show the link model poses of 4DoF orthosis and 6DoF orthosis during the trajectory, respectively. Summary of the experimental protocol is shown in Figure 4.14.

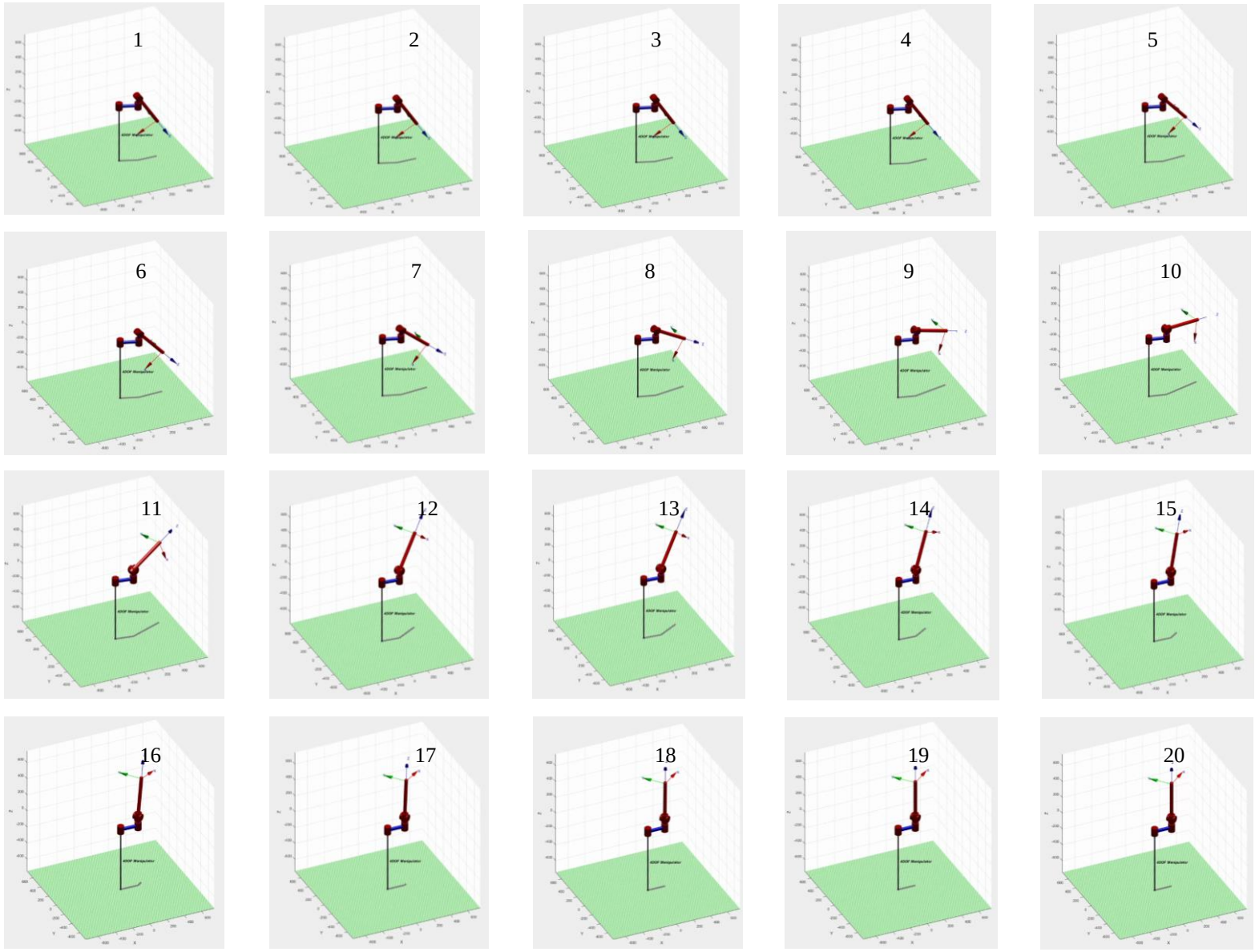

Figure 4.15: Link model of 4DoF orthosis during the trajectory

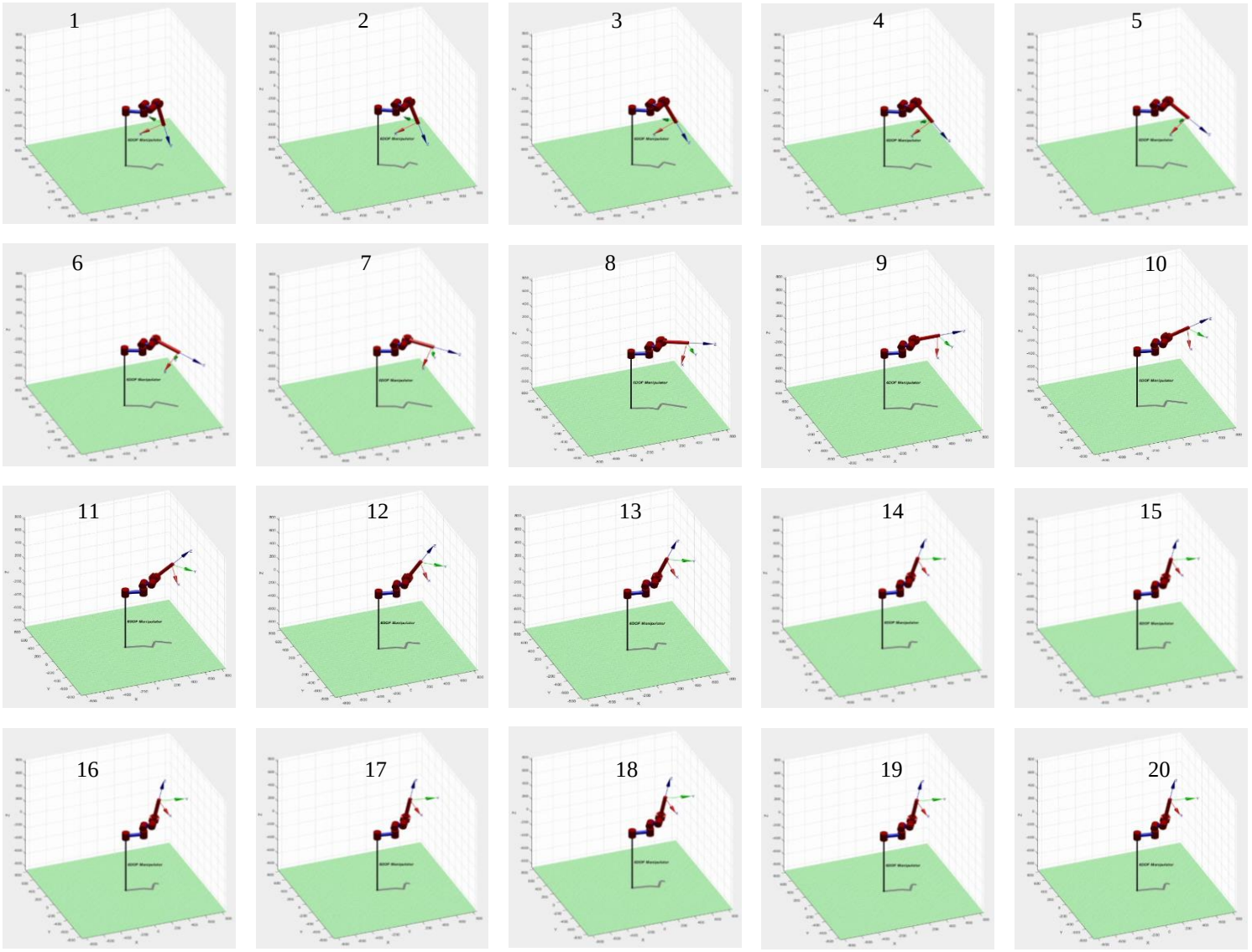

Figure 4.16: Link model of 6DoF orthosis during the trajectory

Simulation experiment Results

Figure 4.17 depicts the manipulability index variation for the trajectories of both conventional 4DoF orthosis and proposed 6DoF orthosis. It can be seen that both curves have obtain a bell shape and have the maximums around step number 10 and 12. However, at the end of the trajectory it can be seen that the values for the 4DoF orthosis have reached zero. This aspect suggests that the manipulator (orthosis) has obtained a singular configuration. At the end of the trajectory 4DoF orthosis is at its maximum reachable boundary where as the 6DoF orthosis can reach that point with several configuration even though it is the maximum reachable point of the residual arm. Furthermore, it can be seen that, even though the manipulability indices of 6DoF orthosis are relatively low at the beginning and the end, compared to the middle region, the values are far from being close to zero (lowest value is 1.6×10^7). Since, manipulability index is a configuration dependant variable, it is clear that the 6DoF orthosis does not have a singular configuration during the trajectory. Hence, it can be deduced that the proposed 6DoF has a higher manipulability compared to the conventional 4DoF orthosis considering the manipulability index variation of the two orthoses.

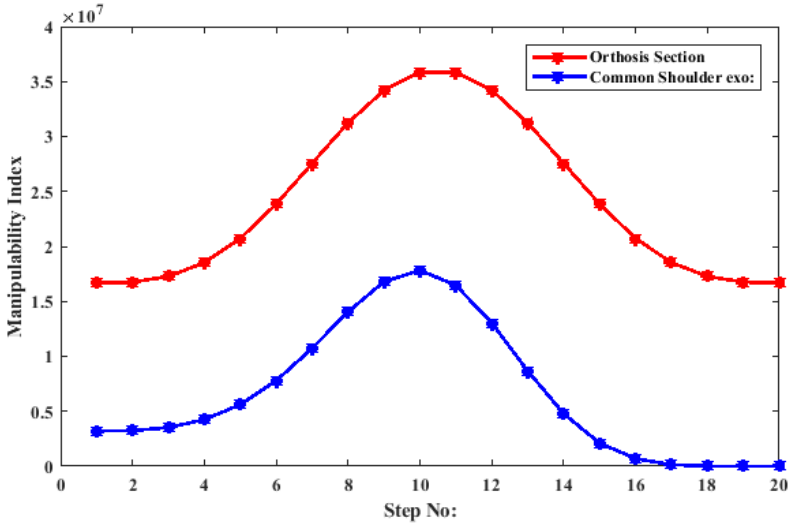

Figure 4.17: Manipulability index variation for the trajectories of both 4DoF and 6DoF orthoses

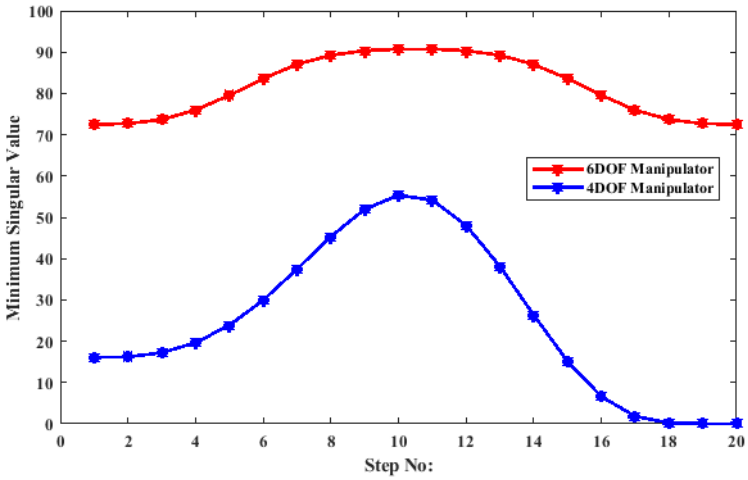

Figure 4.18: Minimum singular value variation for the trajectories of both 4DoF and 6DoF orthoses

Figure 4.18 shows the minimum singular value variation of both 4DoF orthosis and proposed 6DoF orthosis. Minimum singular value describes whether the manipulator is at a singular configuration. It can be seen that the minimum singular value for the 4DoF orthosis reaches at the later steps where as the values for the 6DoF orthosis has varied values between 70 and 100 (not reached zero). This aspect confirms that the proposed 6DoF orthosis has a high manipulability than the conventional 4DoF orthosis.

Figure 4.19 depicts the condition number variation of the two orthoses over the trajectory. It can be seen that the condition number value for the 4DoF orthosis tend to infinity after the 15^{th} step whereas the values for the proposed 6DoF orthosis varies between 6 and 9. Infinite condition number suggests that the 4DoF orthosis has reached a singular configuration. When the condition number of a manipulator is close to 1 it is said that it has high manipulability. Furthermore, if the variation of the conditon number over a trajectory is very high, it implies the manipulator ha too much jerks whereas the less variation of the condition number suggests the smooth motions of the manipulator. Therefore, it can be deduced that apart from the high manipulability of the 6DoF orthosis than the conventional 4DoF orthosis, proposed 6DoF orthosis can also move smoothly than the conventional orthosis.

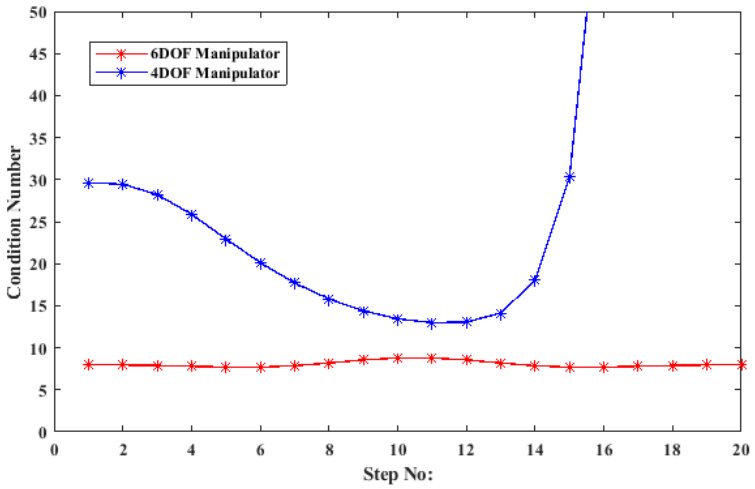

Figure 4.19: Condition number variation for the trajectories of both 4DoF and 6DoF orthoses

Figure 4.20 shows the manipulability ellipsoids generated during the respective trajectories of two orthosis models. In order to get a better view of the ellipsoids, ellipsoids for the 4DoF orthosis is selected differently than that of the 6DoF orthosis. Furthermore, the scale of the ellipsoids drawn after the 15^{th} step of the trajectory of the 4DoF orthosis, are different from the scale used before that step of the 4DoF orthosis. Since manipulability index equals to the volume of the ellipsoid, this scale change had to be brought in (After the 14^{th} step, manipulability indices of the 4DoF orthosis tends to zero.). It can be seen that, at the end of the trajectory, ellipsoid becomes an ellipse in the trajectory of 4DoF orthosis. This suggests that, towards the end of the trajectory, the manipulability of the 4DoF orthosis has lost completely and it is in a singular configuration. Throughout the trajectory, ellipsoids of the proposed 6DoF orthosis have not lost their shape to an ellipse. This aspect shows that the manipulability of the proposed orthosis is very high and it has not obtained a singular configurations. Furthermore, it suggests that the 6DoF orthosis has a higher directional velocity profile than that of the 4DoF orthosis.

Considering all the simulation results on the manipulability measures of both 6Dofs orthosis and 4DoF orthosis, it is clear that that the proposed orthosis has the higher manipulability. The singularity of the 4DoF orthosis has occurred

because it has reached its maximum reachable points at these occasions. Having a high manipulability gives the proposed orthosis the ability to match the different anatomies of the users. Since it has many configurations to reach the same point due to high manipulability, 6DoF orthosis can find a configuration which can suit the anatomical structure of the stump arm of the user. Furthermore, it improves the dexterity of the shoulder orthosis.

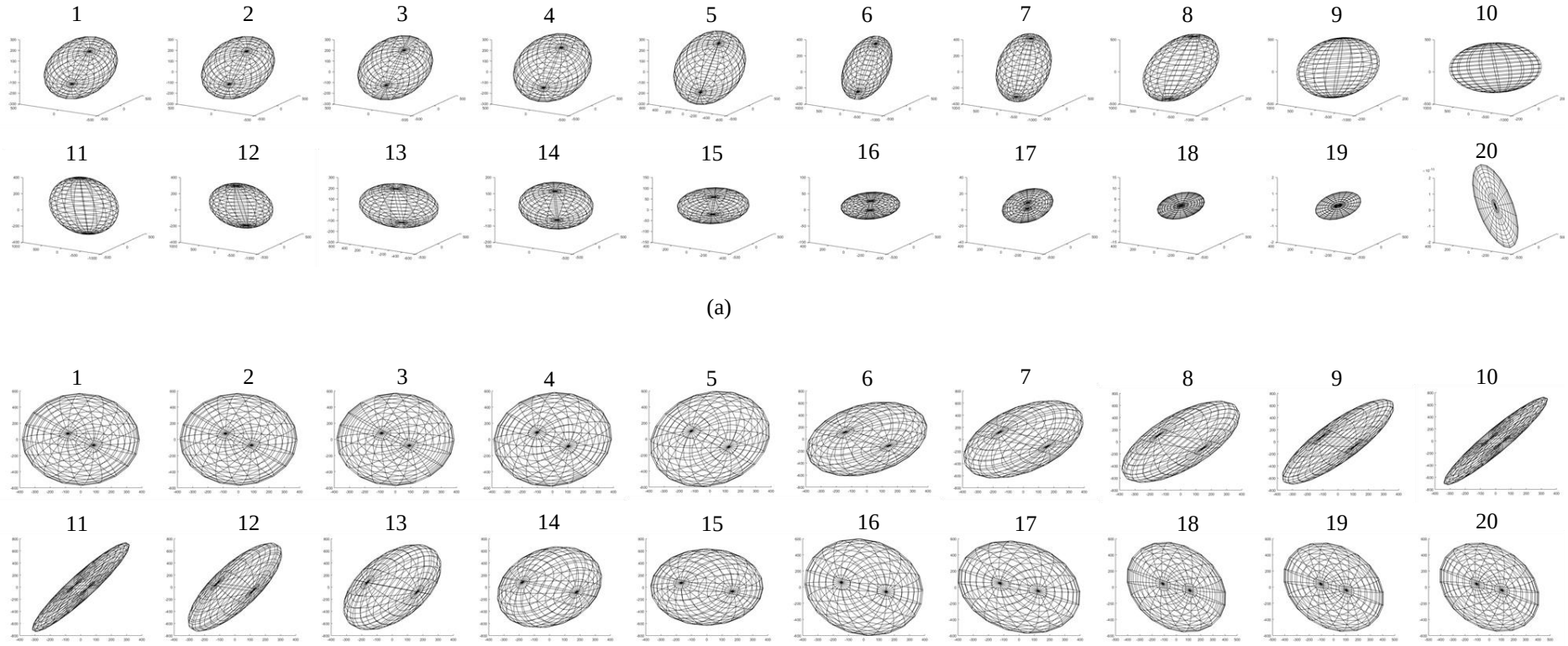

Figure 4.20: Manipulability ellipsoids for the trajectories of both 4DoF and 6DoF orthoses: (a) 4DoF orthosis (b) 6DoF orthosis

4.3 Validation of the proposed trans-humeral ortho-prosthesis

A 9DoF trans-humeral ortho-prosthesis [see Figure 3.1] is proposed in this research. 9 DoF motions consist of 4 DoF motions at the orthosis section and 5 DoF motions at the prosthesis section [11]. The prosthesis enables elbow F/E, forearm S/P, U/R deviation, wrist F/E and compound motion of thumb and index finger whereas orthosis assists shoulder vertical F/E, shoulder Abd/Add, I/E rotation. Shoulder horizontal F/E is kept as a passive DoF.

Even though the orthosis section is designed to achieve 4 DoF, it consists of 6 joints. Therefore, the orthosis section has the properties of a redundant manipulator [94]. In the sense of manipulability, redundancy is a very important property because it can improve the manipulability of a manipulator. Furthermore, a passive DoF in the design effects the manipulability.

4.3.1 Simulation Experiments

Series of simulation experiments were carried out to investigate the manipulability of the trans-humeral ortho-prosthesis. In order to perform the simulation experiments, kinematic model was developed. The kinematic model of the ortho-prosthesis [see Figure 4.21] was developed using the MATLAB Robotic Toolbox environment [see Figure 4.22). Conventional DH parameters of the kinematic model [see Table 4.3] were used to model the ortho-prosthesis.

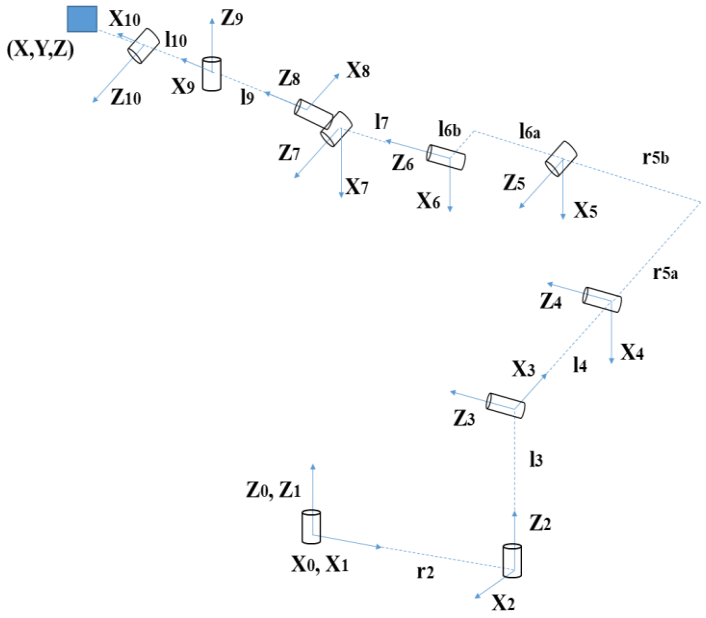

Figure 4.21: Kinematics model of the trans-humeral ortho prosthesis

Table 4.3: DH parameters of proposed trans-humeral ortho-prosthesis

Link	α_i	a_i	d_i	θ_i
1	0	r_2	0	θ_1
2	$-\pi/2$	0	l_3	θ_2
3	0	l_4	0	θ_3
4	$\pi/2$	0	r_{5b}	θ_4
5	$\pi/2$	0	0	θ_5
6	$-\pi/2$	0	$l_{6a} + l_{7a}$	θ_6
7	$-\pi/2$	0	0	θ_7
8	$\pi/2$	0	l_9	θ_8
9	$-\pi/2$	l_{10}	0	θ_9
10	0	l	0	θ_{10}

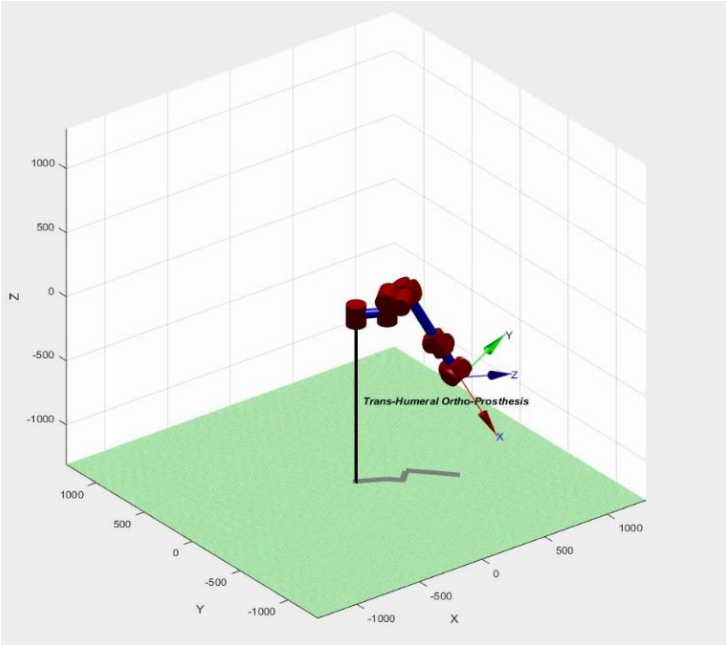

Figure 4.22: Link model of the trans-humeral ortho-prosthesis generated in MATLAB (Robotics toolbox environment)

Experimental protocol

Three trajectories were selected considering the fact that singularities occur at the maximum reachable points. Hence, the trajectories of the hand at the full extension of upper limb were selected. Three motions which were selected for the hand trajectories, are shoulder horizontal F/E, shoulder vertical F/E and shoulder Abd/Add.

The selected trajectories were divided to twenty linearly spaced points. For each point translational Jacobian was calculated. Using the calculated Jacobian matrices, manipulability index, minimum singular value, condition number and manipulability ellipsoids were calculated.

The calculated values were plotted to evaluate whether there is any singular configuration for the end effector (hand) of the trans-humeral ortho-prosthesis. Figure 4.23 shows the summary of the experiment carried out on the link model of the trans-humeral ortho prosthesis.

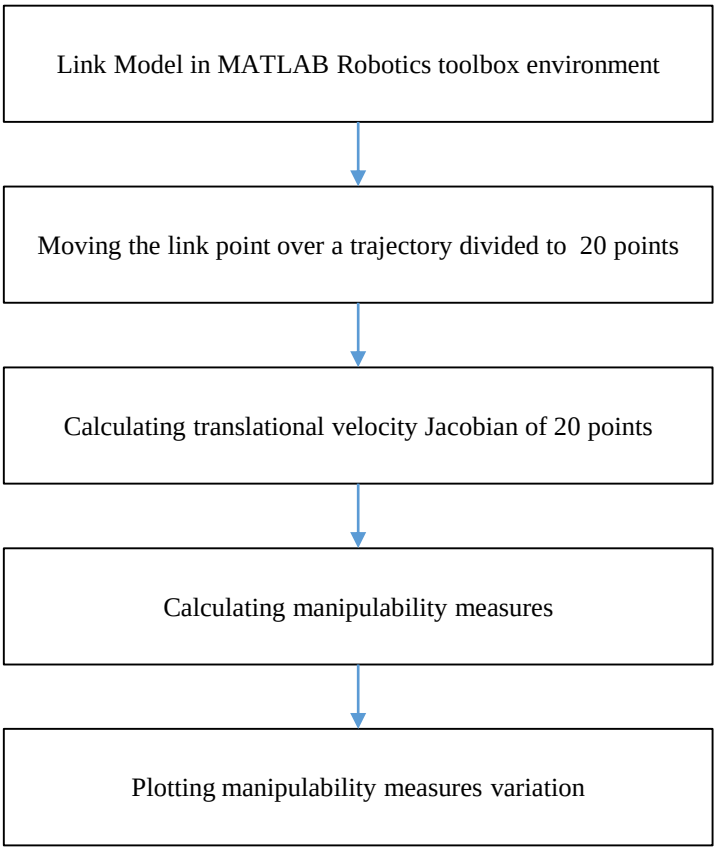

Figure 4.23: Summary of the experimental protocol

Simulation Results

Figure 4.24, Figure 4.25 and Figure 4.26 show the manipulability index variation of the ortho- prosthesis over the three trajectories. Manipulability index variation is almost same for shoulder Abd /Add and shoulder vertical F/E in the sense of shape. Manipulability index drops when the manipulator configuration relatively close to a singular configuration. Even though manipulability index reaches a minimum in Figure 5, it is far from being singular configuration because the lowest value is 1.46108. Manipulability index would not be zero in any configuration since the manipulator has not obtain a singular configuration during the three motions of the shoulder in terms of manipulability index.

Figure 4.27, Figure 4.28 and Figure 4.29 illustrate the minimum singular value

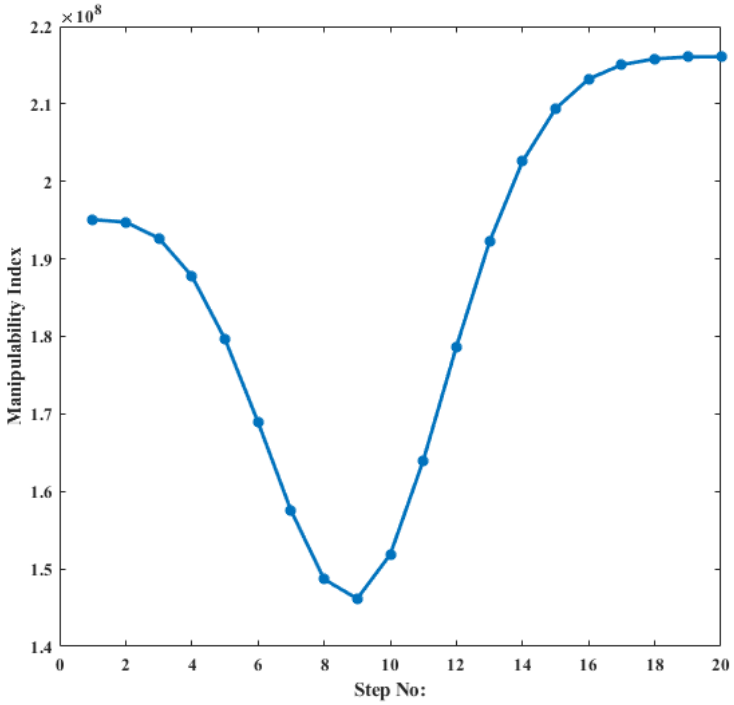

Figure 4.24: Manipulability Index variation for the trajectory during horizontal shoulder F/E

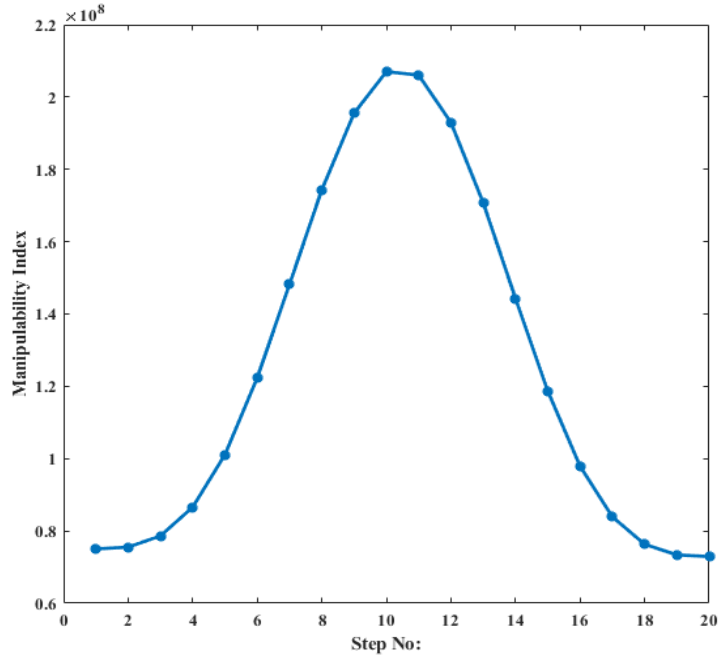

Figure 4.25: Manipulability Index variation for the trajectory during shoulder Abd / Add

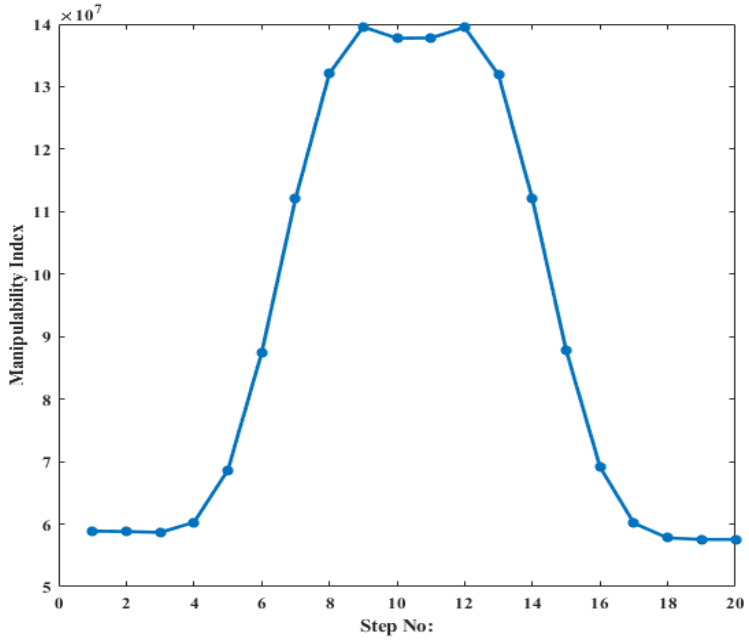

Figure 4.26: Manipulability Index variation for the trajectory during shoulder vertical F/E

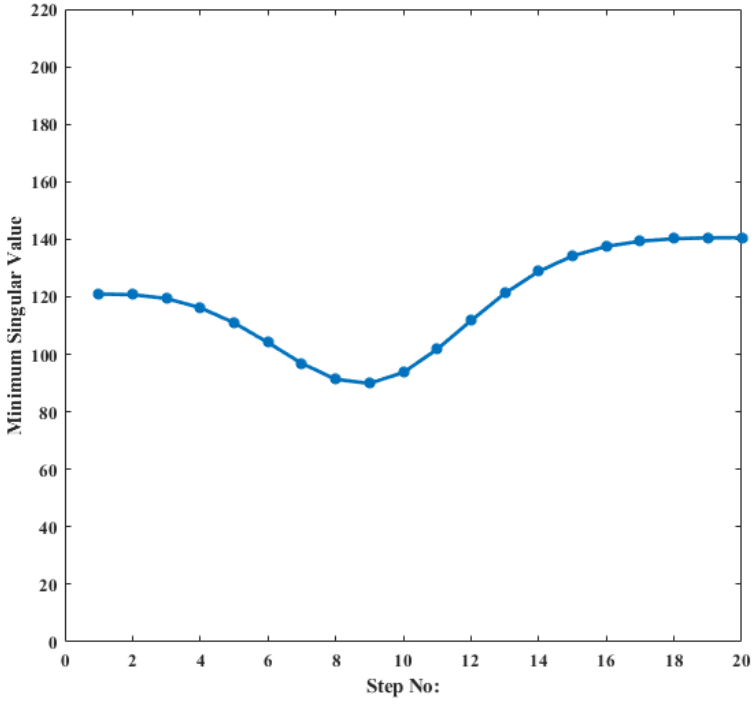

Figure 4.27: Minimum Singular value variation for the trajectory during shoulder horizontal F/E

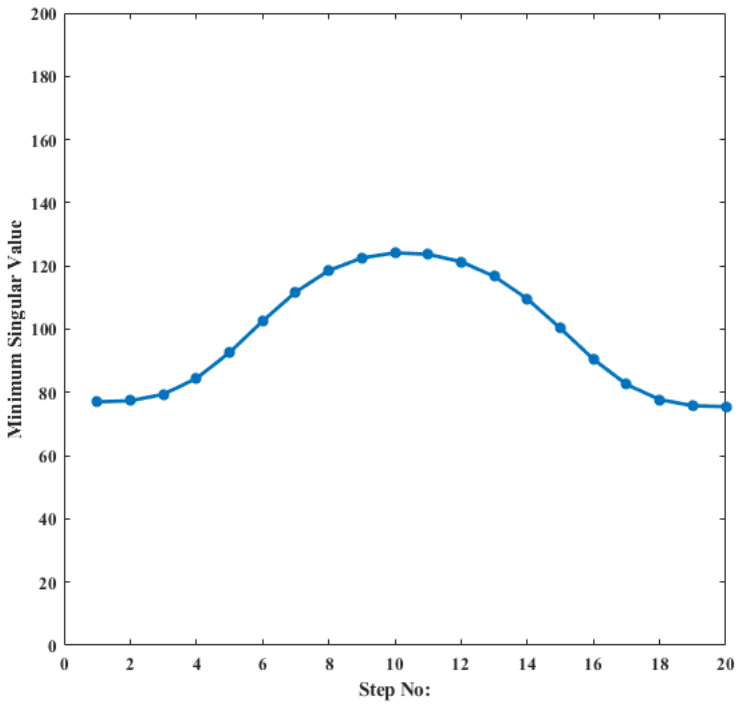

Figure 4.28: Minimum Singular value variation for the trajectory during shoulder Abd / Add

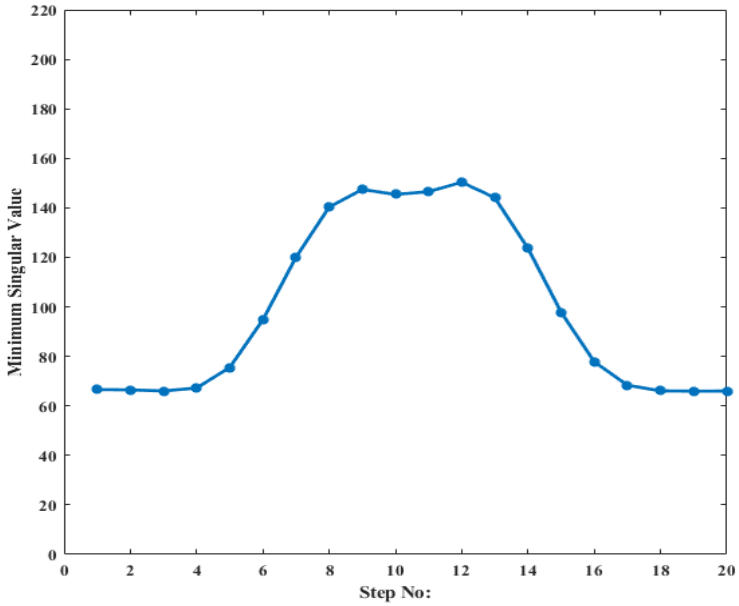

Figure 4.29: Minimum Singular value variation for the trajectory during shoulder vertical F/E

variation of the selected trajectories. It can be seen that there is a drop at the middle of the graph for the shoulder horizontal F/E while other two show com-

plete opposite. Even though the fact remains like that, minimum singular values for all three graphs do not reach zero. Since the condition number is a configuration dependent variable it can be deduced that the hand of the trans-humeral ortho-prosthesis would not have a singular configuration during its motions.

Figure 4.30, Figure 4.31 and Figure 4.32 show the condition number variation of the tans-humeral ortho prosthesis during the selected motions. Apart from proving that manipulator does not fall into a singular configuration during the three motions, they reveal that the manipulator is well conditioned. In all three cases, it can be seen that condition number varies keeping a range between minimum and maximum condition number value to approximately six. Due to the desirable condition number variation it can be concluded that the manipulator is well conditioned and the jerks due to the sudden movements of the manipulator will be reduced. Figure 4.33, Figure 4.34 and Figure 4.35 show the manipulability

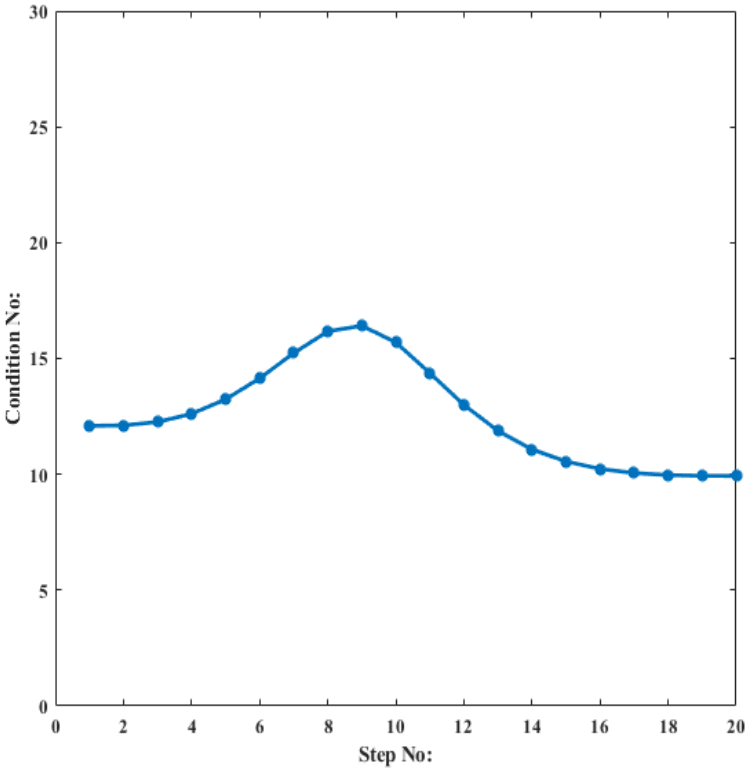

Figure 4.30: Condition number variation for the trajectory during shoulder horizontal F/E

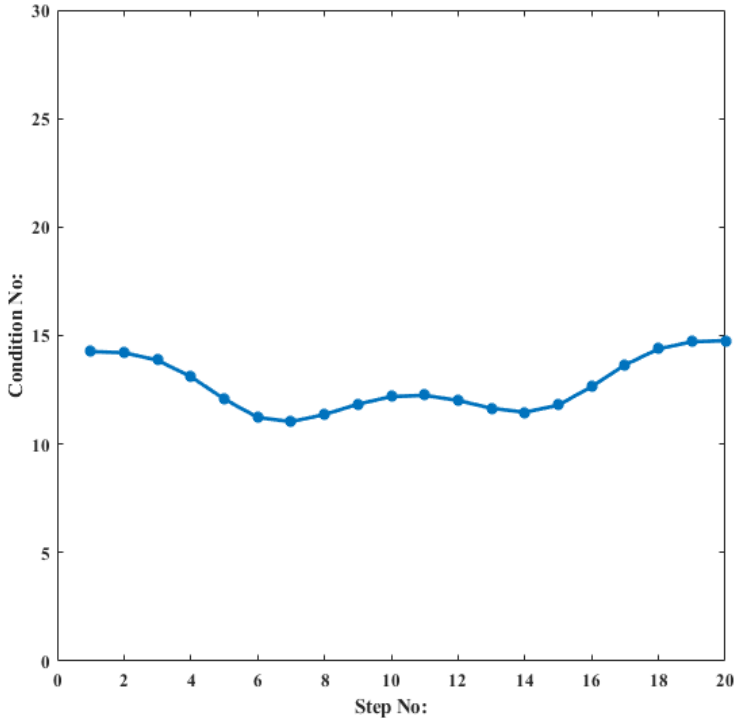

Figure 4.31: Condition number variation for the trajectory during shoulder Abd / Add

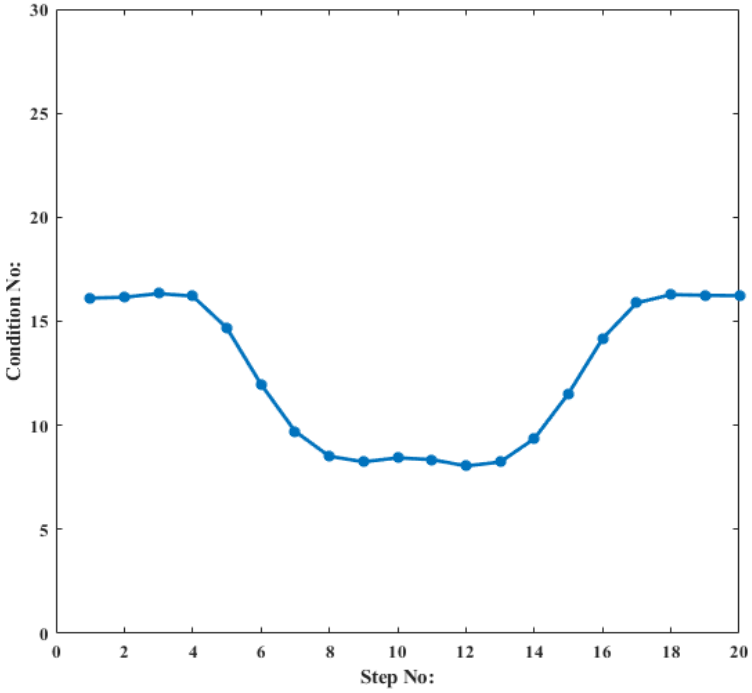

Figure 4.32: Condition number variation for the trajectory during shoulder vertical F/E

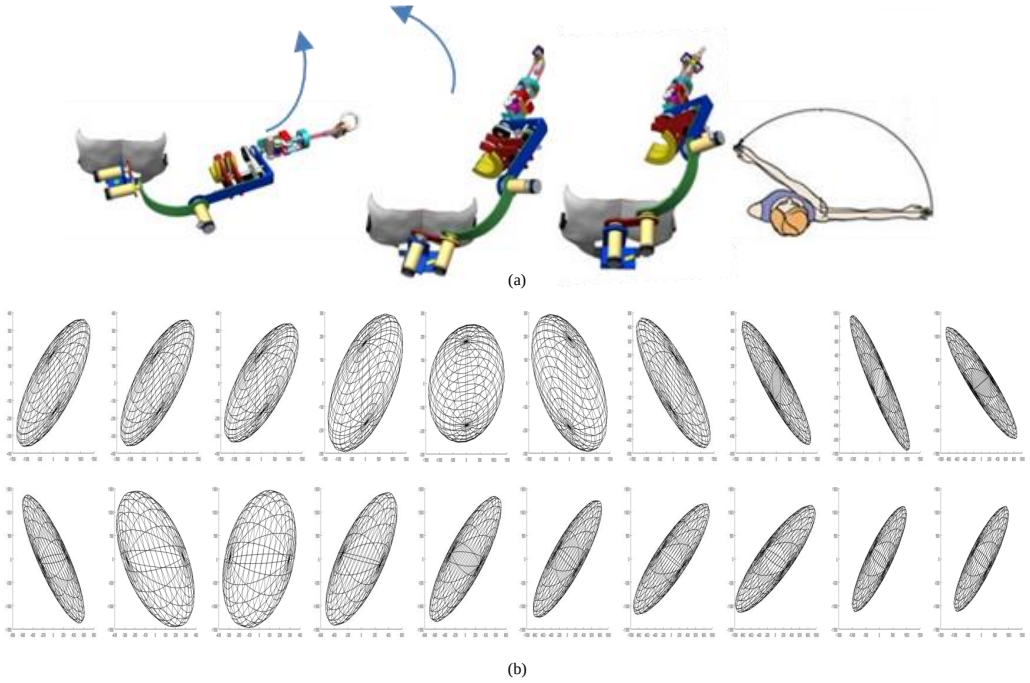

Figure 4.33: (a)Motion of the ortho-prosthesis during Shoulder Horizontal F/E. (b)Manipulability ellipsoids for the trajectory during shoulder horizontal F/E

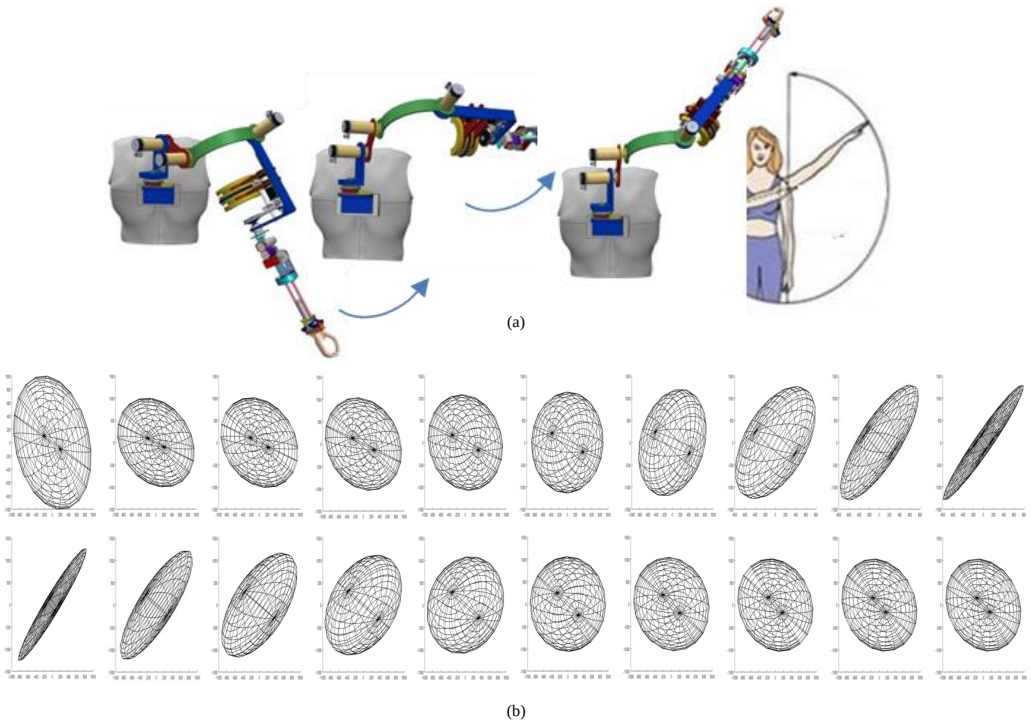

Figure 4.34: (a)Motion of the ortho-prosthesis during Shoulder Abd/Add (b)Manipulability ellipsoids for the trajectory during shoulder Abd/Add

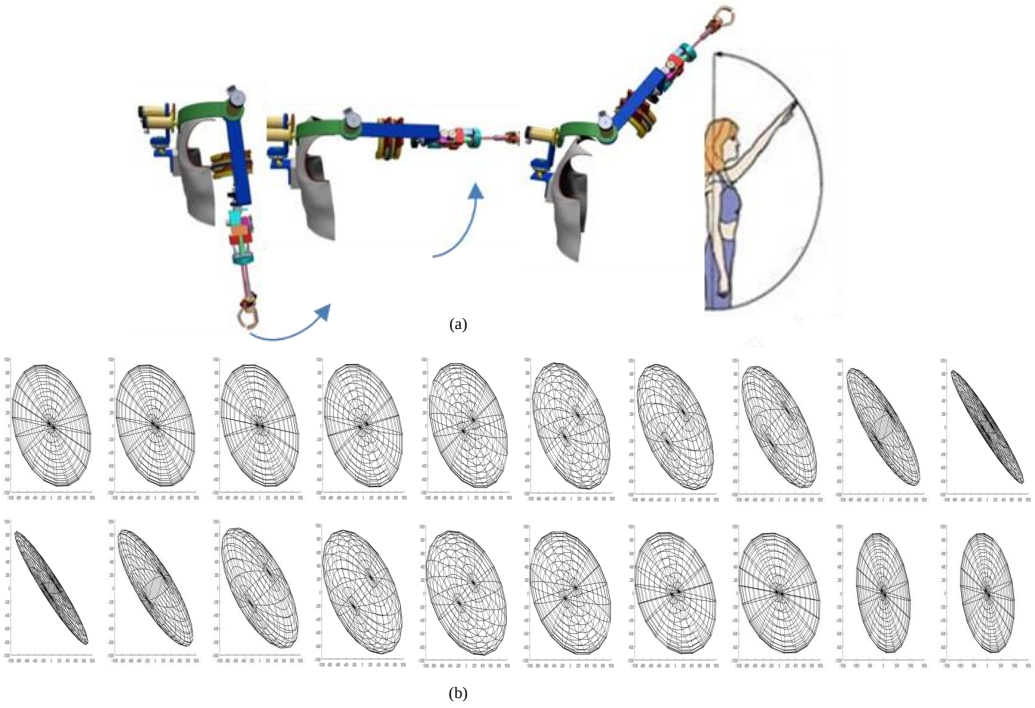

Figure 4.35: (a)Motion of the ortho-prosthesis during Shoulder Vertical F/E (b)Manipulability ellipsoids for the trajectory during shoulder vertical F/E

ellipsoids variation of the selected trajectories. It can be seen from Figure 4.33 that volume of manipulability ellipsoids gradually reducing up to the middle of the trajectory and then increasing. Furthermore, it can be seen that the directional velocity profile (spatial distribution of the ellipsoids) is also reducing up to the middle and increasing up to the end. In Figure 4.34 and Figure 4.35 the highest directional profile is located at the middle. Moreover, there is no single instance throughout all three trajectories where an ellipsoid has become an ellipse. Therefore, it can be concluded that the trans-humeral ortho-prosthesis does not reach a singular configuration at any point of the considered trajectories. In all four manipulability measures considered above, it can be seen that the measures for the trajectories shoulder horizontal F/E is different than the others. When a manipulator obtains its full extension manipulability of the manipulator is completely lost due to boundary singularity. Due to the passive DoF of the orthosis and the the Abd/Add Flat plate [see Figure 3.2) of the serial link mechanism of the orthosis, hand of the ortho-prosthesis would not reach its full extension even

though the manipulator is at the maximum reachable point of the actual human hand. Thus, the hand of the ortho-prosthesis has many configurations to reach the same point (high manipulability).

During the shoulder horizontal F/E, the manipulator reaches relatively closer to its maximum reach than in the other two motions at the middle of the trajectory. This incident causes the main difference of the shape of the shoulder horizontal F/E graph [see Figure 4.24) compared to the other two graphs.

Reachable workspace

Workspace of the end effector of the ortho-prosthesis was determined using the Robotics System Toolbox [95] of MATLAB software. Figure 4.36 shows the reachable workspace of the ortho-prosthesis in three dimensional coordinate frame. Planar motions of the end effector in the main three planes [12] are shown in Figure 4.37, Figure 4.38 and Figure 4.39. Workspace plots of the ortho-prosthesis shows that the achievable workspace of a human hand can be achieved through

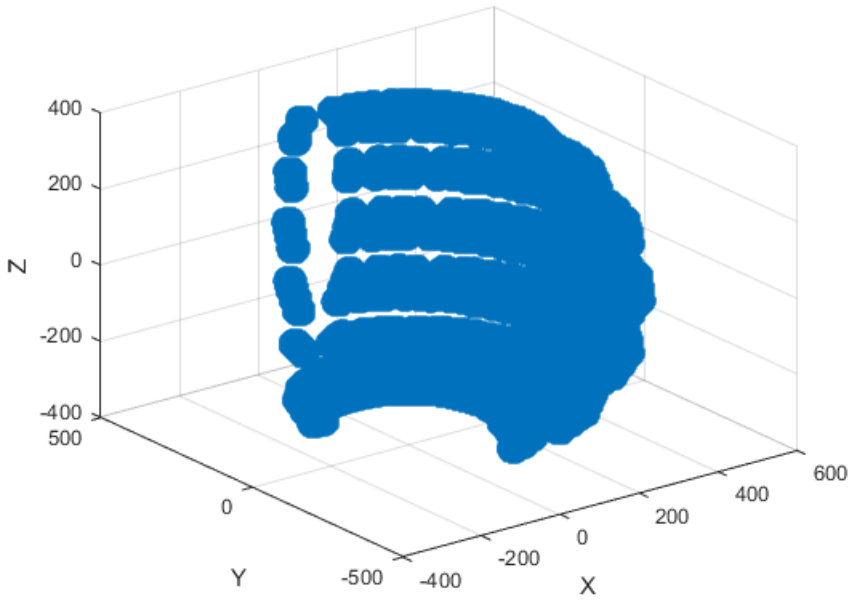

Figure 4.36: Workspace plot for the proposed ortho-prosthesis

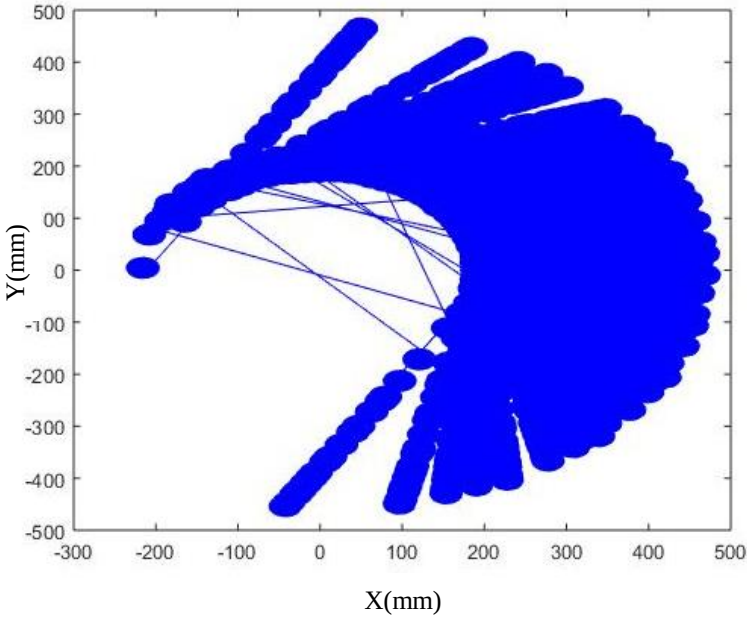

Figure 4.37: Workspace plot for the proposed ortho-prosthesis in the transverse plane

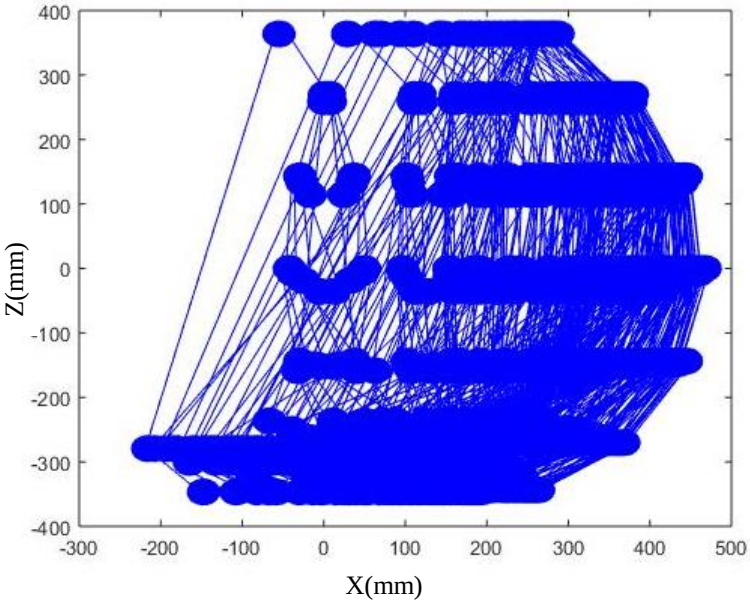

Figure 4.38: Workspace plot for the proposed ortho-prosthesis in coronal plane

this ortho-prosthesis. Furthermore, ortho-prosthesis can adapt according to anthropometry of the user.

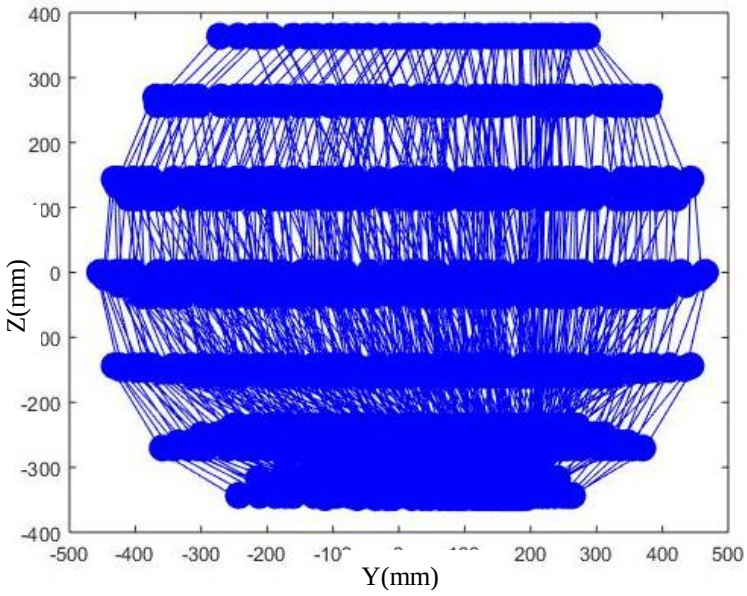

Figure 4.39: Workspace plot for the proposed ortho-prosthesis in sagittal plane

4.3.2 Experiments on the fabricated prototype

The trans-humeral ortho-prosthesis was subjected to several experiments to evaluate the effect of the proposed 6DoF orthosis towards the human like motion generation.

In the experiments, joint motions of the proposed 6DoF orthosis were kept as passive DoF including the powered DoF in the design. The purpose of keeping passive DoF was to allow the natural limb motion and determine whether the shoulder orthosis has any constraints for the natural limb motion. The prototype was worn by a healthy subject by flexing his elbow as shown in Figure 4.41. Therefore, the natural limb motion of the stump arm can be replicated from his motions and the constraints to his limb motion can be easily determined. Subject was given the training to be familiar with the motions of the prototype before starting the experiments.

In both experiments, the prosthesis (MoBio) was controlled through a simulator built inside the V-rep simulation environment [96]. Kinovea video analysis software [97] was used to track the motion captured by the camera.

Monitoring the capability of Human like motion generation

As the first experiment, the ability of the prototype of the trans-humeral ortho-prosthesis to reach towards an object was compared with the motion of the human upper limb towards the same object. Subject was instructed to perform the motion five times and the mean paths for reaching the object was plotted (for both human arm and prototype).

In order to compare the effect of the proposed orthosis and to monitor the effect of the weak stump arm towards the same motion, MoBio was connected to a mannequin with truncated upper limb at the humerus which has the same anthropometry like the test subject and then the reaching motion was performed.

Performing ADL - "Pick and Place"

The second experiment was carried out to monitor the ability of the trans-humeral ortho-prosthesis to complete a given task. The test subjected was asked pick an object placed on a table and put it on another table. Furthermore, he was instructed perform the motions in humerus area in a way which is comfortable for him.

Results

Figure 4.40 depicts the paths obtained for the limb motions mentioned above. If the stump arm of a trans-humeral amputee is inactive, elbow motion and the other motions of the trans-humeral prosthesis have to take over all the motions of the upper limb. Even though the stump arm motion is absent trans-humeral prostheses can perform motions for some motions just like in Figure 4.40. However, these motions stays further away from the natural limb motions. In Figure 4.40, maximum error between the paths of the actual arm and MoBio with constrained humerus, is 185.7mm for "Y" direction. Still it has reached the same end point

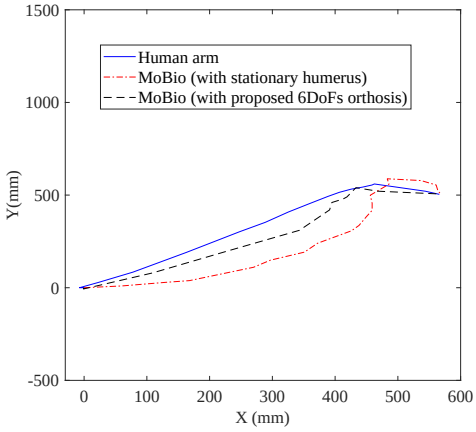

Figure 4.40: Comparison of the paths of human arm, MoBio with stationary humerus and trans-humeral ortho-prosthesis (MoBio with proposed 6DoF orthosis) when reaching the same object.

just like the human upper limb. However, this value is reduced to 3.8mm for the path of MoBio with 6DoF shoulder orthosis. This fact reveals that the proposed 9DoF redundant trans-humeral ortho-prosthesis has enabled the dexterous upper limb motions which are closer to the natural limb motions. Furthermore, the adaptability of the proposed redundant orthosis has caused the reduction of the error between the natural limb motion and motion of the ortho-prosthesis.

Figure 4.41 shows the motion sequence of test subject during the pick and place task. The experiment proved that the test subject can move the ortho-prosthesis as he wanted, because of the high manipulability provided by the proposed 6DoF redundant orthosis. However, there were some limitations of the experiment. Since the experiment used a healthy human subject with flexed elbow, it may have affected the motions. It may have caused the slight deviation from the natural limb motion depicted in the Figure 4.40 for MoBio with orthosis attached to it. Moreover, this error can be reduced further if the power assistance is given to the relevant DoF.

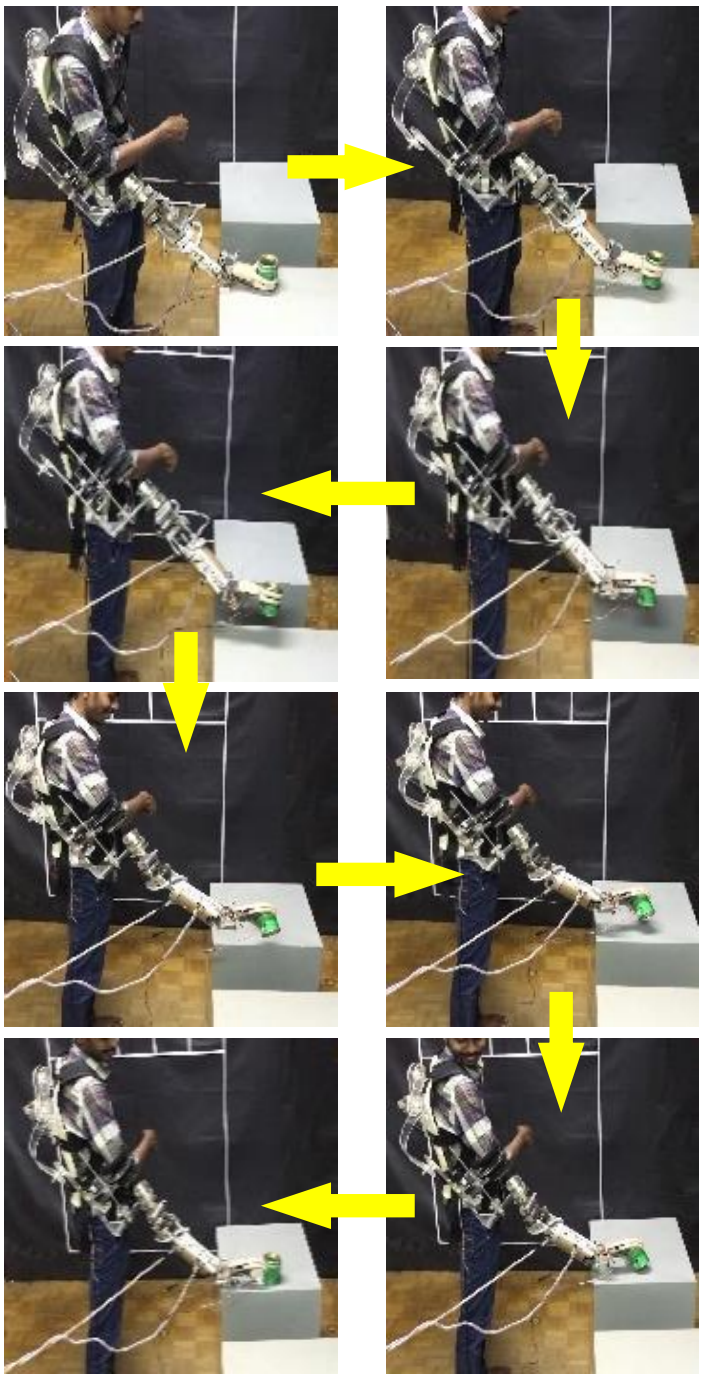

Figure 4.41: Performing pick and place activity while wearing the trans-humeral ortho-prosthesis

Chapter 5

CONCLUSION AND FUTURE DIRECTIONS

5.1 Conclusion

In this thesis a 9DoF trans-humeral ortho-prosthesis was proposed. The concept of upper limb orth-prosthesis is a novel concept and it has been introduced through this thesis. Even though there is no literature available for upper limb ortho-prostheses, the need for a device which can assist the stump arm while bearing the loads applied by the prosthesis was always there. Researches have been carried out all over the world to eliminate the musculo-skeletal disorders occurred due to the prolonged application of the loads by the prosthesis on the stump arm. Those researches are carried out to reduce the weight of the trans-humeral prostheses.

However, the fact that the existing trans-humeral prostheses have not been able to reduce the above mentioned musculo-skeletal disorders, motivated this thesis to look at this problem in different angle and explore different avenues. Literature review provided strong background for the research problem and caused the expansion of the initial motivation. Since the stump arm of the amputee plays a vital role in motion generation of the trans-humeral prosthesis, the motivation was expanded to support the stump arm while bearing the loads of the prosthesis.

As the first phase of the a trans-humeral prosthesis was selected. "MoBio" is a trans-humeral prosthesis developed by Bionics Laboratory of University of Moratuwa, Sri Lanka. However, its fine tunning and validation of its effectiveness

was yet to be carried out. As a contribution of this thesis it was carried out. Experimental results verified that the prosthesis can achieve the full range of motions of elbow F/E, forearm S/P, U/R deviation and wrist F/E, just like the actual human arm. MoBio weighs about 3.2kg which is same as grown human's upper limb. Furthermore, results confirm the fact that the prosthesis can reach a desired object successfully, which is an essential activity in performing ADL.

As the second stage design of the trans-humeral ortho-prosthesis was carried out. Considering the importance of the stump arm motions, orthosis of the trans-humeral ortho-prosthesis was designed as 6DoF manipulator which goes beyond the conventional shoulder orthoses/exoskeletons with 4DoF joint motions. Simulation experiments was carried out to compare the manipulability of both 6DoF and 4DoF manipulators. Simulation results prove that the proposed redundant 6DoF orthosis has the highest manipulability and would not assume singular configurations. Furthermore, improved dexterity of the 6DoF orthosis eliminates the constraints to the natural limb motion of the stump arm.

After finishing the designing stage, simulation experiments have been carried out to investigate manipulability index, minimum singular value, condition number and manipulability ellipsoids variations of the proposed ortho-prosthesis. Results confirmed that the manipulability index values and minimum singular values of the design of the ortho-prosthesis would not reach zero. Instead they have minimum value of 5.75×10^7 for manipulability indices and values over 65.96 for minimum singular values. Moreover, manipulability ellipsoids depicted that the end effector would not have a 2D ellipse at any instance. Hence, it can be deduced that the manipulator will not reach singular configuration during performing motions and it will perform smooth motion due to the desirable condition number variation. Furthermore, it revealed that ortho-prosthesis should be able to perform dexterous motions effectively due to the high manipulability. Moreover, the redundancy supported with a passive DoF of the orthosis section has the major impact on the overall manipulability increase of the trans-humeral

ortho-prosthesis.

As the last phase of this research work a prototype of the proposed trans-humeral ortho-prosthesis was fabricated. With the high manipulability provided by the shoulder orthosis, experimental results have verified that the trans-humeral ortho-prosthesis has the ability to perform dexterous motions. Furthermore, the reduced joint angle misalignment of the trans-humeral ortho-prosthesis, caused by the redundancy of the proposed orthosis, has reduced the error between the paths of human arm and the hand of the ortho-prosthesis to 3.8mm. It is a 181.9mm decrease of the error compared to the error of the path of the hand of the prosthesis when humerus is kept stationary.

5.2 Future Directions

This research work carried out by keeping the joints of the orthosis as passive DoF. Hence, for the future directions, the prototype should be developed with powered DoF according to the design, by adding the motors included in the design.

In order to control the trans-humeral prosthesis a proportional controller is used. However, for the best use of the prosthesis an intelligent system can be incorporated with the propotional controller. Furthermore, controlling algorithm should be extended to control the orthosis section in a way that both orthosis and prosthesis joint motions are synchronized to achieve the desired motions. For this purpose, the ortho-prosthesis must have an intelligent system incorporated with its hardware system.

In this thesis, all the experiments are carried out on healthy human subjects. For the successful validation of the proposed trans-humeral ortho-prosthesis, a trans-humeral amputee should be allowed to wear it and experiments should be carried out on him. After the clinical trials trans-humeral ortho-prosthesis should

be fabricated with designed materials with the modifications added according to the insights and feedbacks of the amputees and medical adepts.

LIST OF PUBLICATIONS

Articles Accepted/Submitted in International Conferences

1. **R. A. M. Abayasiri**, D. G. K. Madusanka, N. M. P. Arachchige, A. T. S. Silva, and R. A. R. C. Gopura, "MoBio: A 5 DOF Trans-humeral Robotic Prosthesis", in *2017 International Conference on Rehabilitation Robotics (ICORR)*, pp. 1627-1632, 2017

2. **R. A. M. Abayasiri**, R. A. R. C. Gopura and R. K. P. S. Ranaweera, "A Trans-Humeral Ortho-Prosthesis: Towards Power Assistive Prostheses", in *4th International Conference on Control, Automation and Robotics (ICCAR)*, pp. 470-475, 2018

3. **R. A. M. Abayasiri** and R. A. R. C. Gopura A Study on Manipulability of a 9 DoF Trans-humeral Ortho-prosthesis, in *112th Annual Sessions, The Institution of Engineers, Sri Lanka*, pp. 619-626, 2018

4. **R. A. M. Abayasiri** and R. A. R. C. Gopura "A Redundant Trans-humeral Ortho-prosthesis with Novel Shoulder Orthosis for Human Like Motion Generation"(Unpublished)

5. **R. A. M. Abayasiri**, R. A. R. C. Gopura and Kazuo Kiguchi "A Trans-humeral Ortho-prosthesis for the amputees with weak stump arms" in *6th Conference on Sri Lanka - Japan Collaborative Research*, p. 16, 2018

REFERENCES

[1] Merriam-Webster, "Robot." [Online]. Available: https://www.merriam-webster.com/dictionary/robot. [Accessed on 22-Aug-2018].

[2] S. Kalan, S. Chauhan, R. F. Coelho, M. A. Orvieto, I. R. Camacho, K. J. Palmer, and V. R. Patel, "History of robotic surgery," *Journal of Robotic Surgery*, vol. 4, no. 3, pp. 141–147, 2010.

[3] C. C. Kemp, A. Edsinger, and E. Torres-Jara, "Challenges for robot manipulation in human environments [grand challenges of robotics]," *IEEE Robotics & Automation Magazine*, vol. 14, no. 1, pp. 20–29, 2007.

[4] T. Fong, I. Nourbakhsh, and K. Dautenhahn, "A survey of socially interactive robots," *Robotics and autonomous systems*, vol. 42, no. 3-4, pp. 143–166, 2003.

[5] R. A. R. C. Gopura, D. S. V. Bandara, K. Kiguchi, and G. K. I. Mann, "Developments in hardware systems of active upper-limb exoskeleton robots: A review," *Robotics and Autonomous Systems*, vol. 75, pp. 203–220, 2016.

[6] K. M. Norton, "A Brief History of Prosthetics." [Online]. Available: https://www.amputee-coalition.org/resources/a-brief-history-of-prosthetics/. [Accessed on 22-Aug-2018].

[7] D. S. V. Bandara, R. A. R. C. Gopura, K. T. M. U. Hemapala, and K. Kiguchi, "Upper extremity prosthetics: current status, challenges and future directions," in *Seventeenth International Symposium on Artificial Life Robot*, Citeseer, 2012.

[8] D. G. K. Madusanka, R. A. R. C. Gopura, Y. W. R. Amarasinghe, and G. K. I. Mann, "Spatial path following scheme for a trans-humeral prosthesis," in *Robotics and Biomimetics (ROBIO), 2017 IEEE International Conference on*, pp. 737–742, IEEE, 2017.

[9] C. Lake and R. Dodson, "Progressive upper limb prosthetics," *Physical Medicine and Rehabilitation Clinics*, vol. 17, no. 1, pp. 49–72, 2006.

[10] C. A. Krueger, J. C. Rivera, D. J. Tennent, A. J. Sheean, D. J. Stinner, and J. C. Wenke, "Late amputation may not reduce complications or improve mental health in combat-related, lower extremity limb salvage patients," *Injury*, vol. 46, no. 8, pp. 1527–1532, 2015.

[11] D. G. K. Madusanka, "Development of a vision aided reach-to-grasp path planning and controlling method for trans-humeral robotic prostheses," PhD [Dissertation]. Moratuwa, University of Moratuwa, 2018.

[12] M. Allami, B. Mousavi, M. Masoumi, E. Modirian, H. Shojaei, F. Mirsalimi, M. Hosseini, and P. Pirouzi, "A comprehensive musculoskeletal and peripheral nervous system assessment of war-related bilateral upper extremity amputees," *Military Medical Research*, vol. 3, no. 1, p. 34, 2016.

[13] R. Gailey, K. Allen, J. Castles, J. Kucharik, and M. Roeder, "Review of secondary physical conditions associated with lower-limb amputation and long-term prosthesis use.," *Journal of Rehabilitation Research & Development*, vol. 45, no. 1, pp. 15–28, 2008.

[14] F. Cordella, A. L. Ciancio, R. Sacchetti, A. Davalli, A. G. Cutti, E. Guglielmelli, and L. Zollo, "Literature review on needs of upper limb prosthesis users," *Frontiers in neuroscience*, vol. 10, p. 209, 2016.

[15] L. Flynn, J. Geeroms, R. Jimenez-Fabian, B. Vanderborght, and D. Lefeber, "Cyberlegs beta-prosthesis active knee system," in *2015 IEEE International Conference on Rehabilitation Robotics (ICORR)*, pp. 410–415, IEEE, 2015.

[16] C. L. Semasinghe, J. L. B. Prasanna, H. M. Kandamby, R. K. P. S. Ranaweera, D. G. K. Madusanka, and R. A. R. C. Gopura, "Transradial prostheses: Current status and future directions," in *Manufacturing & Industrial Engineering Symposium (MIES)*, pp. 1–7, IEEE, 2016.

[17] R. J. Schwarz and C. Taylor, "The anatomy and mechanics of the human hand," *Artificial limbs*, vol. 2, no. 2, pp. 22–35, 1955.

[18] A. R. Tilley, *The measure of man and woman: human factors in design*, vol. 1. John Wiley & Sons, 2002.

[19] K.-N. An, E. Y. Chao, W. P. Cooney III, and R. L. Linscheid, "Normative model of human hand for biomechanical analysis," *Journal of biomechanics*, vol. 12, no. 10, pp. 775–788, 1979.

[20] T. Tsuji, P. G. Morasso, K. Goto, and K. Ito, "Human hand impedance characteristics during maintained posture," *Biological cybernetics*, vol. 72, no. 6, pp. 475–485, 1995.

[21] H. Haken, J. S. Kelso, and H. Bunz, "A theoretical model of phase transitions in human hand movements," *Biological cybernetics*, vol. 51, no. 5, pp. 347–356, 1985.

[22] J. J. Uicker, J. Denavit, and R. S. Hartenberg, "An iterative method for the displacement analysis of spatial mechanisms," *Journal of Applied Mechanics*, vol. 31, no. 2, pp. 309–314, 1964.

[23] F. Piltan, S. H. T. Haghighi, N. Sulaiman, I. Nazari, and S. Siamak, "Artificial control of puma robot manipulator: A-review of fuzzy inference engine and application to classical controller," *International Journal of Robotics and Automation*, vol. 2, no. 5, pp. 401–425, 2011.

[24] T. Yoshikawa, "Analysis and control of robot manipulators with redundancy," in *Robotics research: the first international symposium*, pp. 735–747, MIT press Cambridge, MA, 1984.

[25] T. Yoshikawa, "Manipulability of robotic mechanisms," *The international journal of Robotics Research*, vol. 4, no. 2, pp. 3–9, 1985.

[26] R. M. Murray, *A mathematical introduction to robotic manipulation*. CRC press, 2017.

[27] A. Torabi, M. Khadem, K. Zareinia, G. R. Sutherland, and M. Tavakoli, "Manipulability of teleoperated surgical robots with application in design of master/slave manipulators," in *Medical Robotics (ISMR), 2018 International Symposium on*, pp. 1–6, IEEE, 2018.

[28] "Medical dictionary." [Online]. Available: https://medical-dictionary.thefreedictionary.com/orthosis. [Accessed on 22-Aug-2018].

[29] T. Rahman, W. Sample, R. Seliktar, M. Alexander, and M. Scavina, "A body-powered functional upper limb orthosis," *Journal of rehabilitation research and development*, vol. 37, no. 6, pp. 675–680, 2000.

[30] J. C. Perry, J. Rosen, and S. Burns, "Upper-limb powered exoskeleton design," *IEEE/ASME transactions on mechatronics*, vol. 12, no. 4, pp. 408–417, 2007.

[31] R. A. R. C. Gopura and K. Kiguchi, "Mechanical designs of active upper-limb exoskeleton robots: State-of-the-art and design difficulties," in *Rehabilitation Robotics, 2009. ICORR 2009. IEEE International Conference on*, pp. 178–187, IEEE, 2009.

[32] J. Klein, S. Spencer, J. Allington, K. Minakata, E. Wolbrecht, R. Smith, J. Bobrow, and D. Reinkensmeyer, "Biomimetic orthosis for the neurorehabilitation of the elbow and shoulder (BONES)," in *Biomedical Robotics and Biomechatronics, 2008. BioRob 2008. 2nd IEEE RAS & EMBS International Conference on*, pp. 535–541, IEEE, 2008.

[33] A. Ebrahimi, D. Gröninger, R. Singer, and U. Schneider, "Control parameter optimization of the actively powered upper body exoskeleton using subjective

feedbacks," in *2017 3rd International Conference on Control, Automation and Robotics (ICCAR)*, pp. 432–437, IEEE, 2017.

[34] T. D. R. G. Thalagala, S. D. K. C. Silva, L. K. A. H. Maduwantha, R. K. P. S. Ranaweera, and R. A. R. C. Gopura, "A 4 dof exoskeleton robot with a novel shoulder joint mechanism," in *2016 IEEE/SICE International Symposium on System Integration (SII)*, pp. 132–137, IEEE, 2016.

[35] L. Colizzi, A. Lidonnici, and L. Pignolo, "The aramis project: a concept robot and technical design," *Journal of rehabilitation medicine*, vol. 41, no. 12, pp. 1011–1015, 2009.

[36] L. Pignolo, G. Dolce, G. Basta, L. Lucca, S. Serra, and W. Sannita, "Upper limb rehabilitation after stroke: ARAMIS a robo-mechatronic innovative approach and prototype," in *2012 4th IEEE RAS & EMBS International Conference on Biomedical Robotics and Biomechatronics (BioRob)*, pp. 1410–1414, IEEE, 2012.

[37] Y. Mao and S. K. Agrawal, "Design of a Cable-Driven Arm Exoskeleton (CAREX) for Neural Rehabilitation," *IEEE Transactions on Robotics*, vol. 28, pp. 922–931, Aug. 2012.

[38] Y. Mao, X. Jin, G. G. Dutta, J. P. Scholz, and S. K. Agrawal, "Human movement training with a cable driven arm exoskeleton (carex)," *IEEE Transactions on Neural Systems and Rehabilitation Engineering*, vol. 23, no. 1, pp. 84–92, 2015.

[39] R. A. R. C. Gopura, K. Kiguchi, and Y. Li, "SUEFUL-7: A 7dof upper-limb exoskeleton robot with muscle-model-oriented EMG-based control," in *2009 IEEE/RSJ International Conference on Intelligent Robots and Systems*, pp. 1126–1131, Oct. 2009.

[40] T. Nef and R. Riener, "Three-dimensional multi-degree-of-freedom arm therapy robot (ARMin)," in *Neurorehabilitation technology*, pp. 141–157, Springer, 2012.

[41] A. Frisoli, F. Rocchi, S. Marcheschi, A. Dettori, F. Salsedo, and M. Bergamasco, "A new force-feedback arm exoskeleton for haptic interaction in virtual environments," in *First Joint Eurohaptics Conference and Symposium on Haptic Interfaces for Virtual Environment and Teleoperator Systems. World Haptics Conference*, pp. 195–201, IEEE, 2005.

[42] P. Letier and A. Preumont, "Portable haptic arm exoskeleton," in *Prototyping of Robotic Systems: Applications of Design and Implementation*, pp. 122–145, IGI Global, 2012.

[43] A. Schiele and G. Hirzinger, "A new generation of ergonomic exoskeletons - The high-performance X-Arm-2 for space robotics telepresence," in *2011 IEEE/RSJ International Conference on Intelligent Robots and Systems*, pp. 2158–2165, Sept. 2011.

[44] M. H. Rahman, M. J. Rahman, O. Cristobal, M. Saad, J.-P. Kenné, and P. S. Archambault, "Development of a whole arm wearable robotic exoskeleton for rehabilitation and to assist upper limb movements," *Robotica*, vol. 33, no. 1, pp. 19–39, 2015.

[45] A. Frisoli, L. Borelli, A. Montagner, S. Marcheschi, C. Procopio, F. Salsedo, M. Bergamasco, M. C. Carboncini, M. Tolaini, and B. Rossi, "Arm rehabilitation with a robotic exoskeleleton in virtual reality," in *Rehabilitation Robotics, 2007. ICORR 2007. IEEE 10th International Conference on*, pp. 631–642, IEEE, 2007.

[46] K. Kiguchi, M. H. Rahman, M. Sasaki, and K. Teramoto, "Development of a 3dof mobile exoskeleton robot for human upper-limb motion assist," *Robotics and Autonomous systems*, vol. 56, no. 8, pp. 678–691, 2008.

[47] L. Resnik, S. L. Klinger, and K. Etter, "The deka arm: Its features, functionality, and evolution during the veterans affairs study to optimize the deka arm," *Prosthetics and orthotics international*, vol. 38, no. 6, pp. 492–504, 2014.

[48] L. Resnik, M. R. Meucci, S. Lieberman-Klinger, C. Fantini, D. L. Kelty, R. Disla, and N. Sasson, "Advanced upper limb prosthetic devices: implications for upper limb prosthetic rehabilitation," *Archives of physical medicine and rehabilitation*, vol. 93, no. 4, pp. 710–717, 2012.

[49] K. B. Fite, T. J. Withrow, K. W. Wait, and M. Goldfarb, "A gas-actuated anthropomorphic transhumeral prosthesis," in *2007 IEEE International Conference on Robotics and Automation*, pp. 3748–3754, IEEE, 2007.

[50] S. K. Kundu, K. Kiguchi, and E. Horikawa, "Design and Control Strategy for a 5 DOF Above-Elbow Prosthetic Arm," *International Journal of Assistive Robotics and Mechatronics*, vol. 9, pp. 79–93, 2008.

[51] L. Resnik, J. Cancio, S. Klinger, G. Latlief, N. Sasson, and L. Smurr-Walters, "Predictors of retention and attrition in a study of an advanced upper limb prosthesis: Implications for adoption of the deka arm," *Disability and Rehabilitation: Assistive Technology*, vol. 13, no. 2, pp. 206–210, 2018.

[52] K. B. Fite, T. J. Withrow, X. Shen, K. W. Wait, J. E. Mitchell, and M. Goldfarb, "A gas-actuated anthropomorphic prosthesis for transhumeral amputees," *IEEE Transactions on Robotics*, vol. 24, no. 1, pp. 159–169, 2008.

[53] "A'Manhattan Project'for the Next Generation of Bionic Arms." [Online]. Available: https://spectrum.ieee.org/biomedical/bionics/a-manhattan-project-for-the-next-generation-of-bionic-arms. [Accessed on 22-Aug-2018].

[54] C. D. Brenner and J. K. Brenner, "The use of preparatory/evaluation/training prostheses in developing evidenced-based practice in upper limb prosthetics," *JPO: Journal of Prosthetics and Orthotics*, vol. 20, no. 3, pp. 70–82, 2008.

[55] G. R. Hurley and J. R. Williams, "Modular prosthetic sockets and methods for making same," Mar. 17 2015. US Patent 8,978,224.

[56] L. Resnik, T. Patel, S. G. Cooney, J. J. Crisco, and C. Fantini, "Comparison of transhumeral socket designs utilizing patient assessment and in vivo skeletal and socket motion tracking: a case study," *Disability and Rehabilitation: Assistive Technology*, vol. 11, no. 5, pp. 423–432, 2016.

[57] A. Esquenazi and R. H. Meier, "Rehabilitation in limb deficiency. 4. limb amputation," *Archives of physical medicine and rehabilitation*, vol. 77, no. 3, pp. S18–S28, 1996.

[58] T. A. K. Gaber, C. Gardner, and S. Kirker, "Silicone roll-on suspension for upper limb prostheses: users views," *Prosthetics and orthotics international*, vol. 25, no. 2, pp. 113–118, 2001.

[59] C. Lake, "The evolution of upper limb prosthetic socket design," *JPO: Journal of Prosthetics and Orthotics*, vol. 20, no. 3, pp. 85–92, 2008.

[60] S. Jönsson, K. Caine-Winterberger, and R. Brånemark, "Osseointegration amputation prostheses on the upper limbs: methods, prosthetics and rehabilitation," *Prosthetics and orthotics international*, vol. 35, no. 2, pp. 190–200, 2011.

[61] M. Ortiz-Catalan, B. Håkansson, and R. Brånemark, "An osseointegrated human-machine gateway for long-term sensory feedback and motor control of artificial limbs," *Science translational medicine*, vol. 6, no. 257, pp. 257re6–257re6, 2014.

[62] D. Farina and S. Amsüss, "Reflections on the present and future of upper limb prostheses," *Expert review of medical devices*, vol. 13, no. 4, pp. 321–324, 2016.

[63] G. Li and T. A. Kuiken, "Modeling of prosthetic limb rotation control by sensing rotation of residual arm bone," *IEEE Transactions on Biomedical Engineering*, vol. 55, no. 9, pp. 2134–2142, 2008.

[64] E. Witsø, T. Kristensen, P. Benum, S. Sivertsen, L. Persen, A. Funderud, T. Magne, H. P. Aursand, and A. Aamodt, "Improved comfort and function of arm prosthesis after implantation of a humerus-t-prosthesis in transhumeral amputees," *Prosthetics and orthotics international*, vol. 30, no. 3, pp. 270–278, 2006.

[65] P. K. Tomaszewski, M. Van Diest, S. K. Bulstra, N. Verdonschot, and G. J. Verkerke, "Numerical analysis of an osseointegrated prosthesis fixation with reduced bone failure risk and periprosthetic bone loss," *Journal of Biomechanics*, vol. 45, no. 11, pp. 1875–1880, 2012.

[66] S. Lathers and J. La Belle, "Advanced manufactured fused filament fabrication 3d printed osseointegrated prosthesis for a transhumeral amputation using taulman 680 fda," *3D Printing and Additive Manufacturing*, vol. 3, no. 3, pp. 166–174, 2016.

[67] G. Tsikandylakis, Ö. Berlin, and R. Brånemark, "Implant survival, adverse events, and bone remodeling of osseointegrated percutaneous implants for transhumeral amputees," *Clinical Orthopaedics and Related Research®*, vol. 472, no. 10, pp. 2947–2956, 2014.

[68] D. A. Bennett, J. E. Mitchell, D. Truex, and M. Goldfarb, "Design of a Myoelectric Transhumeral Prosthesis," *IEEE/ASME Transactions on Mechatronics*, vol. 21, pp. 1868–1879, Aug. 2016.

[69] T. Lenzi, J. Lipsey, and J. W. Sensinger, "The ric arma small anthropomorphic transhumeral prosthesis," *IEEE/ASME Transactions on Mechatronics*, vol. 21, no. 6, pp. 2660–2671, 2016.

[70] G. Kejlaa, "Consumer concerns and the functional value of prostheses to upper limb amputees," *Prosthetics and orthotics international*, vol. 17, no. 3, pp. 157–163, 1993.

[71] K. A. Raichle, M. A. Hanley, I. Molton, N. J. Kadel, K. Campbell, E. Phelps, D. Ehde, and D. G. Smith, "Prosthesis use in persons with lower-and

upper-limb amputation," *Journal of rehabilitation research and development*, vol. 45, no. 7, p. 961, 2008.

[72] K. Østlie, R. J. Franklin, O. H. Skjeldal, A. Skrondal, and P. Magnus, "Musculoskeletal pain and overuse syndromes in adult acquired major upper-limb amputees," *Archives of physical medicine and rehabilitation*, vol. 92, no. 12, pp. 1967–1973, 2011.

[73] K. M. Flood, M. E. Huang, T. L. Roberts, P. F. Pasquina, V. S. Nelson, and P. R. Bryant, "Limb deficiency and prosthetic management. 2. aging with limb loss," *Archives of physical medicine and rehabilitation*, vol. 87, no. 3, pp. 10–14, 2006.

[74] I. Vujaklija, D. Farina, and O. C. Aszmann, "New developments in prosthetic arm systems," *Orthopedic Research and Reviews*, vol. 8, pp. 31–39, 2016.

[75] N. A. A. Razak, N. A. A. Osman, H. Gholizadeh, and S. Ali, "Biomechanics principle of elbow joint for transhumeral prostheses: comparison of normal hand, body-powered, myoelectric & air splint prostheses," *Biomedical engineering online*, vol. 13, no. 1, p. 134, 2014.

[76] F. Casolo, "Elbow prosthesis for partial or total upper limb replacements," in *Motion control*, InTech, 2010.

[77] W. D. I. G. Dasanayake, R. A. R. C. Gopura, V. P. C. Dassanayake, and G. K. I. Mann, "Estimation of prosthetic arm motions using stump arm kinematics," in *Information and Automation for Sustainability (ICIAfS), 2014 7th International Conference on*, pp. 1–6, IEEE, 2014.

[78] "The anatomy body." [Online]. Available: http://www.danafarberbostonchildrens.org/why-choose-us/expertise/surgery/rotationplasty.aspx. [Accessed on 22-Aug-2018].

[79] E. MARQUARDT, "The operative treatment of congenital limb malformationpart III," *Prosthetics and Orthotics International*, p. 61.

[80] F. Schiedel and R. Rödl, "Lower limb lengthening in patients with disproportionate short stature with achondroplasia: a systematic review of the last 20 years," *Disability and rehabilitation*, vol. 34, no. 12, pp. 982–987, 2012.

[81] L. E. Ramseier, C. E. Dumont, and G. Ulrich Exner, "Rotationplasty (borggreve/van nes and modifications) as an alternative to amputation in failed reconstructions after resection of tumours around the knee joint," *Scandinavian journal of plastic and reconstructive surgery and hand surgery*, vol. 42, no. 4, pp. 199–201, 2008.

[82] A. S. Niyetkaliyev, S. Hussain, M. H. Ghayesh, and G. Alici, "Review on design and control aspects of robotic shoulder rehabilitation orthoses," *IEEE Transactions on Human-Machine Systems*, vol. 47, no. 6, pp. 1134–1145, 2017.

[83] S. B. Kesner, L. P. Jentoft, F. Hammond, R. D. Howe, and M. Popovic, "Design considerations for an active soft orthotic system for shoulder rehabilitation," 2011.

[84] D. J. Magermans, E. K. J. Chadwick, H. E. J. Veeger, and F. C. T. van der Helm, "Requirements for upper extremity motions during activities of daily living," *Clinical Biomechanics*, vol. 20, pp. 591–599, July 2005.

[85] B. D. Rubin and J. A. Schlechter, "Shoulder Biomechanics, Examination, and Rehabilitation Principles," *AANA Advanced Arthroscopy: The Shoulder E-Book*, pp. 24–33, 2010.

[86] C. Carignan, M. Liszka, and S. Roderick, "Design of an arm exoskeleton with scapula motion for shoulder rehabilitation," in *ICAR'05. Proceedings., 12th International Conference on Advanced Robotics*, 2005.

[87] H. S. Lo and S. S. Xie, "Optimization of a redundant 4r robot for a shoulder exoskeleton," in *2013 IEEE/ASME International Conference on Advanced Intelligent Mechatronics (AIM)*, pp. 798–803, IEEE, 2013.

[88] T. Kijima, K. Matsuki, N. Ochiai, T. Yamaguchi, Y. Sasaki, E. Hashimoto, Y. Sasaki, H. Yamazaki, T. Kenmoku, S. Yamaguchi, *et al.*, "In vivo 3-dimensional analysis of scapular and glenohumeral kinematics: comparison of symptomatic or asymptomatic shoulders with rotator cuff tears and healthy shoulders," *Journal of shoulder and elbow surgery*, vol. 24, no. 11, pp. 1817–1826, 2015.

[89] T. Albrektsson and C. Johansson, "Osteoinduction, osteoconduction and osseointegration," *European spine journal*, vol. 10, no. 2, pp. S96–S101, 2001.

[90] P. Helliwell, "Biomechanics of the upper limbs: Mechanics, modeling, and musculoskeletal injuries," 2007.

[91] F. Parisi and G. Raiola, "Video analysis in youth volleyball team," 2014.

[92] A. Oosterwijk, M. Nieuwenhuis, C. van der Schans, and L. Mouton, "Shoulder and elbow range of motion for the performance of activities of daily living: A systematic review," *Physiotherapy theory and practice*, vol. 34, no. 7, pp. 505–528, 2018.

[93] C.-M. Shih, K.-C. Huang, C.-C. Pan, C.-H. Lee, and K.-C. Su, "Biomechanical analysis of acromioclavicular joint dislocation treated with clavicle hook plates in different lengths," *International orthopaedics*, vol. 39, no. 11, pp. 2239–2244, 2015.

[94] L. Jin, S. Li, H. M. La, and X. Luo, "Manipulability optimization of redundant manipulators using dynamic neural networks," *IEEE Transactions on Industrial Electronics*, vol. 64, no. 6, pp. 4710–4720, 2017.

[95] P. I. Corke, "A Simple and Systematic Approach to Assigning Denavit Hartenberg Parameters," *IEEE Transactions on Robotics*, vol. 23, pp. 590–594, June 2007.

[96] D. G. K. Madusanka, R. A. R. C. Gopura, Y. W. R. Amarasinghe, and G. K. I. Mann, "A simulation environment for control algorithms of tran-

shumeral prostheses," in *International Conference on Emerging Trends in Mechanical Engineering*, pp. 190–196, 2015.

[97] B. Sañudo, D. Rueda, B. d. Pozo-Cruz, M. de Hoyo, and L. Carrasco, "Validation of a video analysis software package for quantifying movement velocity in resistance exercises," *Journal of strength and conditioning research*, vol. 30, no. 10, pp. 2934–2941, 2016.

Appendix A

SIMULATION PROGRAM FOR MANIPULABILITY MEASURES COMPARISON OF 4DOF MANIPULATOR AND 6DOF MANIPULATOR

Before executing this program MATLAB Robotics Toolbox should be running on the computer. Furthermore, the given source codes are generated in MATLAB software.

A.1 Trajectory generation and calculation of manipulability measures of 4DoF manipulator

```
clear

%Defining global variables

deg=pi/180;
L1= 115;
L2= 297.5+135;
r=200;


% L(i) = Link ([q d a alpha]); Defining link
```

```
L(1) = Revolute('d', 0, 'a', r, 'alpha', 0);
L(2) = Revolute('d', L1, 'a', 0, 'alpha', -pi/2);
L(3) = Revolute('d', 0, 'a', 0, 'alpha', pi/2);
L(4) = Revolute('d', L2, 'a', 0, 'alpha', 0);

arm = SerialLink(L, 'name', '4DOF Manipulator');

%Trajectory Generation

qi=[-pi/9,pi/9,5*pi/6,0];
qf=[0,2*pi/9,0,0];
q=jtraj(qi,qf,20);
figure(21)

%plotting link model
arm.plot (q);

ortho=arm.fkine(q);

%Opening files to write

file_ind = fopen('ortho_dummy_manipl.csv','w');
file_sing = fopen('ortho_dummy_sing.csv','w');
file_cond_num = fopen('ortho_dummy_cond.csv','w');

%Calculating mnipulability measures

for i=1:1:20
joint=i;
joint
```

```
%Jacobian of each joint

Ji = arm.jacob0(q(i,:));
Ji

%Manipulability index

Ji_v=Ji(1:3,:);
Ji_v_transpose=Ji_v';
Ji_v
Ji_v_transpose
Manipulability_index = sqrt(det(Ji_v*Ji_v'));
Manipulability_index

%Writing Manipulability index data on the file

fprintf(file_ind,'%f,%f\n',joint,Manipulability_index );

%singular values of jacobian

singular_values_Ji_v=svd(Ji_v);
singular_values_Ji_v

%Writing Singular Values on the file

fprintf(file_sing,'%f,%f,%f,%f\n',joint,singular_values_Ji_v );

%condition Number
```

```
condition_Number=cond(Ji_v);
condition_Number

%Writing Condition Number data on the file

fprintf(file_cond_num,'%f,%f\n',joint,condition_Number );

%Manipulability Ellipsoids

figure(i)
plot_ellipse(Ji_v*Ji_v_transpose);
view(-60,20);

end

%Closingopenedfiles

fclose(file_ind);
fclose(file_sing);
fclose(file_cond_num);

A=ortho(:,4,:);
A
file_pos=fopen('ortho_dummy_pos.csv','w');
fprintf(file_pos,'%f,%f,%f,%f\n',A);
fclose(file_pos);
```

A.2 Trajectory generation and calculation of manipulability measures of 6DoF manipulator

```
%Clearing all the previous variables
clear

%Defining Global Variables
deg = pi/180;
r2= 200;
l3= 115;
l4= 100;
r5a = 135;
r5b = 135;
r=sqrt(r5b*r5b+r5b*r5b);
l6a= 297.5;
t5=pi/4;

%L(i) = Link ([q d a alpha]); Defining link

L(1) = Revolute('d', 0, 'a', r2, 'alpha', 0 );
L(2) = Revolute('d', l3, 'a', 0, 'alpha', -pi/2);
L(3) = Revolute('d', 0, 'a', l4, 'alpha', 0);
L(4) = Revolute('d', 135, 'a', 0, 'alpha', pi/2);
L(5) = Revolute('d', 0, 'a', 0, 'alpha', pi/2);
L(6) = Revolute('d', l6a, 'a', 0, 'alpha', 0);

arm = SerialLink(L, 'name', '6DOF Manipulator');

%Trajectory Generation
```

```
qi=[-pi/6,-pi/9,pi/9,-2*pi/3,3*pi/2,pi/6];
qf=[-pi/18,-pi/9,-pi/9,-4*pi/3,3*pi/2,pi/6];
q=jtraj(qi,qf,20);
figure(21)

%plotting link model
arm.plot (q);

ortho=arm.fkine(q);

%Opening files to write

file_ind = fopen('ortho_Mani_ind_03_27.csv','w');
file_sing = fopen('ortho_sing_03_27.csv','w');
file_cond = fopen('ortho_cond_03_27.csv','w');

%Caluculating Manipulability Measures

for i=1:1:20
joint=i;
joint

%Jacobian of each joint

Ji = arm.jacob0(q(i,:));
Ji

%Manipulability index
```

```
Ji_v=Ji(1:3,:);
Ji_v_transpose=Ji_v';
Ji_v
Ji_v_transpose
Manipulability_index = sqrt(det(Ji_v*Ji_v'));
Manipulability_index

fprintf(file_ind,'%f,%f\n',joint,Manipulability_index );

%singular values of jacob0

singular_values_Ji_v=svd(Ji_v);

singular_values_Ji_v

fprintf(file_sing,'%f,%f,%f,%f\n',joint,singular_values_Ji_v);

%condition Number

condition_Number=cond(Ji_v);
condition_Number

fprintf(file_sing,'%f,%f\n',joint,condition_Number );

%Manipulability Ellipsoids
figure(i)
plot_ellipse(Ji_v*Ji_v_transpose);

end
```

```
%Closing opened files

fclose(file_ind);
fclose(file_sing);
fclose(file_cond);



A=ortho(:,4,:);
A
file_pos=fopen('ortho_pos.csv','w');
fprintf(file_pos,'%f,%f,%f,%f\n',A);
fclose(file_pos);
```

A.3 Trajectory generation and calculation of manipulability measures of proposed trans-humeral ortho-prosthesis

A.3.1 Shoulder Vertical F/E

```
%Clearing all the previous variables
clear

%Defining global variables
r2= 200;
l3= 115;
l4= 100;
r5a = 135;
r5b = 135;
l6a= 297.5;
l7 =135;
l9 = 237.8;
l10 = 20;
l = 69.5;

%L(i) = Link ([q d a alpha]); Defining link

L(1) = Revolute('d', 0, 'a', r2, 'alpha', 0 );
L(2) = Revolute('d', l3, 'a', 0, 'alpha', -pi/2);
L(3) = Revolute('d', 0, 'a', l4, 'alpha', 0);
L(4) = Revolute('d', 135, 'a', 0, 'alpha', pi/2);
L(5) = Revolute('d', 0, 'a', 0, 'alpha', pi/2);
L(6) = Revolute('d', l6a+l7, 'a', 0, 'alpha', -pi/2);
L(7) = Revolute('d', 0, 'a', 0, 'alpha', -pi/2);
L(8) = Revolute('d', l9, 'a', 0, 'alpha', pi/2);
```

```
L(9) = Revolute('d', 0, 'a', l10, 'alpha', -pi/2);
L(10) = Revolute('d', 0, 'a', l, 'alpha', 0);

arm = SerialLink(L, 'name', 'Trans-humeral Ortho-Prosthesis');

%Trajectory Generation

qi=[-pi/6,0,pi/9,-11*pi/18,3*pi/2,pi/6,-pi,pi/2,-pi/2,pi];
qf=[-5*pi/18,pi/9,-pi/9,-7*pi/18,pi/2,pi/6,-pi,pi/2,-pi/2,pi];
q=jtraj(qi,qf,20);
figure(21)
arm.plot (q);

ortho=arm.fkine(q);

%Opening files to write
file_ind = fopen('ortho_pros_VFE_Mani_ind_04_06.csv','w');
file_sing = fopen('ortho_pros_VFE_sing_04_06.csv','w');
file_cond = fopen('ortho_pros_VFE_cond_04_06.csv','w');
for i=1:1:20

%Caluculating Manipulability Measures

joint=i;
joint

%Jacobian of each joint

Ji = arm.jacob0(q(i,:));
Ji
```

```
%Manipulability index

Ji_v=Ji(1:3,:);
Ji_v_transpose=Ji_v';
Ji_v
Ji_v_transpose
Manipulability_index = sqrt(det(Ji_v*Ji_v'));
Manipulability_index

fprintf(file_ind,'%f,%f\n',joint,Manipulability_index );

%singular values of jacob0

singular_values_Ji_v=svd(Ji_v);

singular_values_Ji_v

fprintf(file_sing,'%f,%f,%f,%f\n',joint,singular_values_Ji_v);

%condition Number

condition_Number=cond(Ji_v);
condition_Number

fprintf(file_cond,'%f,%f\n',joint,condition_Number );

%Manipulability Ellipsoids
figure(i)
plot_ellipse(Ji_v*Ji_v_transpose);
```

```
end

%Closing the opened files

fclose(file_ind);
fclose(file_sing);
fclose(file_cond);

A=ortho(:,4,:);
A
file_pos=fopen('ortho_pros_pos_VFE.csv','w');
fprintf(file_pos,'%f,%f,%f,%f\n',A);
fclose(file_pos);
```

A.3.2 Shoulder Horizontal F/E

```
%Clearing all the previous variables

clear

r2= 200;
l3= 115;
l4= 100;
r5a = 135;
r5b = 135;
l6a= 297.5;
l7 =135;
l9 = 237.8;
l10 = 20;
l = 69.5;

%L(i) = Link ([q d a alpha]); Defining length

L(1) = Revolute('d', 0, 'a', r2, 'alpha', 0 );
L(2) = Revolute('d', l3, 'a', 0, 'alpha', -pi/2);
L(3) = Revolute('d', 0, 'a', l4, 'alpha', 0);
L(4) = Revolute('d', 135, 'a', 0, 'alpha', pi/2);
L(5) = Revolute('d', 0, 'a', 0, 'alpha', pi/2);
L(6) = Revolute('d', l6a+l7, 'a', 0, 'alpha', -pi/2);
L(7) = Revolute('d', 0, 'a', 0, 'alpha', -pi/2);
L(8) = Revolute('d', l9, 'a', 0, 'alpha', pi/2);
L(9) = Revolute('d', 0, 'a', l10, 'alpha', -pi/2);
L(10) = Revolute('d', 0, 'a', l, 'alpha', 0);
```

```
arm = SerialLink(L, 'name', 'Trans-Humeral Ortho-Prosthesis');

%Trajectory Generation
qi=[-pi/6,-pi/9,pi/9,-pi,3*pi/2,pi/6,-pi,pi/2,-pi/2,pi];
qf=[pi/9,4*pi/9,pi/18,-pi,3*pi/2,pi/6,-pi,pi/2,-pi/2,pi];
q=jtraj(qi,qf,20);
figure(21)
arm.plot (q);

ortho=arm.fkine(q);

%Opening files to write
file_ind = fopen('ortho_pros_HFE_Mani_ind_04_06.csv','w');
file_sing = fopen('ortho_pros_HFE_sing_04_06.csv','w');
file_cond = fopen('ortho_pros_HFE_cond_04_06.csv','w');

%Calculating manipulabilty measures
for i=1:1:20
joint=i;
joint
%Jacobian of each joint

Ji = arm.jacob0(q(i,:));
Ji

%Manipulability index

Ji_v=Ji(1:3,:);
Ji_v_transpose=Ji_v';
```

```
Ji_v
Ji_v_transpose
Manipulability_index = sqrt(det(Ji_v*Ji_v'));
Manipulability_index
fprintf(file_ind,'%f,%f\n',joint,Manipulability_index );

%singular values of jacob0

singular_values_Ji_v=svd(Ji_v);
singular_values_Ji_v
fprintf(file_sing,'%f,%f,%f,%f\n',joint,singular_values_Ji_v);

%condition Number

condition_Number=cond(Ji_v);
condition_Number

fprintf(file_cond,'%f,%f\n',joint,condition_Number );

%Manipulability Ellipsoids

figure(i)
plot_ellipse(Ji_v*Ji_v_transpose);

end

%Closing the opened Files
fclose(file_ind);
fclose(file_sing);
fclose(file_cond);
```

A.3.3 Shoulder Abd/Add

```
%Clearing all the previous variables
clear
%Defining Global variables
r2= 200;
l3= 115;
l4= 100;
r5a = 135;
r5b = 135;
l6a= 297.5;
l7 =135;
l9 = 237.8;
l10 = 20;
l = 69.5;

%L(i) = Link ([q d a alpha]); Defining length

L(1) = Revolute('d', 0, 'a', r2, 'alpha', 0 );
L(2) = Revolute('d', l3, 'a', 0, 'alpha', -pi/2);
L(3) = Revolute('d', 0, 'a', l4, 'alpha', 0);
L(4) = Revolute('d', 135, 'a', 0, 'alpha', pi/2);
L(5) = Revolute('d', 0, 'a', 0, 'alpha', pi/2);
L(6) = Revolute('d', l6a+l7, 'a', 0, 'alpha', -pi/2);
L(7) = Revolute('d', 0, 'a', 0, 'alpha', -pi/2);
L(8) = Revolute('d', l9, 'a', 0, 'alpha', pi/2);
L(9) = Revolute('d', 0, 'a', l10, 'alpha', -pi/2);
L(10) = Revolute('d', 0, 'a', l, 'alpha', 0);

arm = SerialLink(L, 'name', 'Trans-Humeral Ortho-Prosthesis');
```

```
%Trajecory generation
qi=[-pi/6,-pi/9,pi/9,-2*pi/3,3*pi/2,pi/6,-pi,pi/2,-pi/2,pi];
qf=[-pi/18,-pi/9,-pi/9,-4*pi/3,3*pi/2,pi/6,-pi,pi/2,-pi/2,pi];
q=jtraj(qi,qf,20);
figure(21)
arm.plot (q);

ortho=arm.fkine(q);

%Oening file to write
file_ind = fopen('ortho_pros_Mani_ind_AA_04_06.csv','w');
file_sing = fopen('ortho_pros_sing_AA_04_06.csv','w');
file_cond = fopen('ortho_pros_cond_AA_04_06.csv','w');

%Calculating Manipulability measures
for i=1:1:20
joint=i;
joint

%Jacobian of each joint
Ji = arm.jacob0(q(i,:));
Ji

%Manipulability index
Ji_v=Ji(1:3,:);
Ji_v_transpose=Ji_v';
Ji_v
Ji_v_transpose
Manipulability_index = sqrt(det(Ji_v*Ji_v'));
```

```
Manipulability_index
fprintf(file_ind,'%f,%f\n',joint,Manipulability_index );

%singular values of jacob0
singular_values_Ji_v=svd(Ji_v);
singular_values_Ji_v
fprintf(file_sing,'%f,%f,%f,%f\n',joint,singular_values_Ji_v);

%condition Number
condition_Number=cond(Ji_v);
condition_Number
fprintf(file_cond,'%f,%f\n',joint,condition_Number );

%Manipulability Ellipasoids

figure(i)
plot_ellipse(Ji_v*Ji_v_transpose);

end

%Closing the opened files
fclose(file_ind);
fclose(file_sing);
fclose(file_cond);

A=ortho(:,4,:);
A
file_pos=fopen('ortho_pros_pos_AA.csv','w');
fprintf(file_pos,'%f,%f,%f,%f\n',A);
fclose(file_pos);
```

Appendix B

ENGINEERING DRAWINGS OF PROSPOSED TRANS-HUMERAL ORTHO-PROSTHESIS

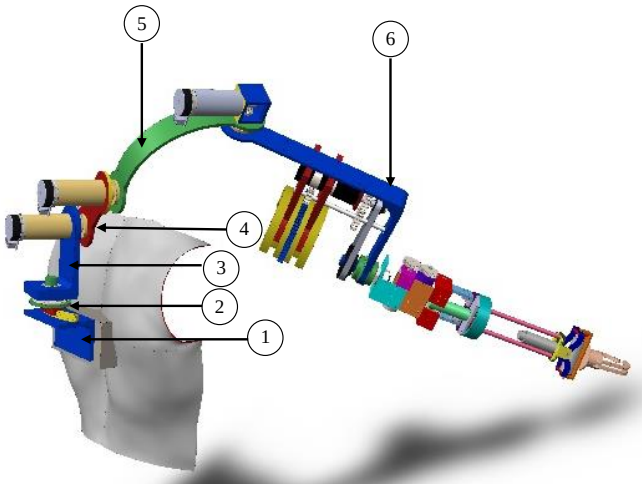

Figure B.1: Components of proposed trans-humeral ortho-prosthesis

Table B.1 shows the components labeled in the Figure B.1. Engineering drawings of these components are availble under this section. (For more details on the components of the proposed trans-humeral ortho-prosthesis, refer to the Computer Aided Design model of the ortho-prosthesis attached herewith.)

Table B.1: Description of the components of the proposed trans-humeral ortho-prosthesis

Item No:	Component
1	Back Stage
2	Thrust Bearing Holder
3	Vertical L Plate
4	Abd/Add Flat Plate
5	Abd/Add Curve Plate
6	F/E L Plate

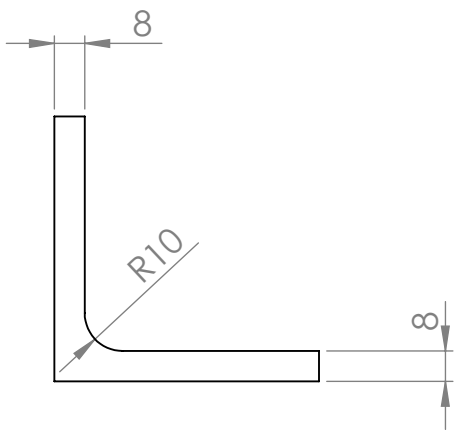

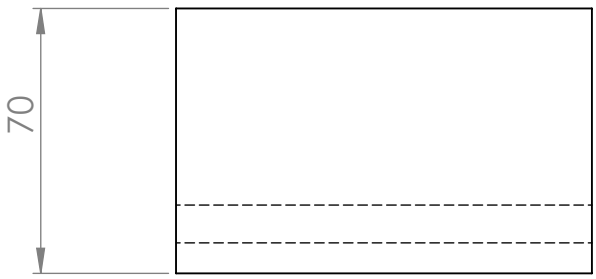

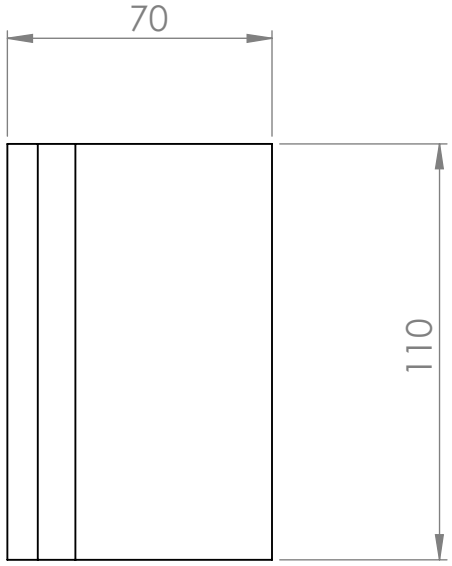

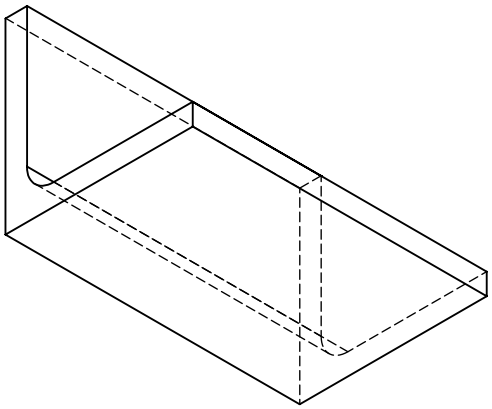

UNLESS OTHERWISE SPECIFIED:DIMENSIONS ARE IN MILLIMETERS

DO NOT SCALE DRAWING | REVISION

	NAME	SIGNATURE	DATE
DRAWN	RAM ABAYASIRI		
CHK'D			
APPV'D			
MFG			
Q.A			

TITLE:

BACK STAGE

MATERIAL:

DWG NO. 1

A4

WEIGHT:

SCALE:1:2

SHEET 1 OF 1

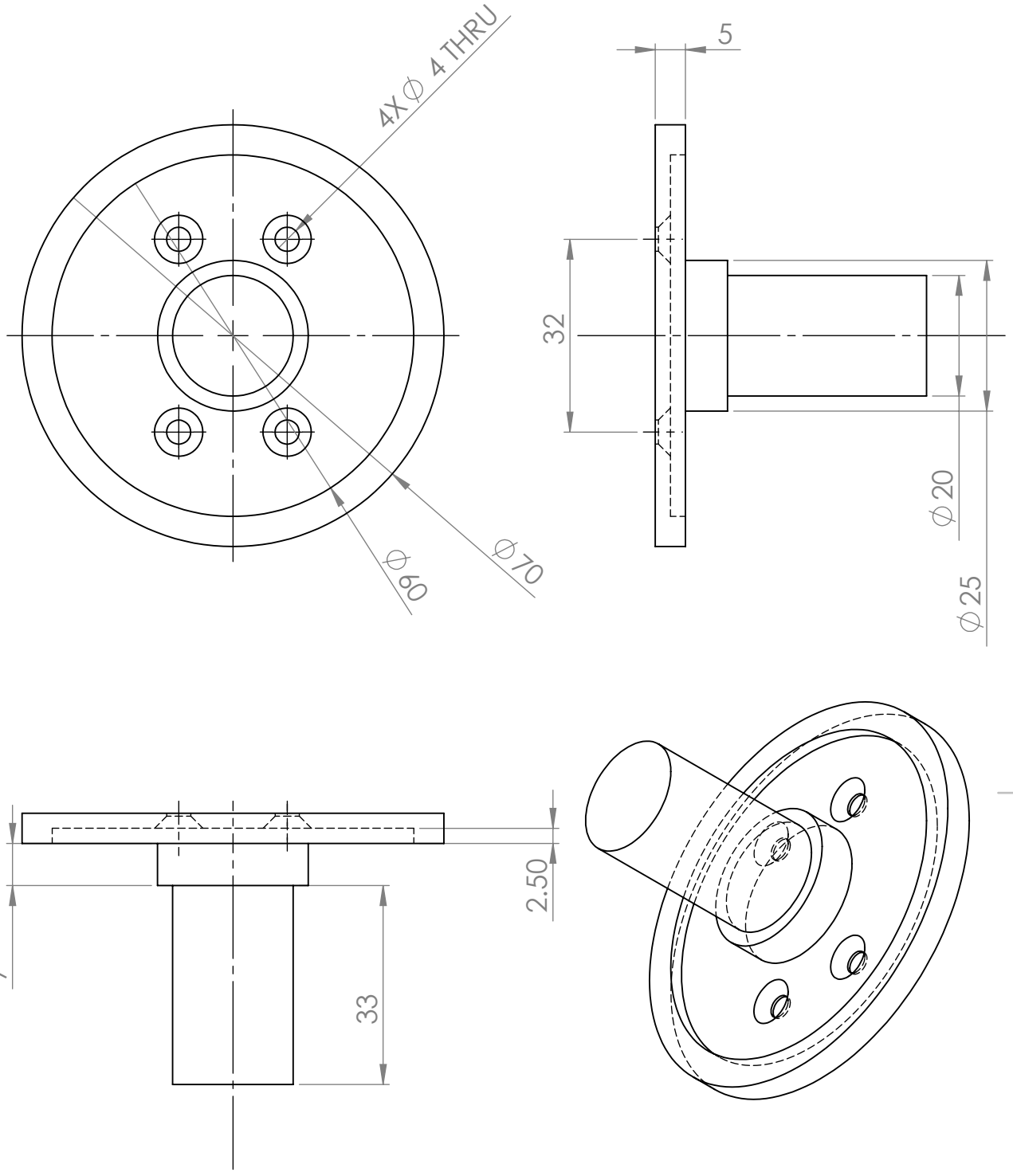

UNLESS OTHERWISE SPECIFIED:DIMENSIONS ARE IN MILLIMETERS

DO NOT SCALE DRAWING | REVISION

	NAME	SIGNATURE	DATE
DRAWN	RAM ABAYASIRI		
CHK'D			
APPV'D			
MFG			
Q.A			

TITLE:

THRUST BEARING HOLDER

MATERIAL:

ALUMINIUM

DWG NO. 2

A4

WEIGHT:

SCALE:1:1

SHEET 1 OF 1

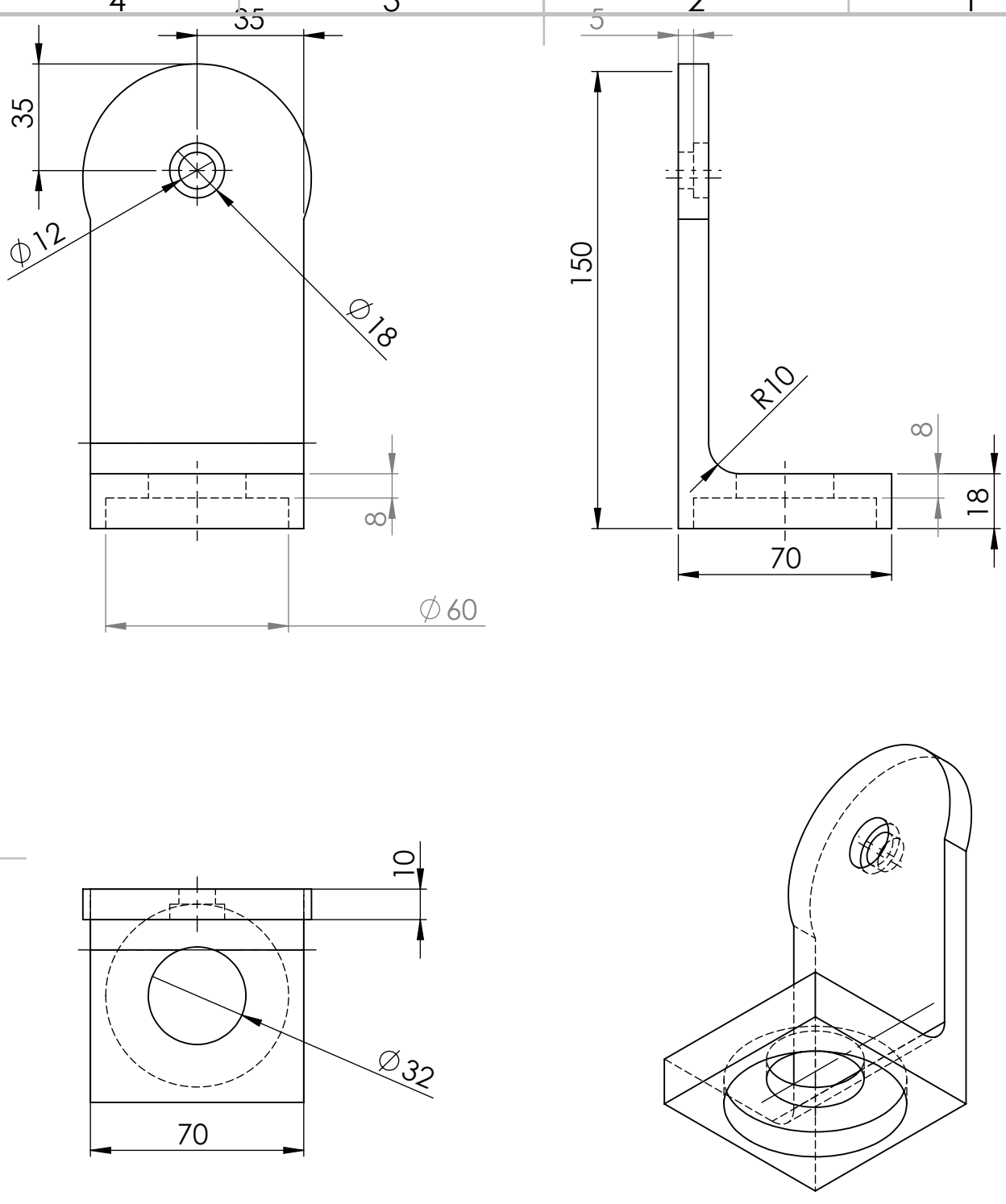

UNLESS OTHERWISE SPECIFIED:DIMENSIONS ARE IN MILLIMETERS

DO NOT SCALE DRAWING | REVISION

	NAME	SIGNATURE	DATE
DRAWN	RAM ABAYASIRI		
CHK'D			
APPV'D			
MFG			
Q.A			

TITLE:

VERTICAL L PLATE

MATERIAL:

ALUMINIUM

DWG NO.

3

A4

WEIGHT:

SCALE:1:2

SHEET 1 OF 1

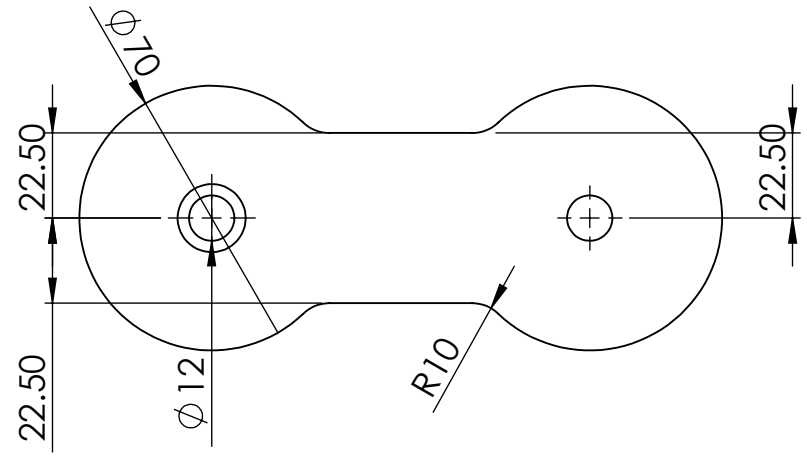

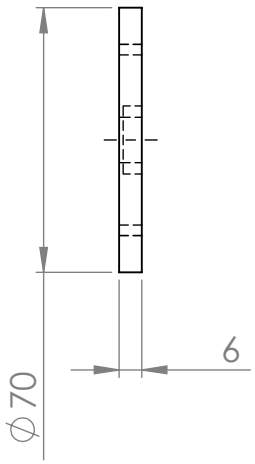

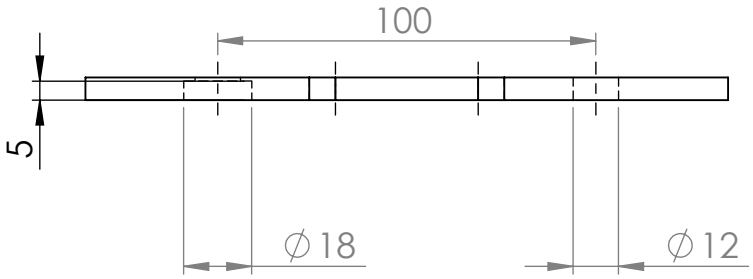

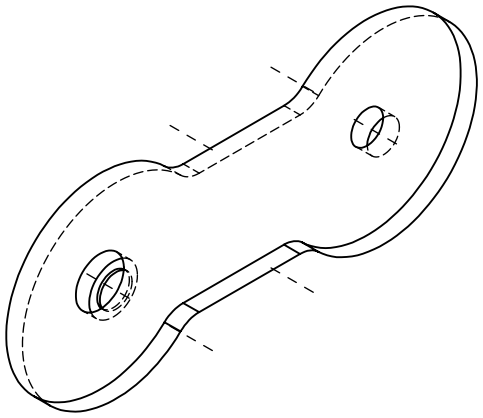

UNLESS OTHERWISE SPECIFIED:DIMENSIONS ARE IN MILLIMETERS

DO NOT SCALE DRAWING | REVISION

	NAME	SIGNATURE	DATE
DRAWN	RAM ABAYASIRI		
CHK'D			
APPV'D			
MFG			
Q.A			

TITLE:

ABD/ADD FLAT PLATE

MATERIAL:

ALUMINIUM

DWG NO.

4

A4

WEIGHT:

SCALE:1:2

SHEET 1 OF 1

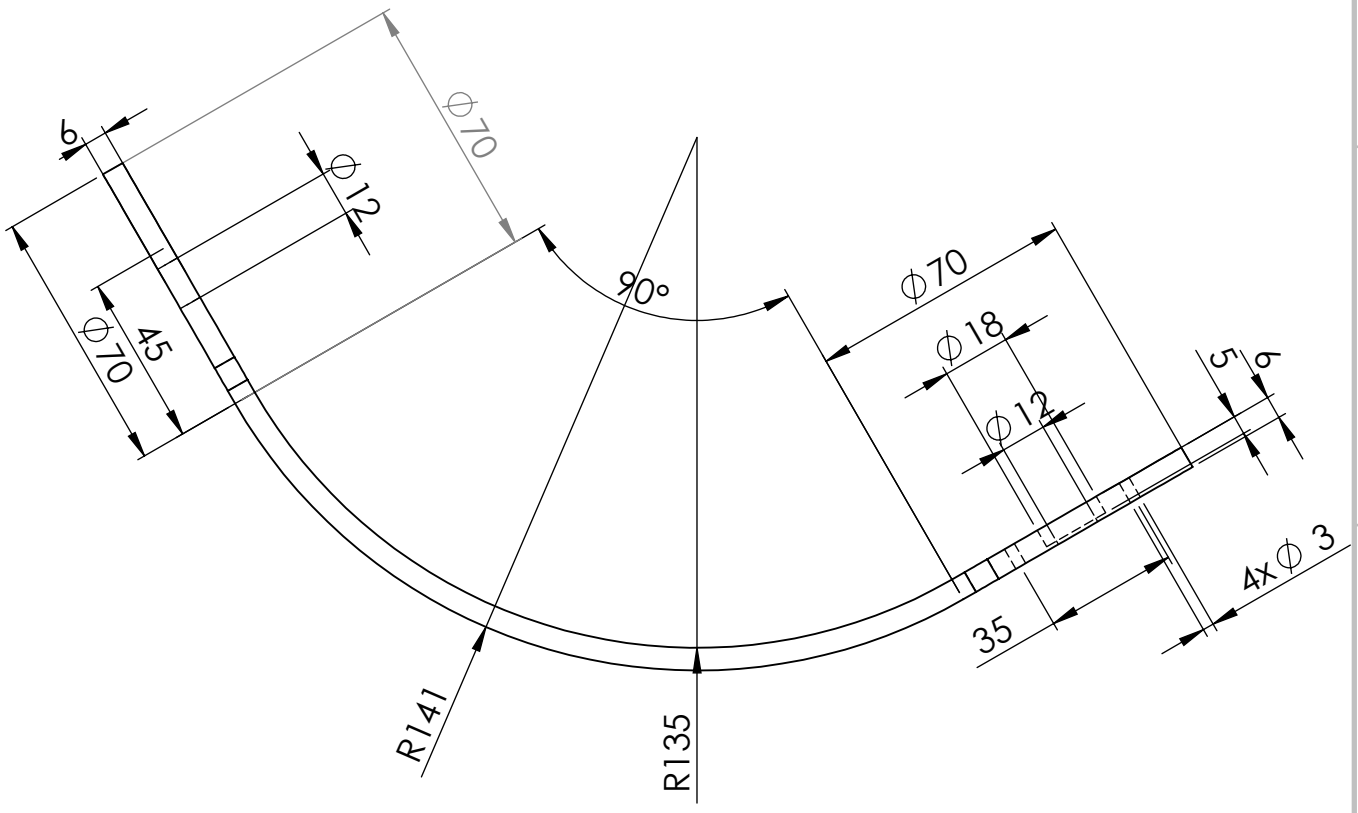

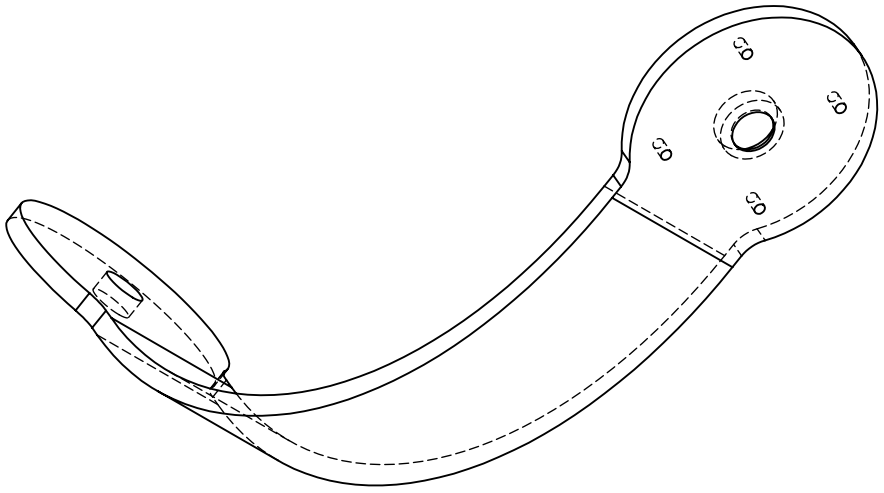

UNLESS OTHERWISE SPECIFIED:DIMENSIONS ARE IN MILLIMETERS

DO NOT SCALE DRAWING | REVISION

	NAME	SIGNATURE	DATE
DRAWN	RAM ABAYASIRI		
CHK'D			
APPV'D			
MFG			
Q.A			

TITLE:

ABD/ADD CURVE PLATE

MATERIAL:

ALUMINIUM

DWG NO.

5

A4

WEIGHT:

SCALE:1:2

SHEET 1 OF 1

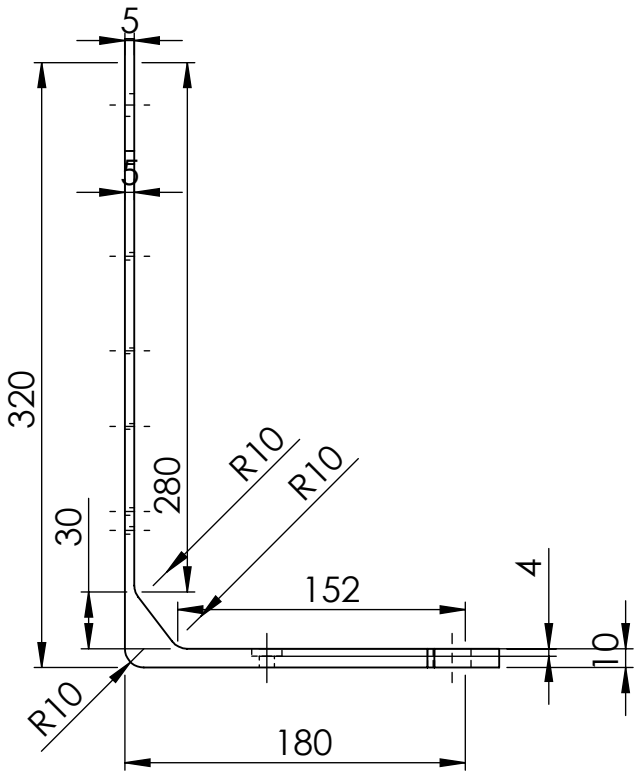

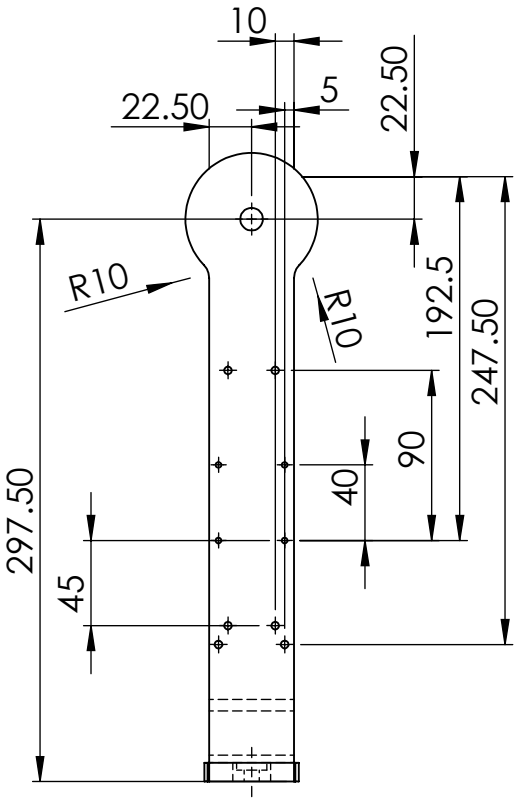

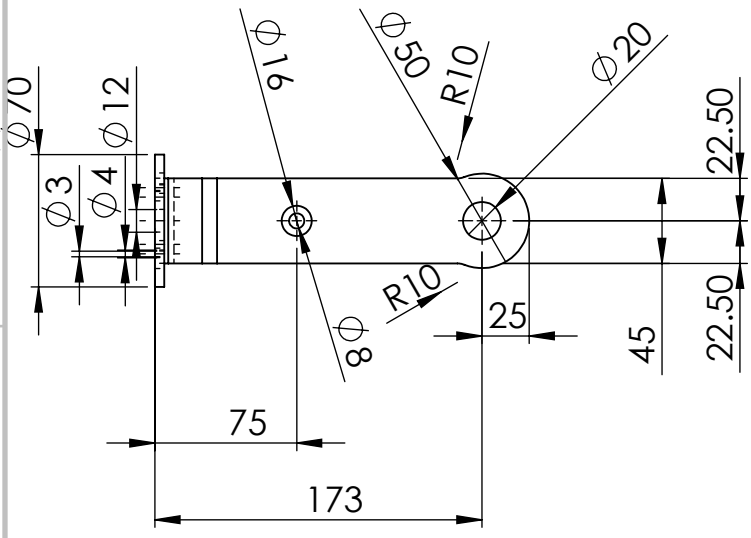

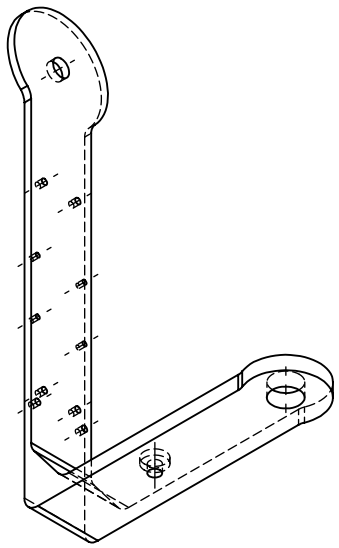

UNLESS OTHERWISE SPECIFIED:DIMENSIONS ARE IN MILLIMETERS

DO NOT SCALE DRAWING | REVISION

	NAME	SIGNATURE	DATE
DRAWN	RAM ABAYASIRI		
CHK'D			
APPV'D			
MFG			
Q.A			

TITLE:

F/E L PLATE

MATERIAL:

ALUMINIUM

DWG NO.

6

A4

WEIGHT:

SCALE:1:4

SHEET 1 OF 1